University of Nottingham

UK | CHINA | MALAYSIA

Fine Sediment Loads and Dynamics in Baleh River, Sarawak.

JOYCE ANAK JANGGU

Thesis submitted to The University of Nottingham

for the degree of Master of Research

September 2023

Abstract

Dams are well known to cause changes in sediment dynamics in downstream rivers, as a result of sediment trapping by the dam and changes in flow competence. While a major programme of dam building is underway in the tropics, the vast majority of fluvial geomorphic studies of dams globally have taken place in temperate and Mediterranean climate regions. More generally, sediment loads in tropical system are less well known than those in more northerly regions. Hence, there are fundamental and applied knowledge gaps related to fluvial processes in tropical rivers.

This thesis provides baseline data on fine sediment loads in the Baleh River (Sarawak, Malaysia Borneo) prior to damming. Baleh dam is due for completion in 2027. This thesis is part of a larger project designed to feed into the development of a Functional Flow regime for Baleh dam, prior to its operation. It provides insights into fine sediment loads near the catchment outlet over a one-year period, and information on spatial variation in suspended sediment concentration along the 100km length of the river.

A continuously logging sensor was installed near the Baleh confluence with the Rajang. This recorded data on turbidity over a one-year period, which were converted to suspended sediment concentration (SSC) via the instrument's internal calibration set up. Data were related to discharge obtained from a nearby gauging station. Spatial patterns of SSC were assessed using drone and satellite images. Sensor signals in both these remote-sensing tools were converted to SSC using a combination of field samples and regression-based calibration.

It was estimated that the Baleh conveyed approximately 15 million tonnes annually into the Rajang. SSCs at the monitoring station were typically around 135mg/L (median concentration). Loads and concentrations both varied between months, although strong season patterns (wet versus dry seasons) were less evident. The study year was rather unusual, showing less pronounced seasonal hydrograph than normal for the Baleh.

The satellite images suggested while there are major changes in SSC along the Baleh, these are very complex and locally variable. Marked increases and decreases in SSC occur, as turbid and clean tributaries discharge their water to the mainstem respectively. However, the relative direction of these changes differs over time, with individual tributaries sometimes

delivering water that is less turbid and sometimes more turbid than the mainstem. An overall increase in SSC along the 100km length survey was only evident when flows were relatively low.

Drone-based analyses indicated highly variable SSCs in confluence zones. Marked contrast in SSC was evident across spatial distances of only a few meters, with little missing of tributary and mainstem waters until several hundred metres downstream. The higher resolution (cm) of drone images compared to the satellite (10m) meant that they provided much more detail of such local contrasts. Together, the three approaches (time series data, satellite analysis of catchment scale patterns, and drone-based assessment of confluence zones) provided useful insights into fine sediment loads and dynamics in the Baleh prior to damming.

Acknowledgements

I would like to express my deepest gratitude to Prof Christopher Gibbins in guiding me throughout this project.

I would also like to thank Celine, Azam and Leon for your support and guidance whenever I needed some help.

A big thank you to Karen and SEB team for the support and advise in everything related to Baleh.

Lastly, a big thank you to my family for their unwavering support during this period of study.

List of Abbreviations

SSC	Suspended Sediment Concentration
GAM	Generalized Additive Model
ADCP	Acoustic Doppler Current Profiler
HEP	Hydroelectric Project
GFF	Geomorphic Functional Flows
FF	Functional Flows
CFRD	Concrete Face Rockfill Dam
MASL	Metres Above Sea Level
MW	Megawatt
DID	Department of Irrigation and Drainage
Rh.	Rumah
HEC-RAS	Hydrologic Engineering Centre – River Analysis System
Q	Discharge
WL	Water Level
RMSE	Root Mean Squared Error
NDSSI	Normalized Difference Suspended Sediment Index
GCP	Ground Control Point
GPS	Global Positioning System
RGB	Red, Green, Blue
DN	Digital Number
CMOS	Complementary Metal Oxide Semiconductor

List of Units

km	kilometre
cm	centimetre
km^2	square kilometre
m^3	cubic metre
mg/L	milligram per litre

Mm^3	million cubic metre
ton	tonnes
m^3/s	cubic metre per second
$\boldsymbol{\rho_B}$	reflectance value of the blue band
$\boldsymbol{\rho_{NIR}}$	reflectance value of the near infrared band

List of Tables

List of Figures

Table of Contents

1. Introduction, Aims and Objectives of Thesis

All rivers convey sediment from headwaters to downstream areas. This natural process includes both coarse and fine sediments, as well as dissolved material (Fondriest Environmental, 2014). Coarse sediments are important for aquatic habitat as they create physical structures at a range of scales, extending, for example, from boulder clusters to gravel bars, and up to morphological units such as riffles (Leopold, 1964). Coarse sediments can also trap nutrients, and create spawning and rearing grounds for fish and other aquatic organisms (Hauer, 2015, Pusch, 2008). Fine sediments are also important as they contribute to nutrient transfer and cycling, as well as physical habitat diversity (Bernhardt, 2005, Wallace, 2002). However, fine sediment, when in high concentrations, can create problems for the physico-chemical quality of water and has implications for habitat and river ecosystems (Wood and Armitage, 1997).

While fine sediment occurs naturally, the delivery of high volumes of fine sediment into river channels is accelerated by human activities such as logging, agriculture, construction and mining (Thapa, 2011, Wang, 2016). Conversely, dams, which are designed to harness water resources, may reduce river fine sediment loads. Due to their ability to trap sediments, dams lead to sediment starvation in downstream areas, which can cause fluvial disequilibrium (Basson, Beck, 2003, McCartney et al., 2001). In addition to these gross changes, trapping by dams can alter the sediment size composition downstream since they tend to trap a higher proportion of coarse than fine sediments, while changes in flow competence alter the ability of the river to entrain and transport different size fractions of its sediment load. This results in changes in sediment size on the riverbed, with impacts on ecological processes and bed conditions downstream from the dam (Power et al., 1996, Soukhaphon et al., 2021, Williams and Wolman, 1984).

Although there has been a considerable amount of work published on the impact of dams on fine sediment dynamics in temperate regions, very little work has been published in tropical systems. Tropical studies are needed because natural patterns of sediment conveyance have been argued to be different in tropical regions compared to those in other climate regions (Chong et al., 2021), so the relative effects of tropical dams may differ. A key difference is that tropical systems often convey their fine sediment loads continuously, while in temperate and Mediterranean systems most of the load is conveyed in a few, shorter periods of time (during high flows). The magnitude and impact of fine sediments trapped by dams are significant in

the context of geomorphic functional flows (GFFs), which are often proposed as a solution to restore or maintain more natural sediment dynamics in dammed systems. The starting point for GFFs is an understanding of fine sediment dynamics prior to damming. In practice this has rarely been addressed, so many or most FFs are developed retrospectively, after dam closure.

This research is part of a larger project to understand the baseline conditions of Baleh River prior to the completion of the Baleh Dam. Baleh River is located in Central Borneo, in the Malaysian state of Sarawak. It is situated within the Kapit Division (an administrative region) and is a tributary of the Rajang, Malaysia's longest river. The Baleh Dam is a Concrete Faced Rockfill (CFRD) Dam situated at an elevation of 225 metres above sea level (Sarawak Energy Berhad, 2019). It is located 105 kilometres upstream from the Baleh's confluence with the Rajang River. The dam is currently under construction and is expected to be complete in 2027. The owner and developer of Baleh Dam, Sarawak Energy Berhad, has commissioned research to inform the development of functional flows (FF), extending from those needed to maintain natural flood and low flow regimes, to maintain temperatures and fluvial processes, and to river ecology. The research described in this thesis is one part of the FF project and focuses on assessing baseline conditions related to fine sediment prior to the completion of the Baleh Dam. The research has three objectives:

1. To estimate the annual fine sediment load of the Baleh and assess monthly and seasonal patterns to this load;

2. To assess longitudinal patterns of Suspended Sediment Concentration (SSC) along the Baleh, from the dam site to its confluence with the Rajang (i.e. riverscale patterns), especially the influence of tributaries in altering mainstem SSCs;

3. To assess patterns of mixing around confluence zones, particularly how these vary with flow.

These aims and objectives nest within an overarching goal to assess the utility of using remote sensing tools for assessment of fine sediment. Baleh is remote, inaccessible and large, and these attributes mean that conventional spot sampling and time series recording using turbidity sensors may not provide the necessary insights. Satellite based surveys provides an alternative for such large rivers, because the river width and length mean that image resolution in the order of tens of metres still has the potential to provide insights into spatial

patterns at the catchment scale. However, satellite data may be too coarse to resolve more detailed patterns around confluences. For this reason, drone measurement can be used to complement satellite data, and especially to see whether fine scale patterns may not be discernible in satellite images. Hence, as part of the overarching goals, some comparisons of satellite versus drone images are made.

2. Literature Review

2.1. Contents

This literature review discusses fine sediment and its significance, as well as the impacts of dams on fine sediment dynamics. The review also covers various methods of assessing fine sediments at both large and small scales; it highlights the strengths and weaknesses of the various methods of assessing fine sediment at these two scales. This informs the methods used for the thesis.

2.2. Sources, Transport and Function of Sediment

Sediments are the products of disintegration and decomposition of rocks, and find their way to streams and rivers as a result of erosion and run-off (Ponce, 2014). Disintegration and decomposition of solid geology occur as a result of multiple, naturally occurring geomorphic processes, caused by the dynamic activity of water, ice, snow wind, plants, animal and humans (Augustyn et al., 1998). In addition to geomorphic processes, human activities such as deforestation and overcultivation accelerate the production of sediment (Fondriest Environmental, 2014). Czuba et al. (2011) found that heavy rainfall over areas with loose soil and minimal vegetation can carry loose particles into waterways through runoff. They also discovered that most of the sediment load in the waterways they studied was transported during flood events.

Sediments with grain size of more than 8mm travel as bedload (Wilcock et al., 2009), where they are transported along the bottom of the channel and are moved by rolling, sliding and saltation, depending on the strength of the flow (Chanson, 2004). Examples of bedload include gravel and cobbles transported in upland rivers as described by Ancey (2020), Collinson (2005), Hassan et al. (2013). Granules and pebbles, with grain sizes between 2mm and 8mm (Wentworth, 1922) are transported through saltation where they are intermittently lifted and bounced along the river bed (Bagnold, 1973, Gilbert and Murphy, 1914, Niño et al., 1994).

Sediments whose grain size has a diameter of less than 2 mm are referred to as fine sediment and typically comprised of sand, silt and clay particles (Naden, 2010). Unlike coarser sediments, fine sediments are transported by means of suspension (Owens et al., 2005) and when in suspension, the fine sediment is referred to as suspended load. Dissolved load refers

to material which has grain size of less than 0.001mm, and is carried in solution. Ions such as calcium, potassium and chloride are dissolved in water from the chemical weathering of bedrock and soils.

Rivers convey sediment from higher elevation parts of catchments to the oceans. This is referred to as sediment transport or conveyance. Sediment transport is not a continuous process, but rather a stop-start process which is influenced by water flow, terrain, weather, and human activities.

Zimmermann (2013) states that sediment transport in rivers comes in three phases. In the first phase where there is low flow, only fine sediments are mobilized. Not all fine sediments are mobilised – those behind boulders and shadowed (hidden) by large gravel and cobbles may remain on the bed. In phase two, where there is higher flow, medium sized sediments are mobilized along with the finer one – this is a common type of sediment transport in rivers and is referred to as partial mobility (Lenzi et al., 2006). In the last phase of sediment transport where river flow is very high, all grain sizes are mobilized (i.e. including the largest ones present) such that the entire channel bed is entrained and transported. This is referred to as full mobility and occurs only during extreme high flows (Lenzi et al., 2006).

Transported sediments are periodically deposited on the river bed and remain stored until competent flows re-suspend and transfer them downstream (Piqué et al., 2014). According to Hauer et al. (2018), the processes of sediment transport, deposition and subsequent re-entrainment are a fundamental aspect of habitat creation and integrity of river ecosystems. Depending on the local sediment supply and energy environment, different types of habitats occur along the river network, changing systematically from upland to lowland environments. These different habitats support different types of ecosystem (Cinco-Castro et al., 2022, Hauer, 2015, Montgomery and Buffington, 1997). Sediments are also critical for coastal zones, creating estuaries and deltas, and are critical for beach and sand dune formation (Fondriest Environmental, 2014).

2.3. Fine Sediment and its relationship with Flow

Fine sediment plays a fundamental role in the quantity and quality of aquatic habitat (Owens et al., 2005, Hauer et al., 2018). Its role in transporting nutrients is especially significant (Naden, 2010).

Holeman (1968), Panin (2004), Syvitski et al. (2005) and Walling (2006) concluded that about 13.5 to 22 billion tonnes of fine sediment are transported into the oceans per year. The Murray River in Australia is estimated to deliver 100 million tonnes of fine sediment load per year and has an estimated SSC ranging from 100 – 500mg/L (Authority, 2019, CSIRO, 2018, Milliman and Meade, 1983). In the USA, USBR (2023) reported that the Colorado River is estimated to deliver about 150 million tonnes of fine sediment and an estimated SSC ranging from 10 – 100mg/L at the delta of the Colorado River in Mexico (Board, 2023, USBR, 2019). The Nile River in Egypt is estimated to transport about 200 million tonnes of sediment per year, with an estimated SSC of 100 – 1,000mg/L (Lemma et al., 2019).

In Spain, the Ebro River, upstream of the Mequinenza Reservoir, is estimated to have suspended sediment load of about 0.6 million tonnes per year, while the Matarranya and Algars Rivers have sediment loads of about 480 million tonnes and 280 tonnes respectively per year (Tena and Batalla, 2013). In South East Asia, the Mekong River is estimated to transport about 160 million tonnes of sediment load per year (Thi Ha et al., 2018) with the SSC ranging from 100 – 1,000mg/L (MRC, 2019). In South America, the Amazon River is estimated to transport about 2 billion tonnes of fine sediment load per year with SSC up to 10,000mg/L (Milliman and Meade, 1983).

In tropical regions, high sediment loads are contributed by the erodible soils and high rainfall-runoff. The relationship between SSC and flows is complex. The relationship is not always linear where SSC may peak at a certain flow rate and then decline as flow increases. The relationship between flows and SSC can be assessed using hysteresis analysis (Lloyd et al., 2016). The hysteresis occurs because SSC for a given discharge during the rising limb of the hydrograph is typically different from the falling limb due to the time lag between flow curve and SSC curve (Mukundan et al., 2013). Different flows and sediment transport processes can be identified using hysteresis patterns, and inferences can be drawn about sources (Nadal-Romero et al., 2008).

Once it settles on the bed, fine sediment creates a physical habitat that is distinct from that formed by coarser sediment. Areas of finer bed therefore support different species with different requirements to those associated with gravel or boulder beds. At small scales, patches of fine sediment add to local habitat heterogeneity and so can contribute to increasing biodiversity within river reaches. At larger scales, there tends to be a transition in the prevalence of deposited fine sediment moving from headwater areas to lower, coastal sections of rivers. This again can lead to turnover in biological community composition, with communities changing from those associated with high energy, transport dominated environments to those associated with low energy, depositional ones (Vannote et al., 1980).

Fine sediment deposited not on the riverbed but on river floodplains is equally important in shaping river ecosystems (Owens et al., 2005). Periodic floods cause floodplain inundation, and associated settlement of fine material that forms the floodplain. These floodplains are ecologically important in many regions. Seasonally flooded floodplain wetlands are important nursery grounds for fish (Burgess et al., 2013). Floodplain agriculture depends on the nutrients present within fine material; the importance of floodplain agriculture globally means that transport and deposition of fine sediment can be argued to be important for many millions of people.

Finally, in the coastal zone, deltas are formed as a consequence of fine sediment deposition (Naden, 2010). Deltas are important for biodiversity because they harbour species unique to these particular environments (Giosan et al., 2014, Volke et al., 2015). Large deltas such as the Mekong are critical for agriculture (Bank, 2021, Hui et al., 2022). Deltas, estuaries and beaches, because they are no longer replenished become vulnerable to erosion by rising sea levels (International Hydopower Association, 2020). A case study of the Aswan Dam in Egypt showed that upon the completion of the dam, the trapping efficiency was at 99% with little sediment reaching to the delta (Schellenberg et al., 2017).

Overall, fine sediments are an important element of fluvial systems. However, large volumes of fine sediment, leading to high concentration of suspended sediment and excessive deposition on the bed, can have detrimental effects on fish and other aquatic organisms. The impacts of excessive fine sediment are further discussed in the next section.

2.4. Impacts of Excessive Fine Sediment

Excessive amounts of fine sediment in watercourses, either in suspension or deposited on the bed, can lead to a variety of problems. Human problems include obstruction or clogging storm sewers, which can lead to flooding, and excessive sediment deposition, which can alter river flow and reduce the depth, making river navigation difficult (Shaffer, 2017).

High SSC results in water becoming highly turbid, hindering animals' ability to locate food (e.g. visual predators such as fish). Additionally, the murky water prevents natural vegetation from growing in water (EPA, 2005) as it blocks the sunlight needed for photosynthesis. This turbidity reduces plant productivity and, in doing so, alters primary productivity and, accordingly, the basis of the aquatic food chain (Håkanson, 2006). As well as a reduction in the depth of the photic zone, high SSC can increase the temperature of the water; thus, fine sediment becomes part of a multiple aquatic ecosystem stressor problem (Collins and Zhang, 2016).

Excessive sediment deposited on stream bed can reduce the quality of the natural benthic habitat (Kondolf and Wolman, 1993, Milner et al., 2003). For example, Kemp et al. (2011) found that excessive fine sediment loadings cause entrapment and suffocation of fish progeny, eventually leading to a decrease in fish populations. Fine sediments can also transport toxic compounds into the river (Ali, 2017). Nutrients, especially nitrogen and phosphorus from large-scale, intensive agriculture, may be transported along with fine sediment, causing eutrophication – a process which leads to oxygen depletion as a result of excess algal growth (USDA, 1993). This may be especially problematic in the tropics where warm water encourages rapid plant growth.

2.5. Dams and Sediment Deficits

Dams have a variety of functions, including flood control, potable water supply, water for agriculture and industry, and the production of hydroelectric power. Dams function to hold back water for various purposes. By having a dam structure across a river section, the hydrological regime of the river is modified, changing naturally dynamic flow regimes to more stable, less variable flow. This, in turn, causes hydro-morphological modifications that include armouring, stabilisation, changes in bedform morphology, 'terrestrialization' of gravel bars and bed incision, which alter ecological systems (Alexandra, 2021). For example, a study of the

sediment budget at Lower Red River in Vietnam by Lu et al. (2015) showed that as a result of the Tac Ba dams, hungry-water effects occurred downstream of the dam; erosion became the dominant process, with erosion increasing from 3.7 to 40.9 metric tonnes per year.

A river with a natural flow regime is approximately in a sediment transport equilibrium (Wohl et al., 2015). However, dams also trap sediment, and this may cause disequilibria. Retaining sediment behind the reservoir contributes to geomorphological changes downstream, as the very material that habitat is built from is no longer supplied. It is estimated that 70-90% of fine sediment loads from the catchment area are retained in reservoirs (Vörösmarty et al., 2003), with a variety of effects that include agricultural areas downstream of the dam becoming less fertile (Pacini et al., 2013).

In the tropics, Liu et al. (2013) found that the sediment load after the completion of the Manwan Dam on Mekong River decreased; this is consistent with the study by Lu and Siew (2006) who reported that the presence of dams in the upper Mekong has caused significant decline in sediment flux along the lower Mekong. Lu and Siew (2006) found 40% reduction in monthly SSC at several gauging stations at the Lower Mekong River. In addition, a study by Kummu and Varis (2007) estimated that the annual sediment flux at the Lower Mekong River has reduced by half, from 70 x 10^9 kg to 31 x 10^9 kg, since the completion of the Manwan Dam.

Sediment accumulated behind the dam wall is in proportion to the supply of material from upstream. Accumulation of sediment behind a dam wall is spatially variable. Fine sediments are accumulated near the dam and coarser sediments are accumulated farther upstream of the dam (Figure 2-1). This buildup can lead to the storage capacity of the reservoir being reduced in the long run. The rate of reduction in storage capacity depends on local climate and landcover, which influence sediment runoff. A study of the Dez Dam in Iran found that excessive sedimentation has caused the reservoir bed to rise by about 2 meters per year, resulting in a storage capacity loss of about 19% during its 40 years of operation (Schellenberg et al., 2017). Such reductions can affect various reservoir functions, including water provision and HEP production.

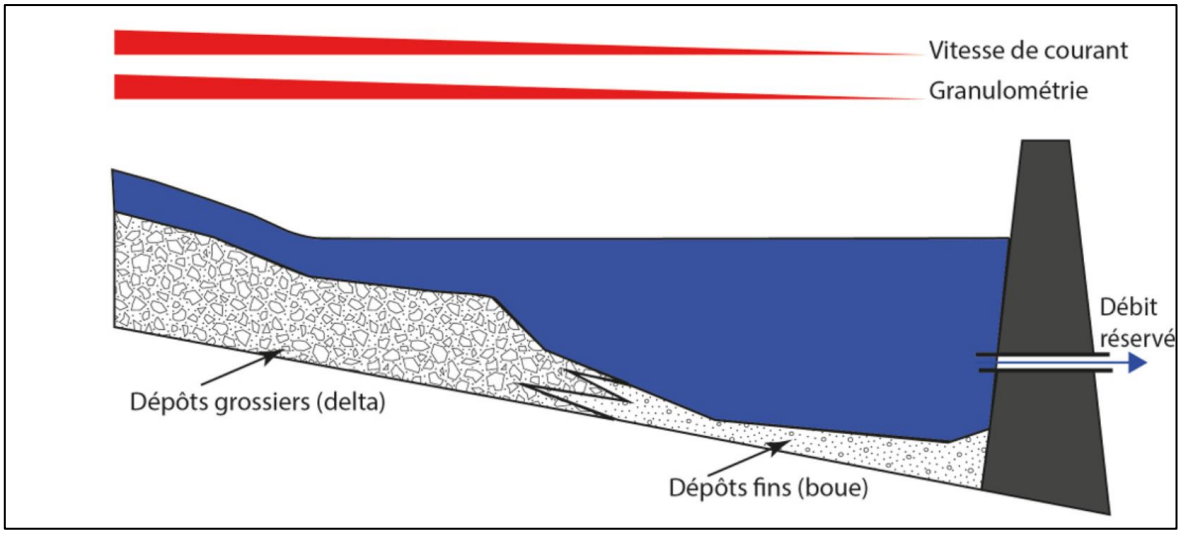

Figure 2-1: Influence of dams on sediment grain size sorting upstream of the structure; coarser grain at the upstream end and finer grain near the structure (Alexandra, 2021)

2.6. Methods of Assessing Suspended Sediment Concentration

Various methods can be used to assess the quantity and spatiotemporal distribution of fine sediment carried in suspension. The two common methods are collecting spot samples of water to measure SSC directly, and continuous measurements of turbidity via an *in-situ* sensor and conversion of these data to SSC using a calibration. Recent developments in remote sensing technology have permitted more thorough spatial analyses. Each method has its strengths and weaknesses, and these are elaborated below.

2.6.1. Spot Sampling

The spot sampling method involves collecting water samples using a sampling device such as a bottle or a container, at a desired location. The sampler is submerged at the desired depth and the sample is collected via the opening of the bottle or container. Once the sample is obtained, it is transported to the laboratory for analysis, where the concentration of suspended sediment is determined via filtration (American Public Health Association, 2012).

This method is reliable, well-documented and widely used (Wren et al., 2000). It is also cost effective compared to continuous monitoring techniques and requires minimal equipment (Carling, 1995). Although it is simple and cost-effective, it also has its limitations. Spot

sampling only provides a snapshot of sediment concentration in that specific point in time and does not show the temporal variability of the sediment concentration over time, which is often influenced by high flow events such as intense rains storms and major floods (Horowitz, 2008, Walling and Collins, 2016). Thus, the key limitation to spot sampling is that it may miss the suspended sediment concentrations at high or low flow, and this would result to inaccurate computation of the suspended sediment loads. Automated water sample collection devices have been designed to get around this problem, but they have limited capacity due to the number of bottles they can house.

As well as having poor temporal resolution, spot sampling does not capture spatial variability. In practice it tends to be used at a few locations along a river to detect major changes in concentration but is not useful for detecting complex small-scale patterns such as confluence mixing zones. Overall, spot sampling at a single location lacks spatial and temporal variability associated with the transport of suspended sediment (Haddadchi, 2017).

2.6.2. Continuous Monitoring

The continuous monitoring of turbidity is excellent at providing insights into temporal variation in sediment concentration, giving better insight into the sediment transport and sediment load pattern and how it relates to flow variability (Hester, 2008). Continuous monitoring systems via a turbidity sensor at the site can be automated and remotely operated, which minimizes the need for frequent site visits and reduces the logistical challenges and cost (Langendoen, 2014). Hence, this method is suitable for sites that are remote and difficult to access regularly. As this method can be remotely operated, having remote access to the real-time data also facilitates real-time decision making and adaptive management strategies. The biggest advantage of this method is that its long-term continuous monitoring datasets can be easily integrated with other environmental data such as hydrological or climate data, allowing for comprehensive analysis and trend identification (Gray, 2009). Load data can be estimated by integrating SSC with flow volume.

The drawback to this method is its high cost of installation and operation, as it relies upon sensors, data loggers, reliable power sources and sturdy structures to mount the instrument. Continuous monitoring systems are usually preferred for remote sites, but the installation and

maintenance can be logistically challenging and the deployment of the sensor needs to consider protection against vandalism or damage (Wagner, 2006).

The accuracy and reliability of continuous monitoring systems are dependent on sensor performance and calibration. Hester (2008) also states that any drift or movement to the sensor, or if the sensor malfunctions, can undermine data reliability. Accordingly, sensors require regular calibration and maintenance. They also suffer from the same low spatial resolution at manual spot samples, and arguably are more limiting due to their high cost, which means rarely more than one or two are installed per study catchment. A typical design is to have them located at the upstream and downstream ends of study sections in order to estimate fine sediment budgets – i.e. difference between inputs and output from a section of interest.

2.6.3. Detecting Spatial Patterns

Spatial analysis involves examining the spatial distribution of sediment suspended within the water column. One of its key strengths is that it helps to identify hotspots or localized areas with high sediment concentration. These hotspots help us understand the sediment sources, sedimentation processes and potential impacts on aquatic ecosystems (Hodge, 2014). Limited sampling density can lead to uncertainty in characterizing the spatial pattern and distribution of sediment concentration. Subsequent to this, spatial interpolation techniques are often used to estimate sediment concentration at unmeasured locations, but applying this technique would introduce uncertainty, depending on field sample resolution (Langendoen, 2014). However, with appropriate calibration and validation, suspended sediment concentration can be estimated across continuous spatial areas from remote sensing images (Hossain et al., 2010) either from satellite or drones.

High resolution spatial data on sediment concentration can be integrated with geospatial data such as land use or land cover maps, and topographical maps (Wheaton, 2010). The integration helps elucidation of controls on local variation in SSC, makes visual presentation appealing and easier to communicate with stakeholders and the community at large (Hodge, 2014). Through spatial analysis, the assessment of changes in sediment concentration over time is possible by comparing multiple datasets/images (Aziz et al., 2021, Cui et al., 2022).

Spatial analysis can be conducted at different scales, depending on research objectives or questions. Hodge (2014) states that, at smaller scales, fine-scale processes, such as sediment plumes, small-scale turbulence or localized sediment sources, dominate sediment dynamics. However, at larger scales, factors such as basin morphology, land use and regional sediment sources become more influential. In order to assess large scale variability for water bodies such as reservoirs or oceans, satellite images are appropriate (Ody et al., 2022, Choo et al., 2022). On the other hand, for small spatial scale variability, remote sensing method using unmanned aerial vehicle (UAV) have been proven to be useful, e.g. for small to medium sized rivers (Hemmelder et al., 2018, Larson et al., 2018).

While remote sensing approaches offer great potential to understand spatial patterns continuously over large areas, they have limitations. Depending on scale of interest in relation to image resolution, the choice of method is critical. Moreover, techniques for converting the signal received by a sensor into an estimate of SSC are still quite new, so issues of uncertainty or accuracy still limit confidence. Wheaton (2010) cites that spatial analysis relies on the availability of representative sediment data at multiple locations of the study area.

2.7. Key Points

Fine sediments are sediments with grain size less than 2mm and comprised of sand, silt and clay particles. They are transported in suspension, and their movement in water is highly influenced by river flow. The relationship between SSC and flow is often complex and non-linear. In general, much less has been published about suspended sediment in tropical systems than in temperate ones. Tropical systems tend to have relatively high fine sediment loads due to the nature of rainfall and erodible soils, and the temporal distribution of the annual sediment load is different to that in other climate regions (Chong et al., 2021).

Dams are a major barriers that obstruct sediment transport, causing geomorphic changes downstream of the dam, leading to more erosion as a result of hungry-water effect (Kondolf, 1997). Studies have shown that dams retain more than 70% of the fine sediment loads in the reservoir, casing reductions in fine sediment loads downstream. In the Mekong, studies have found that there has been a 40% reduction in suspended sediment concentration downstream of the dam. The Mekong, however, is a rare example of a tropical dam study – in their review Chong et al. (2021) highlighted the current paradox, which is that while most new dam

building is in the tropics, very few studies exist for this climate region. Hence, due to the poor knowledge base, we have a limited ability to anticipate and predict the likely consequences of dams in tropical systems.

This literature review also explored the various methods of assessing suspended sediment concentration in rivers. It showed that the methods should be chosen depending on research objectives. For this study, which investigates both the temporal and spatial characteristics of fine sediment in a very large system (main channel > 100km long), multiple methods are appropriate:

1. Continuous monitoring using turbidity sensors to estimate the sediment load at the basin outlet,
2. Spatial analysis using satellite images to assess the spatial variability of suspended sediment along the whole river length, and
3. Spatial analysis using unmanned aerial vehicle (UAVs) to assess the spatial variability of sediment around confluences.

3. Study Area and Methods

3.1. The Baleh Catchment and Baleh Hydroelectric Project (HEP)

Baleh Catchment

The Baleh catchment is a sub-basin of the Rajang River Basin and has a catchment area of 5,625km^2. Figure 3-1 shows the location of Baleh catchment as depicted by the light green zone. The triangle indicates the location of Baleh HEP within the catchment, and the circles indicate the confluences of Baleh River (Rh. Bawai A, Kerangan Ara, Merirai, Putai and Nanga Entawau River). SSC sampling sites are located at the confluences of Merirai and Putai, while Teluk Buing, indicated as a black square, serves as the gauging station used to estimate the inflow at Baleh.

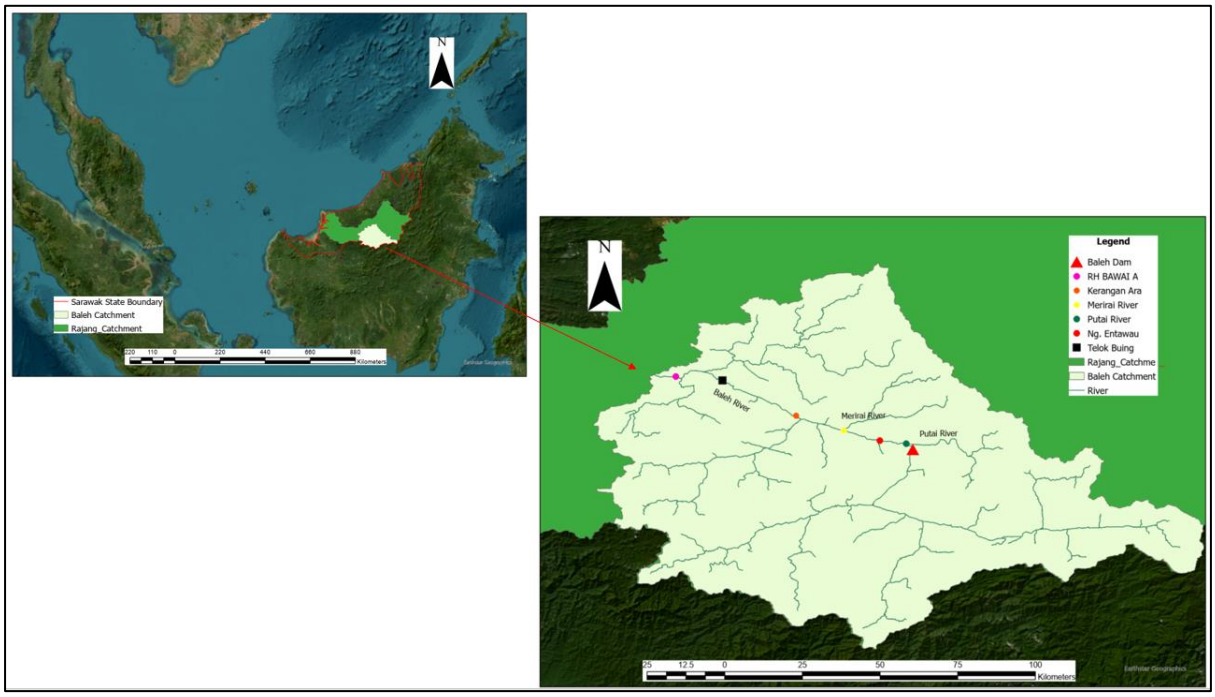

Figure 3-1: Locality of Baleh catchment, Baleh Dam, Confluences and Gauging Stations

Staub (2000) reported that the Rajang River Basin is approximately 50,000 square kilometres (km^2) with elevations surpassing 2000 metres above sea level (masl). According to Lum (2023), a portion of the Upper Baleh region is designated as a national park, with more than 80% of the catchment covered by mixed dipterocarp, primary and secondary forest, and agricultural plantations (Chong, 2023, Lum, 2023). The geology of the area consists of sandstone and shale from the Belaga and Nyalau formation (Ling et al. (2016). Based on the Sarawak classification system, the soils in Baleh are mainly Red-Yellow Podzols (Tie, 1982).

Lum (2023) examined the land cover change within Baleh catchment from 2000 – 2019. Land cover classes used in the analysis were forest, bare earth, built-up areas, disturbed vegetation and river channel. The study concluded that there were no significant large scale forest clearances in the catchment, with less than 5% change over the period. She found that the intensity of the forest degradation in Baleh was highest at the start of the period and decreased as the years passed, with the highest forest loss observed between 2001 – 2008. These results are consistent with the study by Gaveau et al. (2014), regarding the shift in the logging trend in Malaysian Borneo, where the logging boom occurred in the 1970s and thereafter shifted to industrial plantation sometime in 2005.

Chong et al. (2021) analysed the hydrological flow regime of Baleh, prior to damming. According to the study, the annual total rainfall in Baleh exceeds 5000 mm in most years with an average of 250 days of measurable precipitation per year. The temperature in the area is also high throughout the year with a mean annual daily maximum temperature of 33°C. Their study uses the rain gauges and water level data from within the catchment of Baleh to develop the long-term inflow series from 1967 – 2017. Information on Baleh's hydrology as presented below is extracted from this paper. Based on the median monthly discharges at Baleh (Figure 3-2), the wet months are found to be from November to March and the dry months are from May to August. In terms of baseflow (Figure 3-3), during the dry months it is found to be less than 500m^3/s. while for the wet months baseflow ranges from 500 – 800m^3/s.

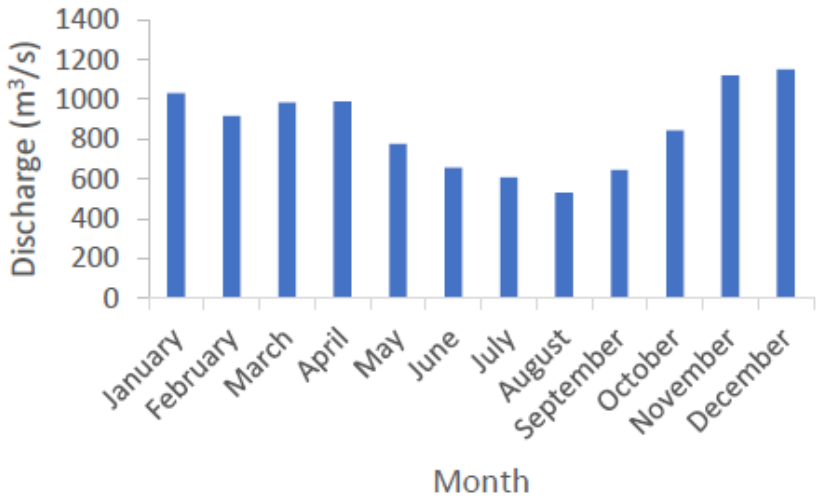

Figure 3-2: Median Monthly Discharges at Baleh (1967 - 2017) [Source: (Chong et al., 2021)]

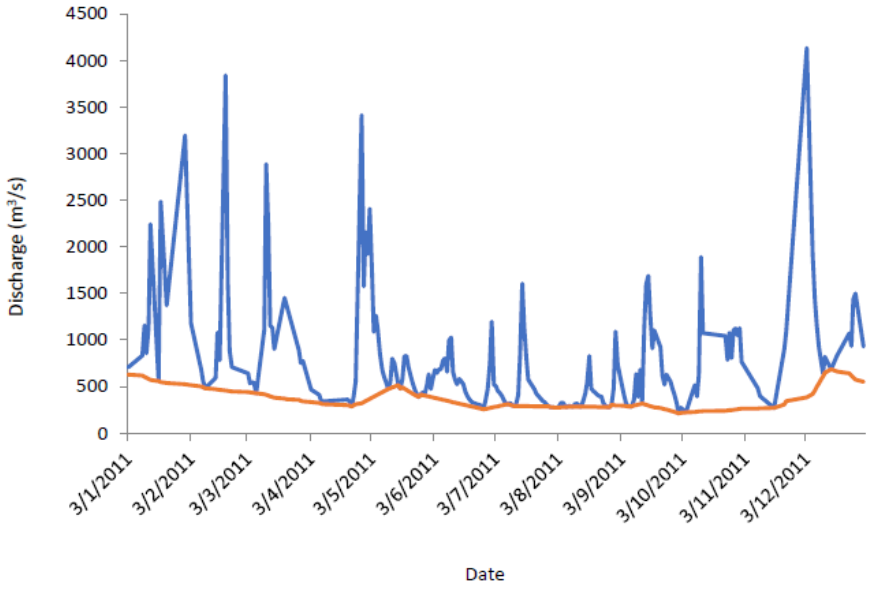

Figure 3-3: Example of an annual hydrograph at Baleh, indicating the daily discharge magnitude (blue line) and baseflows (orange line) [Source: (Chong et al., 2021)]

The long-term median flow for Baleh is estimated to be 873m^3/s, with the flow at 90th percentile estimated at 376m^3/s and the 10th percentile, 1915m^3/s. The flow duration curve for each year of record (1967 – 2017) is plotted in Figure 3-4. The inset diagram Figure 3-4 indicates the overall long-term flow duration curve. From the period of the record, it was found that 1970 and 2014 represent the extreme wet and dry years respectively. Median flow (Q50) varies a lot, with a two-fold difference between these wet and dry years (approximately 1800 and 900m^3/s respectively).

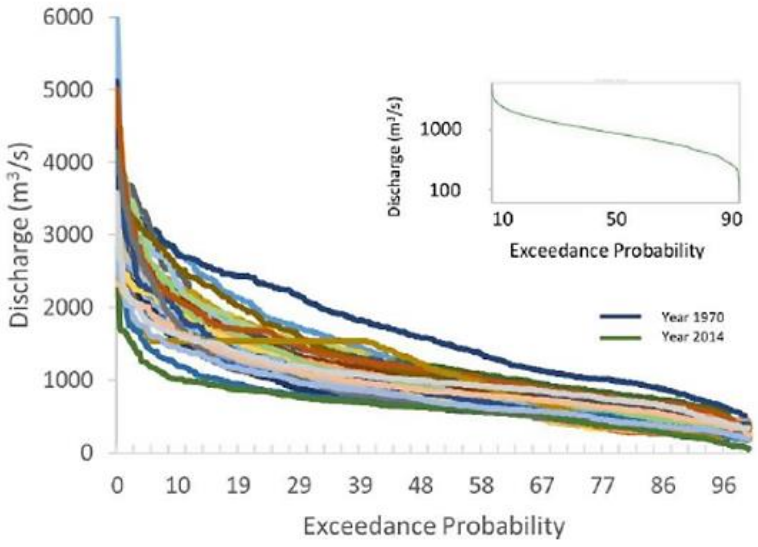

Figure 3-4: Flow duration curve for years 1967 - 2017, The inset shows the long-term flow duration curve [Source: (Chong et al., 2021)]

Baleh Hydroelectric Project

The construction of the hydroelectric dam, as depicted in Baleh HEP's locality in Figure 3-1, is well underway. The Baleh HEP is a key infrastructure for hydro-industrialization to meet the rising energy demands from energy intensive industries within the Sarawak Corridor of Renewable Energy (SCORE) (Sarawak Energy Berhad, 2019). Sarawak Energy Berhad, the developer of Baleh HEP, has announced that the project would be completed by 2027 (Borneo Post, 2022).

Baleh HEP is designed as a 185 m high concrete-face-rockfill dam, with an installed capacity of 1,285MW. It is located 95km upstream from the confluence of Rajang River (1° 48' 9.00" N, 113° 46' 22,00" E), in the Kapit division of Sarawak, Malaysia. Upon completion, the dam will impound a reservoir with an area of 588km^2 and volume of 29,868 x 10^{6}m^3 at full supply level.

3.2. Methods

This section describes the methods used to estimate the suspended sediment concentration at the study sites, as well as the method used to estimate the discharge, for the purpose of estimating the suspended sediment loads. It also discusses the remote sensing approaches used to assess the spatial distribution and patterns of SSC within the Baleh River.

3.2.1. Continuous Monitoring of Turbidity

3.2.1.1. Suspended Sediment Concentration Data

A multi-parameter sensor, Proteus Water Quality Probe by Proteus Instruments (Figure 3-5) was used to measure the SSC at Baleh River. Prior to installation by Sarawak Energy Berhad, the sensor was calibrated on site in accordance with the user manual (Proteus, 2023). The calibration proceeded in the following sequence;

(i) Calibration for dissolved oxygen: This step involved exposing the sensor to open air to achieve 100% dissolved oxygen saturation.

(ii) Calibration of pH: Buffer solutions of pH values 4 and 7 were utilized to calibrate the sensor.

(iii) Calibration of conductivity: A standard solution with a conductivity of 500 microsiemens per centimeter (µS/cm) was employed for this calibration.

(iv) Calibration of turbidity: A standard solution with a turbidity of 1000 Nephelometric Turbidity Units (NTU) was used for this calibration.

(v) Calibration of Ammonium: Standard solutions of 1mg/L and 10mg/L were used for this calibration process.

It is installed at Rumah (Rh) Bawai A, approximately 90km downstream from Baleh Dam. Its locality is shown in Figure 3-1. This station was installed and commissioned by Sarawak Energy Berhad on 1st February 2022 to collect a range of water quality data of the Baleh River, including measurement of SSC.

Figure 3-5: Proteus Water Quality Probe by Proteus Instruments to measure SSC at Baleh River (Source:(Proteus, 2023))

This sensor provides SSC data in milligrams per litre (mg/L) with a 15-minute time interval. As the SSC data is available on a 15-minute time interval, the average daily SSC data is calculated to correlate with the estimated daily flow data. Another station was installed at the dam site at the beginning of this research project. However, due to a major flood, this sensor was washed out within 2 months of installation. Hence the thesis is based solely on the data from Rh. Bawai A station.

3.2.1.2. River Flow

Teluk Buing water level station (owned and operated by Sarawak's Department of Irrigation and Drainage (DID) has a long record of data; from 1966 to the present date. Teluk Buing is 20km upstream from Rh. Bawai A and its location is shown in Figure 3-1.

Bannigan (2013) conducted a river survey in 2013 which covered a distance of 12km downstream of the gauge site and obtained 24 cross sections. A HECRAS model was developed and fitted to previous DID gaugings by adjusting the bed roughness coefficient. The fit is considered to be reasonable over the full range of measured discharges; the fitted HEC-RAS rating curve at Teluk Buing is shown in Figure 3-6. This fitted rating curve was then extrapolated to high discharges using the same HECRAS model and the extrapolated rating curve is shown in Figure 3-7.

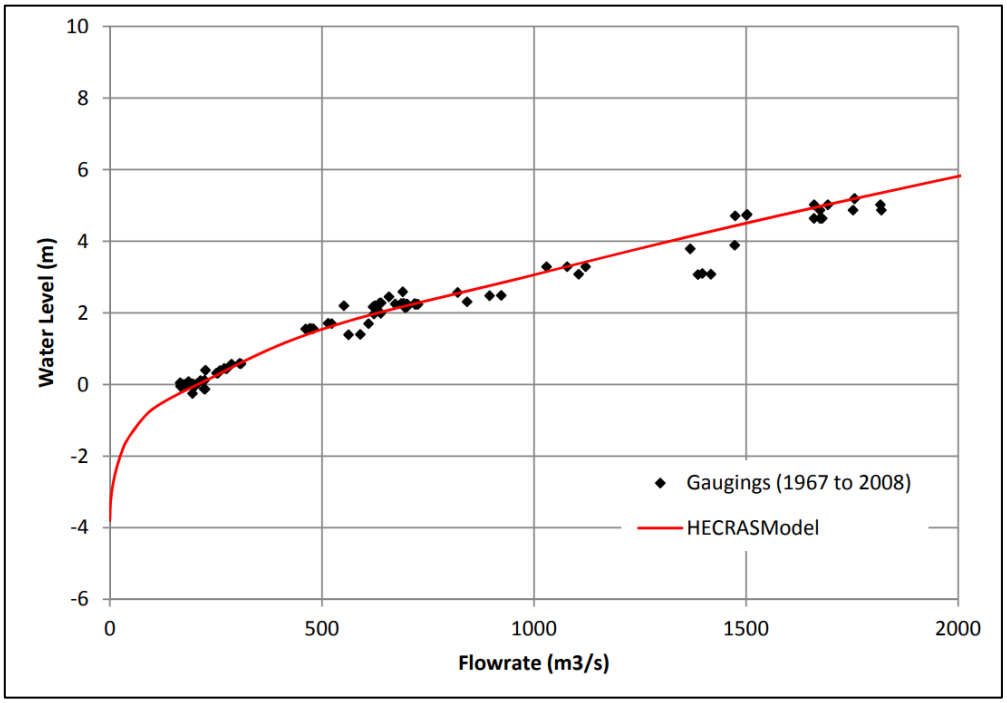

Figure 3-6: Fitted HECRAS rating curve (Source: (Bannigan, 2013))

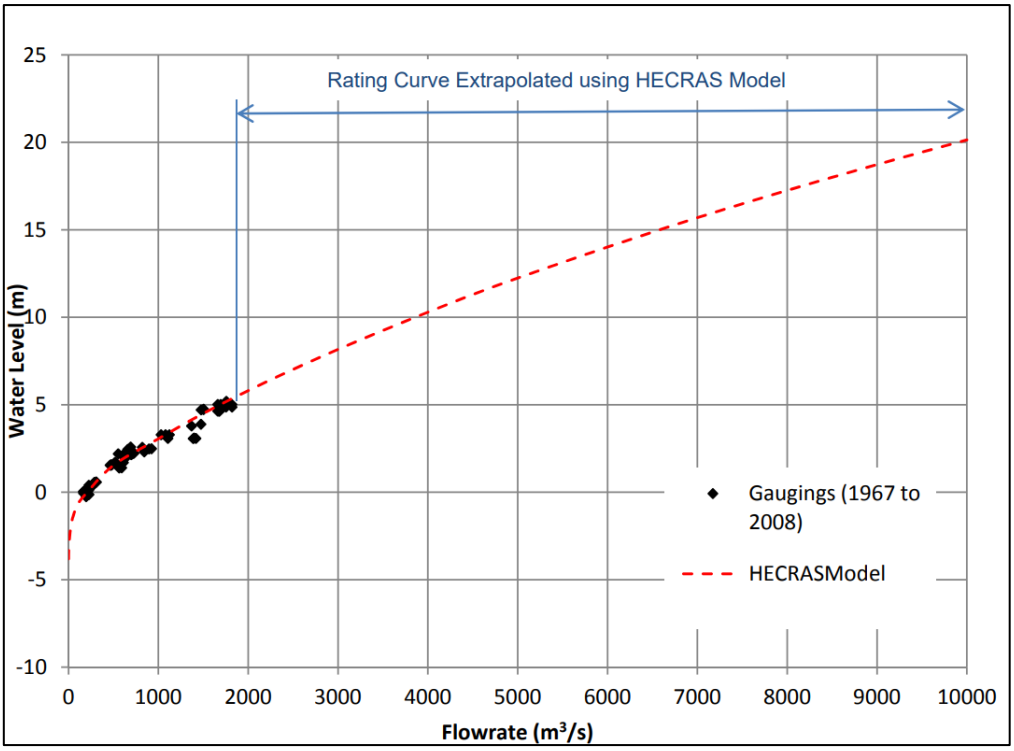

Figure 3-7: Extrapolated Rating Curve

From the rating curve, Bannigan (2013) concluded that the water level measurements at Teluk Buing can be converted to discharge using the following equations;

$Q = 5.807 \times (WL + 3.9)^{2.221}$ for WL < - 2.2m *(Equation 3-1)*

$Q = 3.6616 \times (WL + 3.9)^{2.894}$ for -2.2m ≤ WL < 1.5m; and, *(Equation 3-2)*

$Q = 120.22 \times (WL + 1.2)^{1.4393}$ for WL > 1.5m. *(Equation 3-3)*

Where,

Q = discharge (m^3/s) and,

WL = water level (m).

Using the established rating curve equation by Bannigan (2013), the flows at Rh. Bawai A is estimated using transposition method based on catchment area factor. The equation for estimation of discharge at Rh. Bawai A is as per Equation 3-4.

$$\text{Discharge at Rh. Bawai A} = \text{Inflow at Teluk Buing} \times \frac{\text{Catchment Area of Rh. Bawai A}}{\text{Catchment Area of Teluk Buing}}$$

(Equation 3-4)

The water level data at Teluk Buing, as provided by DID, is on a daily timestep and only available up to 31st December 2022. The discharges at Rh. Bawai A are calculated up to 31st December 2022 using Equation 3-4.

3.2.1.3. Suspended Sediment Load

Given that the suspended sediment concentration data is available from 1st February 2022, and the discharge at Rh. Bawai A, is up to 31st December 2022, the period of this study is from 1st February 2022 – 31st December 2022. Since the discharge data is on a daily timestep, the suspended sediment load is to be analysed at a daily timestep, using the average daily suspended sediment concentration data at Rh. Bawai A, recorded using the sensor as shown in Figure 3-5.

To calculate the suspended sediment load in ton/day, SSC in mg/L is first converted to ton/m^3 and inflow (m^3/s) is converted to m^3/day. After the conversion, the sediment load in ton/day is calculated as per Equation 3-5.

$$Sediment\ Load\ (ton/day) = SSC\ (ton/m^3) \times Flow\ (m^3/day) \qquad \textit{(Equation 3-5)}$$

3.2.2. Remote Sensing at River Scale Using Satellite Images

The method of Hossain et al. (2010) uses the Sentinel-2 MSI Multispectral Instrument, Level 2A imagery to compute the Normalized Difference Suspended Sediment Index (NDSSI). This method has been widely used and NDSSI has proven to be good in representing the spatial distribution and patterns of SSC in rivers and lakes. Table 3-1 below shows the obtained coefficient of determination, R^2 and Root Mean Square Error (RMSE) values of literatures that uses the same method. Generally, R^2 exceeds 0.6, while errors range from less than 1 to approximately 70mg/L. This index is applied to satellite data to map the spatial distribution and variation of SSC along the length of Baleh River.

Table 3-1: R^2 and RMSE values of literature that apply the method developed by Hossain et al. (2010)

Source	Study Area	Satellite Source	R^2	RMSE (mg/L)
Hossain et. al., 2010	Mississippi River, USA	Landsat	0.68	-
Paulista et. al., 2023	Teles Peles River, Brazil	Sentinel	0.79	-
Pereira et. al., 2019	Jaguaribe River, Brazil	RapidEye	0.6	48
Womber et. al., 2021	Lake Tana, Ethiopia	Modis Terra	0.81	42.96
Liew et. al., 2003	Jinsha Tributary, China	Landsat	0.79	-
Isidro et.al., 2018	Didipio, Phillipines	Pleiades	0.65	519
Wang et.al., 2010	Chaohu Lake, China	HJ-1	0.74	16.68
Kaba et.al., 2014	Lake Tana, Ethiopia	Modis Terra	0.95	16.5
Rajendran et.al.,2023	Arabian Gulf	Sentinel	0.58	0.15
Zhang et.al.,2022	Yangtze River, China	Sentinel	0.79	24.87
Arisanty et.al.,2017	Barrito Delta, Indonesia	Landsat	0.7	-
Shahzad et.al., 2018	Indus Delta	Landsat	0.88	67.24
Zhang et.al.,2014	Yellow River, China	Landsat	0.97	-
Wirabumi et.al., 2020	Menjer Lake, Indonesia	Planetscope	0.78	-
Adjovu et.al.,2021	Lake Mead, USA	Landsat	0.96	-
Munir et.al., 2019	Padang, Jakarta, Indonesia	Sentinel	0.81	-

Similar to Hossain et al. (2010)'s method, this study uses Sentinel-2 MSI Multispectral Instrument, Level 2A imagery with 10m resolution to analyze the spatial distribution and pattern of SSC at Baleh River.

The length of river used for this was constrained by the resolution of the satellite images relative to the river width. For much of its lower length, the Baleh is 150-200 m wide so satellite image resolution (10 m) is adequate for mapping SSC. We used a minimum river width of 10 m to set the upstream point at which satellite based analysis was no longer feasible.

To estimate the SSC, Band 2 (Blue) and Band 8 (Near Infrared) were employed to calculate the NDSSI (Hossain et al., 2010). The NDSSI is calculated by taking the difference between the reflectance values of Band 2 and Band 8, and then dividing that difference by the sum of the reflectance values of those bands. The equation is depicted in Equation 3-6. The resulting NDSSI value should range from -1 to 1, with higher values indicating turbid water and lower values indicating clearer water.

$$NDSSI = \frac{\rho_B - \rho_{NIR}}{\rho_B + \rho_{NIR}} \qquad \textit{(Equation 3-6)}$$

Where $\boldsymbol{\rho_B}$ and $\boldsymbol{\rho_{NIR}}$ are the reflectance values of the Blue and NIR Band. The value of $\boldsymbol{\rho_B}$ and $\boldsymbol{\rho_{NIR}}$ are taken from Landsat 8's Band 2 and Band 5 respectively (USGS, 2018).

Figures 3-8, 3.9 and 3-10 shows the NDSSI imagery prepared from Sentinel-2 MSI: Multispectral Instrument, - Level 2A. Three image sets were chosen, to represent low flows (July 2021), normal or average flows (September 2022) and high flows (December 2020). Figures 3-11, 3-12 and 3-13 shows the magnified NDSSI imageries for the respective flows.

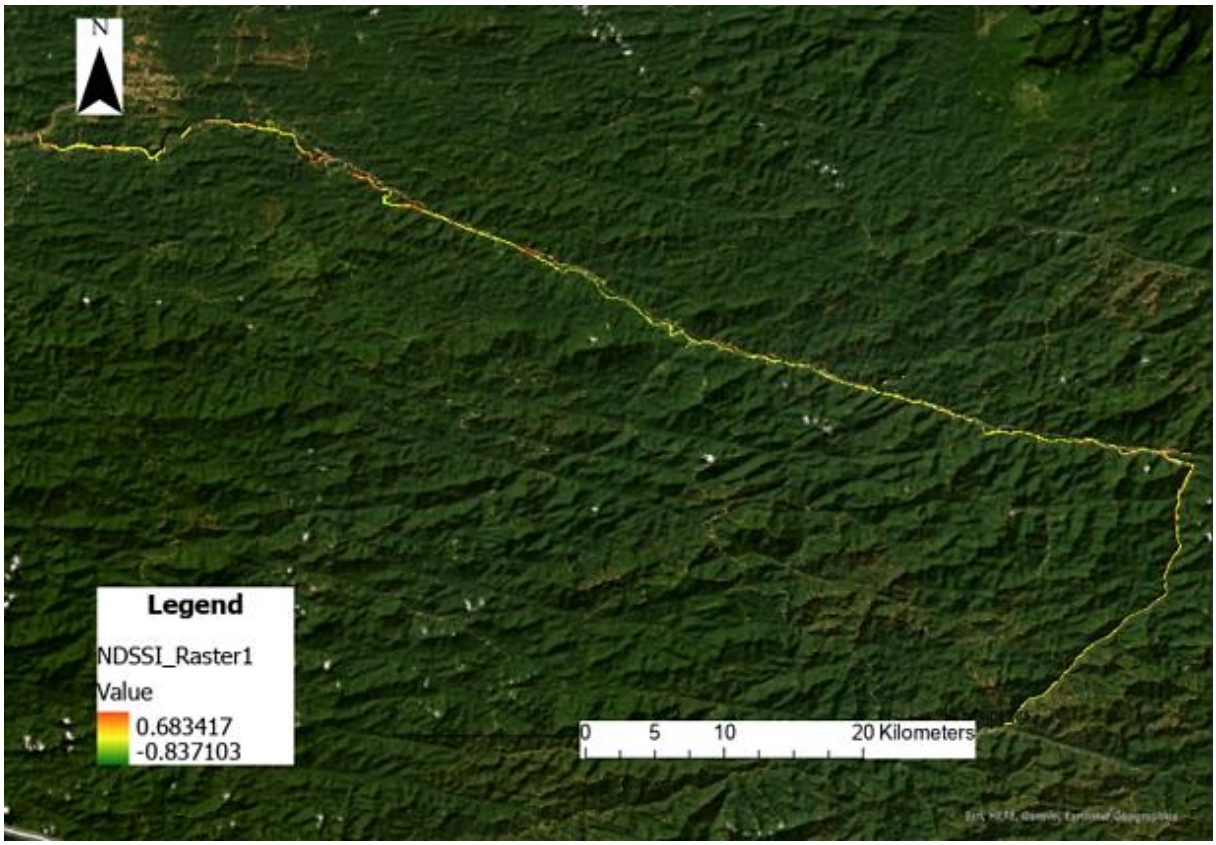

Figure 3-8: NDSSI Imagery for Baleh River on July 2021, representing low flow.

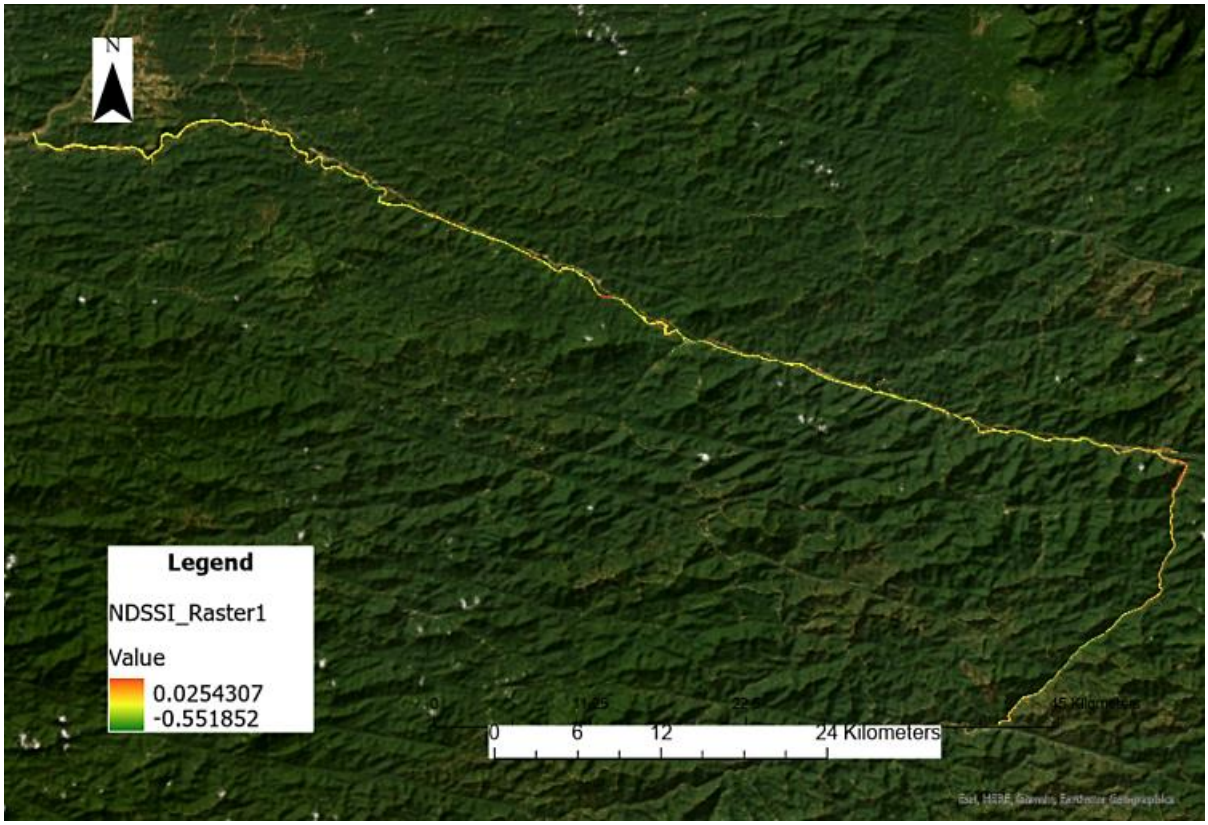

Figure 3-9: NDSSI Imagery for Baleh River on September 2022, representing average flow.

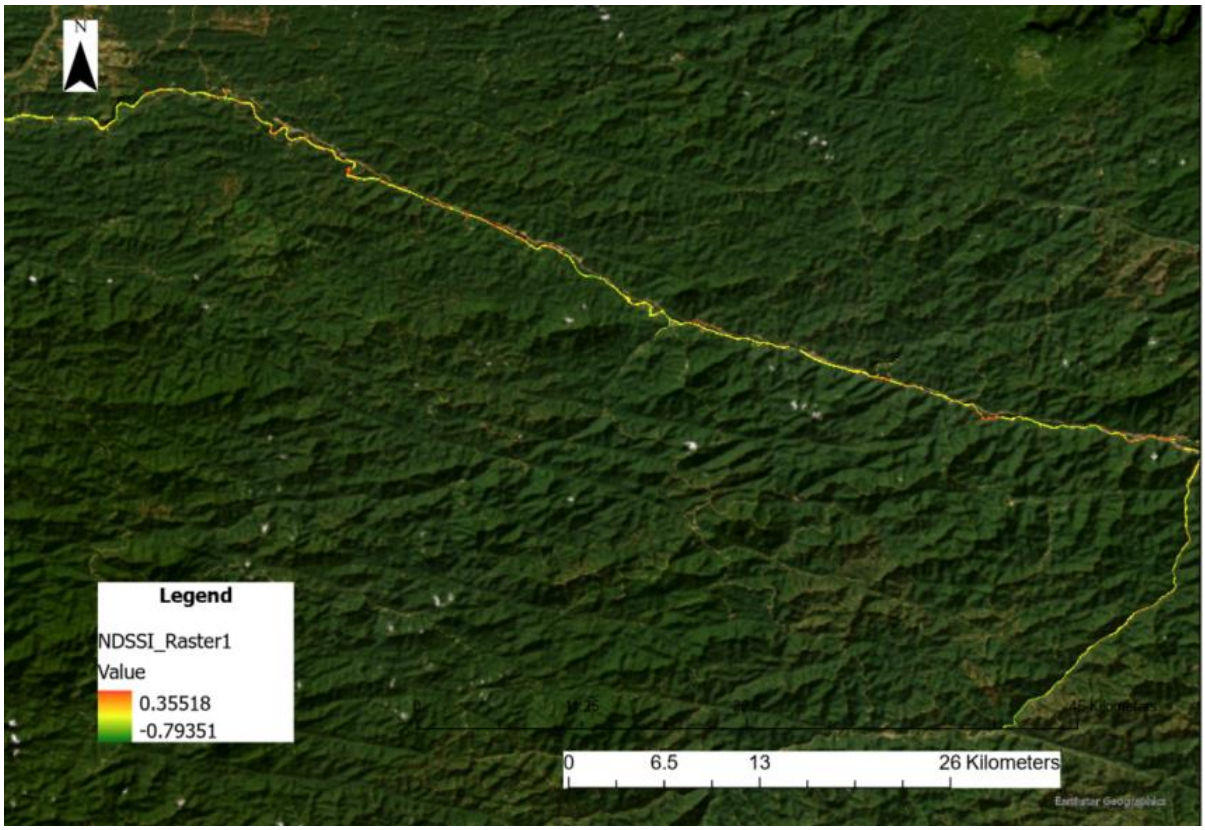

Figure 3-10: NDSSI Imagery for Baleh River on December 2020, representing high flow.

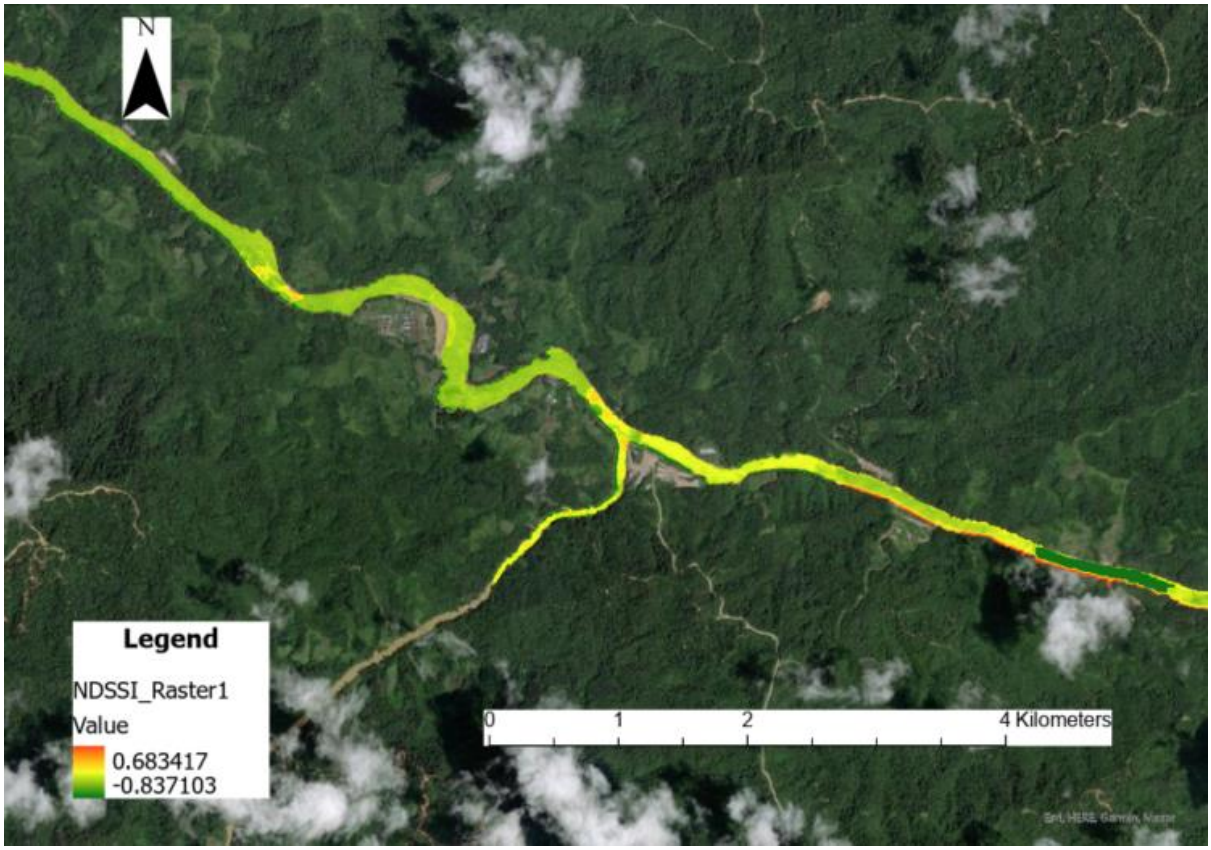

Figure 3-11: Magnified NDSSI Imagery of Baleh River on July 2021 (low flow)

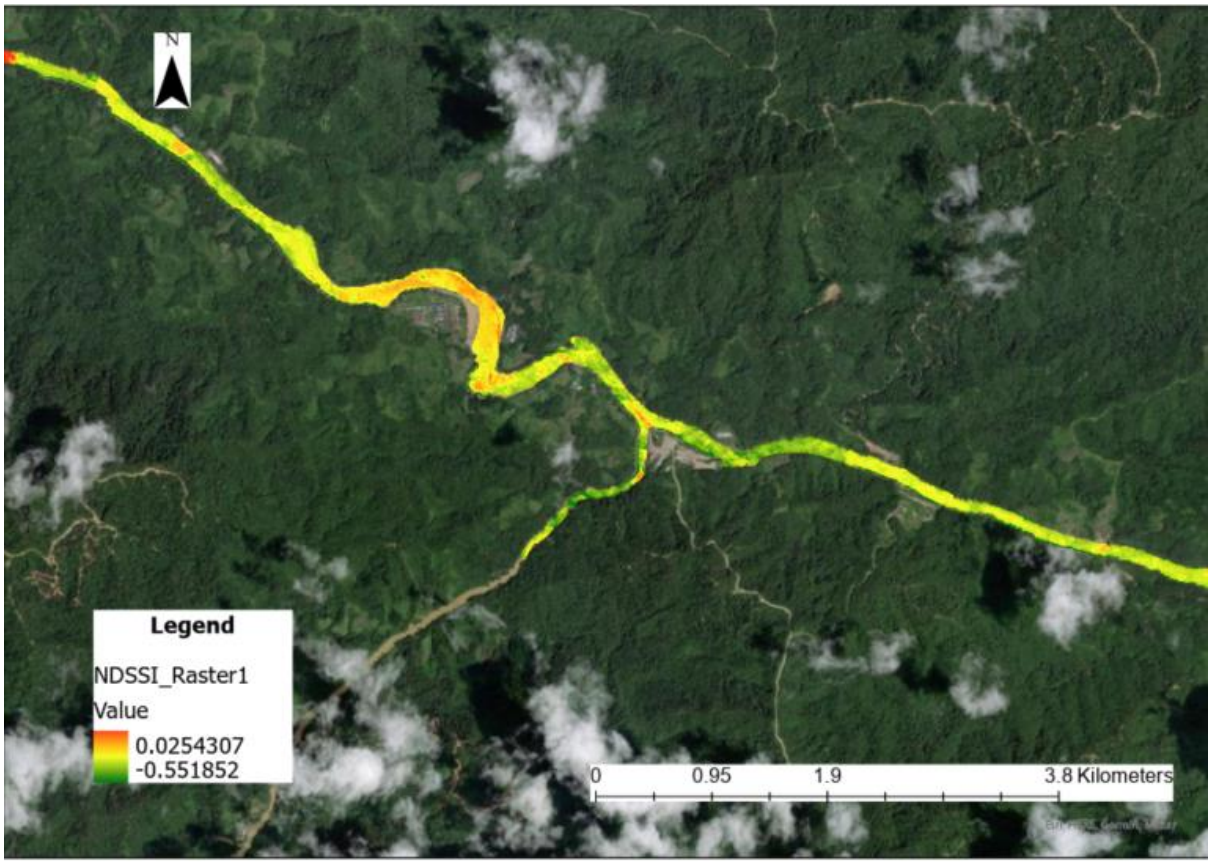

Figure 3-12: Magnified NDSSI Imagery of Baleh River on September 2022 (average flow).

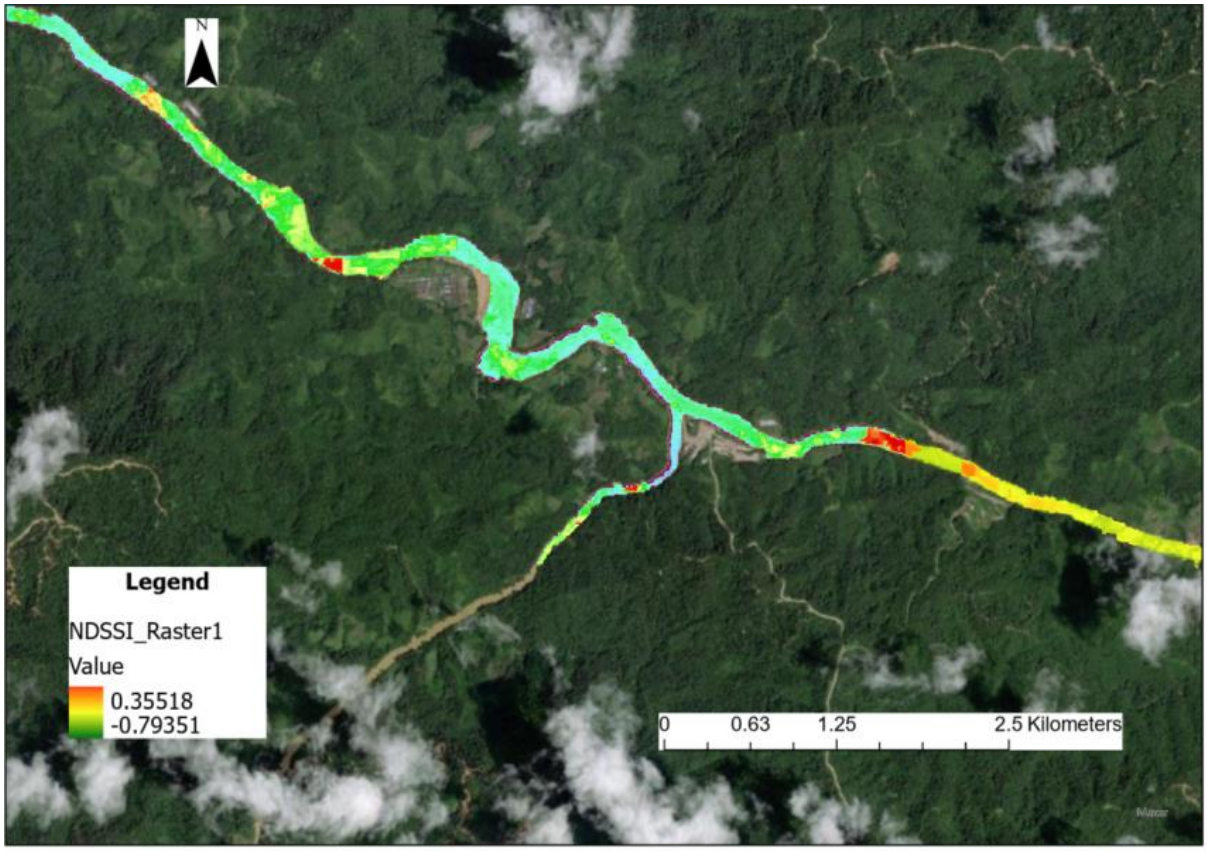

Figure 3-13: Magnified NDSSI Imagery of Baleh River on December 2020 (high flow).

The NDSSI values were correlated with near real-time in-situ SSC measurement, to provide a quantitative estimation of the SSC at Baleh River using a calibration data set. In-situ measurement of SSCs were collected at various sampling points along Baleh River, at the confluence of Merirai and Putai on 16th and 17th September 2022. The location of these SSC sampling points is obtained from a handheld GPS as described in Section 3.2.3.1, with their locations illustrated on Figures 3-14 and 3-15. The SSC samples were processed in the lab as detailed in Section 3.2.3.1.

These in-situ measurements (a total of 80 samples) were correlated with the respective NDSSI values of the same coordinate, with Sentinel imagery acquired on 16th September 2022. The best relationship between NDSSI and the SSC measurements was a polynomial equation with an order of 2 (Figure 3-16) and this equation was used to convert NDSSI values to SSC. There is clearly an appreciable error around this modelled fit, which is discussed later.

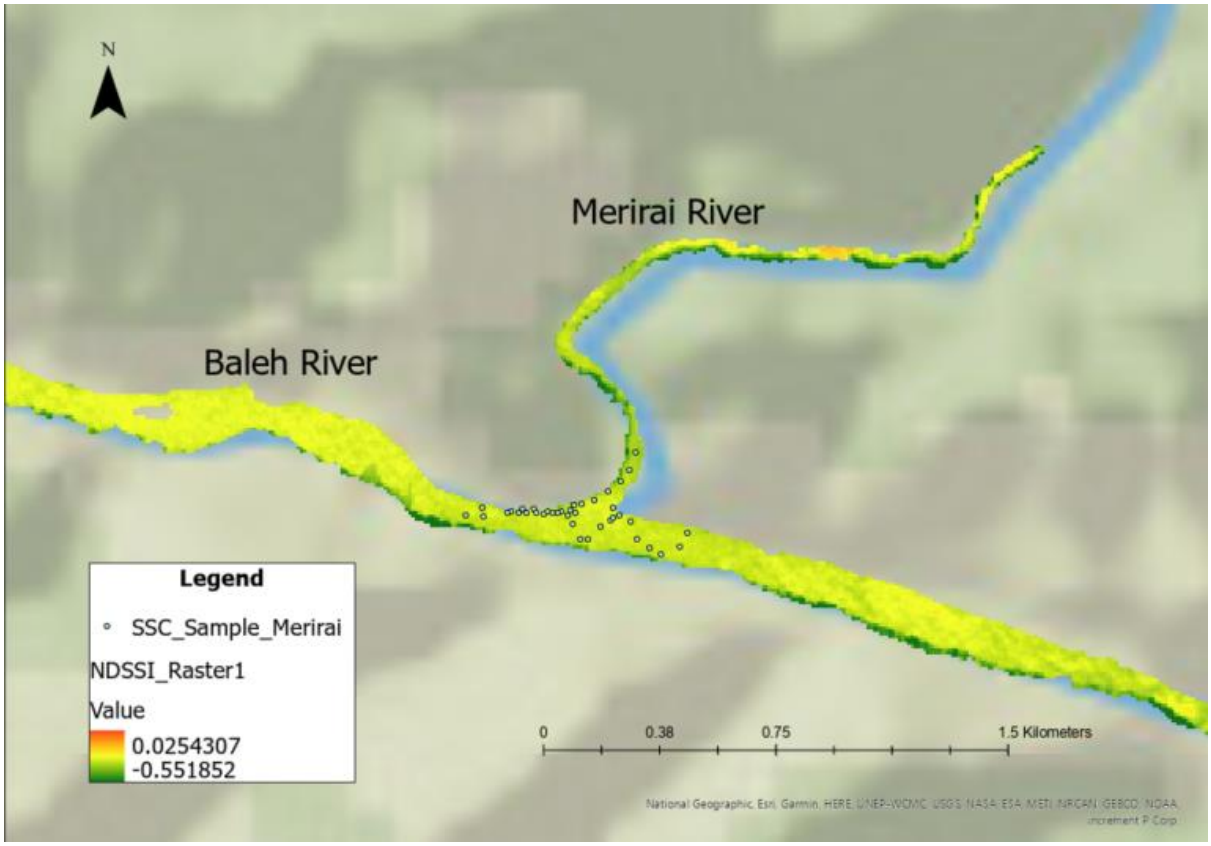

Figure 3-14: Location of SSC sampling points at Merirai confluence with the NDSSI map

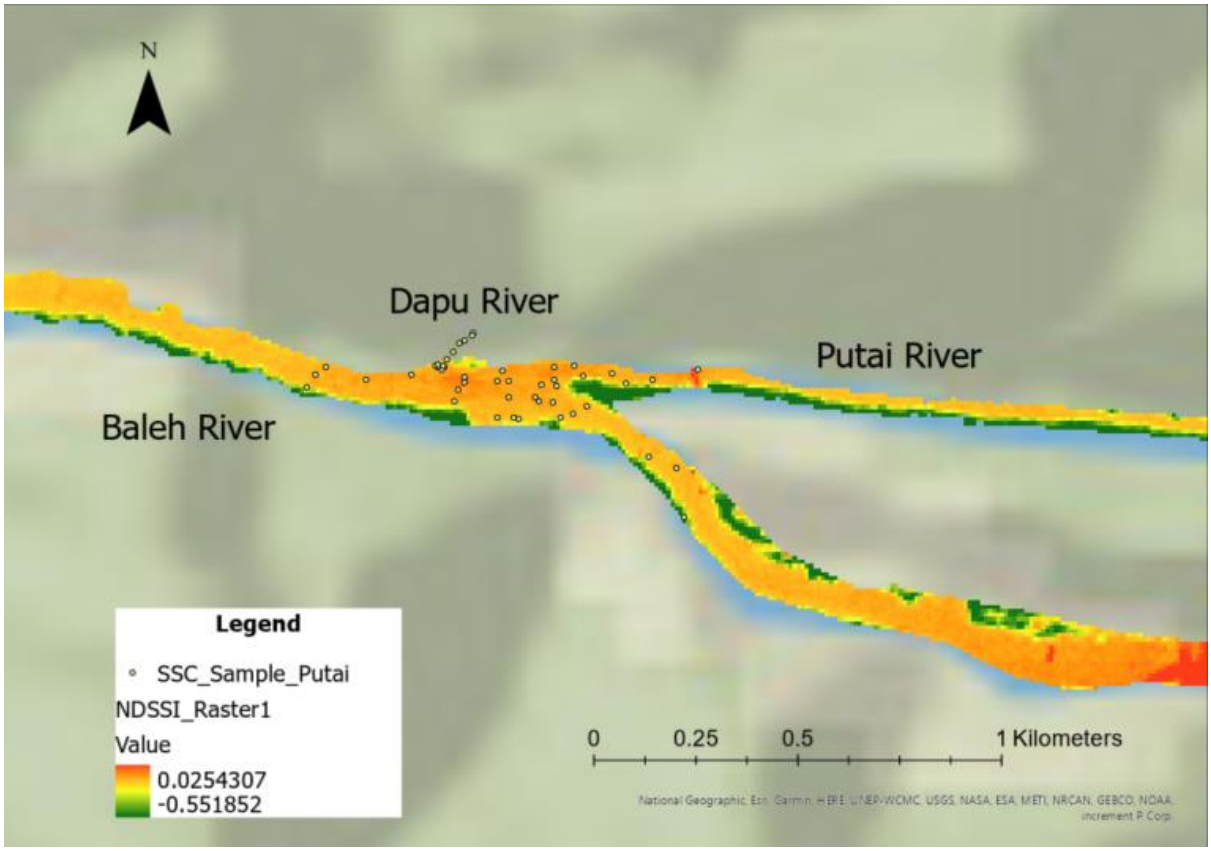

Figure 3-15:Location of SSC sampling points at Putai confluence with the NDSSI map

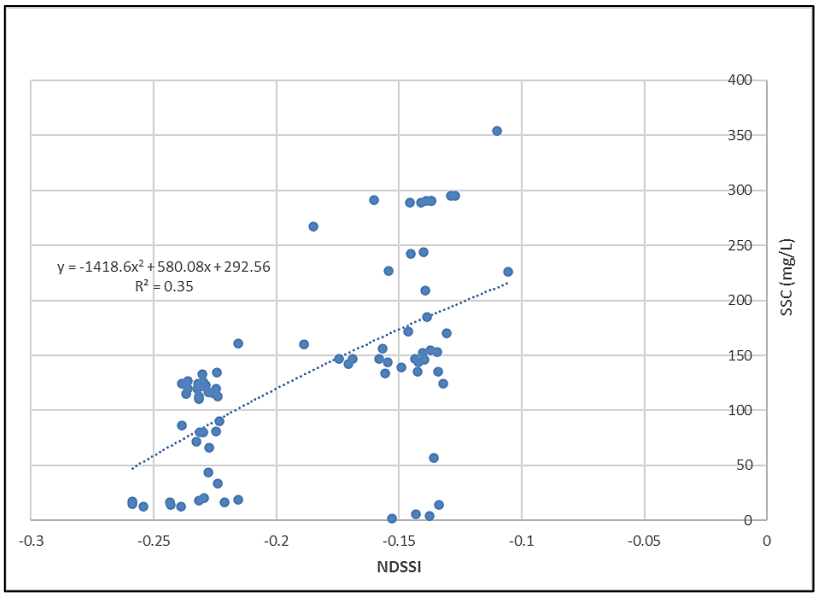

Figure 3-16: Polynomial equation between NDSSI and in-situ measurement of SSC at Baleh on 16th September 2022

$$SSC = -1418.6(NDSSI)^2 + 580.08(NDSSI) + 292.56 \qquad \textit{(Equation 3-7)}$$

3.2.3. Remote Sensing at Reach Scale Using Drone Images

This part of the work involved obtaining images from drones of selected locations, from which SSC was estimated. To calibrate and validate these estimates, field samples were collected from points with known coordinates. These two steps are detailed below.

3.2.3.1. SSC Measurement

The study sites at river reach level are the Putai and Merirai tributary confluences; both are downstream of the dam site. Figure 3-1 show the locality of both tributaries.

To obtain the SSC data for these two sites, a total of 80 water samples were collected (Figures 3-17 and 3-18). The samples were collected at locations that include the upstream of the confluence, mixing zone, and downstream of the confluence. This was done to capture the full range of different SSC values present across the reaches.

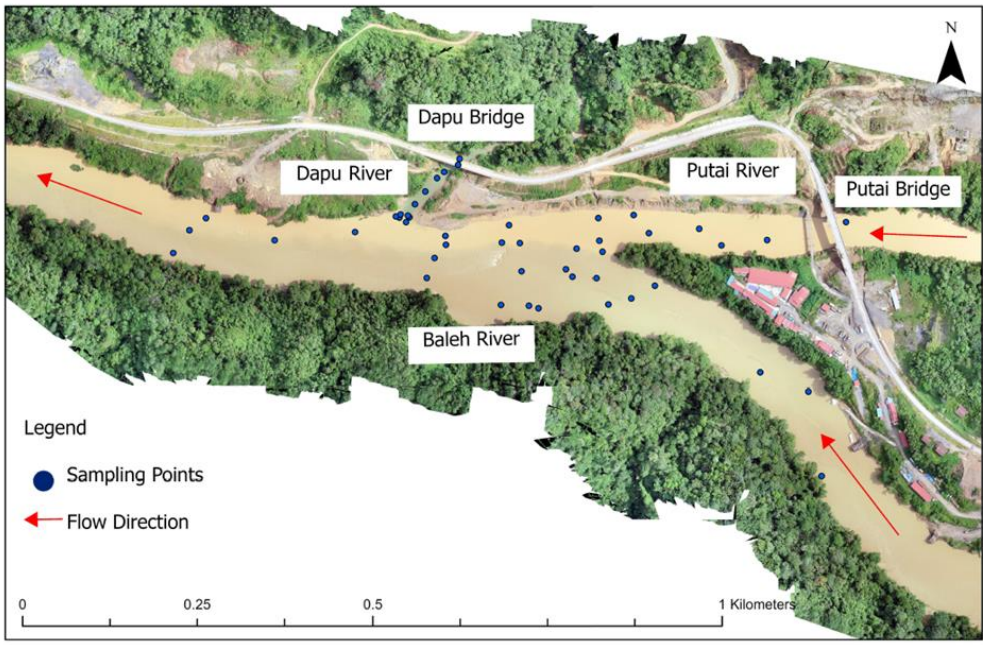

Figure 3-17: The study site of Putai-Baleh confluence where the blue circles indicate the water sampling points.

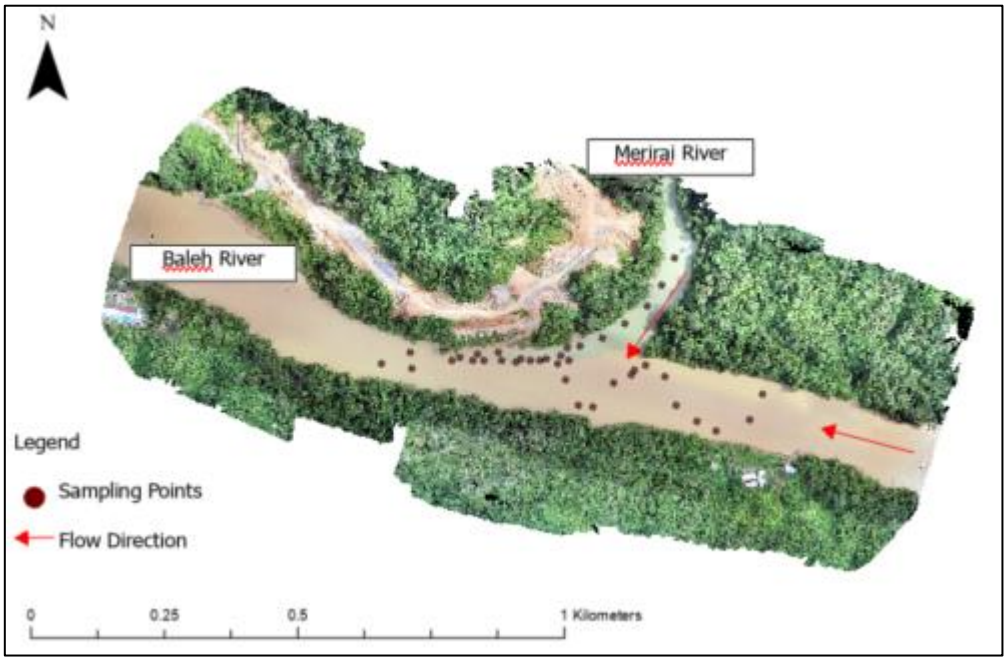

Figure 3-18: The study site of Merirai-Baleh confluence with red circles indicating the water sampling points.

The water samples were locally coordinated using a handheld GPS, Garmin GPS Map 66S with an accuracy of ± 3m. Prior to obtaining the water samples, the handheld GPS was calibrated with a known elevation at Baleh HEP site to validate its reading. Then, 500ml of river water

was collected from each sampling point at both Putai and Merirai confluences. At Putai confluence, the sampling was conducted on 16th September 2022 from 10:00 – 10:30 am where 47 samples were obtained. At Merirai confluence, the sampling was conducted on 17th September 2022 from 10:30 – 11:00 am where another 39 samples were obtained.

SSC values of samples were determined using a vacuum filtration apparatus following the standard protocol APHA 2540 (American Public Health Association, 2012). For this, glass microfiber filters with pore size of 1.5 microns were used. As a preparation step of the filter membrane, each filter membrane was washed with 300ml of purified water and vacuum apparatus used to remove all traces of water. The filter membrane was then dried in the oven at 105 degrees Celsius for 12 hours. Then, the filter membrane was cooled in a desiccator for 30 minutes and after that, the filter membrane was weighed. The drying, cooling and weighing process was repeated until a constant weight is obtained or when the weight change was less than 4% of the previous weighing.

Once the preparation of the filter membrane was complete, 500ml of water sample was filtered through the filter membrane and oven dried at 105 degrees Celsius for 12 hours. The oven-dried filter membranes were then cooled in the desiccator for 30 minutes. After cooling, the oven-dried filter membranes were then weighed. The differences in weight of the oven-dried filter membranes, before and after filtration were divided by the volume of water sample to derive the SSC in mg/L. Out of the 80 samples, 45 samples were used to derive a calibration relationship, while the remaining 35 samples were used to validate the calibration model.

3.2.3.2. Drone Image Acquisition

At Putai confluence, four Ground control Points (GCPs) were positioned at both Putai and Dapu bridge respectively. They were locally coordinated using Garmin GPS Map 66S. A DJI Phantom 4 Pro drone with a built-in Real-Time Kinematics (RTK) was deployed to collect the images of the confluence and flown at a height of 120 metres. The drone flight took place from 9.15AM – 10.00AM on 16th September 2022. Immediately afterwards, water samples were collected.

As for Merirai confluence, three GCPs were positioned at the right bank of the main stem and the confluence. They were also locally coordinated using Garmin GPS Map 66S. Similar with

the drone mission at Putai confluence, the same drone was deployed and flown with the same height of 120 metres. The drone flight at Merirai confluence took place on 17th September 2022 from 9.45AM – 10.30AM. This is followed immediately by the collection of water samples.

For both sites, the drone images were taken first, immediately prior to collecting the water samples to avoid specular water reflection (sun glint) on the images which increased as the days warmed up and clouds dissipated. Doing this ensured two things; the images captured have no sun glint, and the images captured will not have any major temporal hydro morphological change from the time the water samples were collected. Fortunately, on both days of the drone flights there was no major difference in the observed river flow during the flight and collection of water samples.

The drone camera has a 12.4 megapixels CMOS sensor with a sensor size of 6.2 x 4.6mm (1/2.3”). 771 and 631 images were collected from Putai and Merirai confluence respectively. The white balance of the camera was pre-set to ‘sunny’ which was adjusted according to the physical white balance card to ensure that the Digital Number (DN) values can be retrieved from the white and black ages. The camera settings were ISO 200, shutter speed 1/800 second and aperture of F7.1.

The drone images captured on 16th and 17th September 2022, of Putai and Merirai, were employed to calibrate the Red, Green and Blue (RGB) Digital Numbers (DN) with the measured SSC at both sites. In addition to these initial images, additional drone imageries of the same sites were acquired to discern the spatial patterns of SSC under varying flow conditions at these confluences. No additional SSC samples were taken during these additional drone flight missions. Following Baleh’s historical seasonal flow pattern as per Chong et al. (2021), the acquisition dates of the drone images and its respective flow conditions are as follows;

- 11th and 12th March 2022, represent the wet condition,
- 16th and 17th July 2023, represent the dry flow condition and,
- 16th and 17th September 2022 (initial images), represent the average or normal flow conditions.

3.2.3.3. Production of Orthomosaics

The drone images were processed and stitched using the Pix4DMapper Version 4.8.0 (Pix4D) to produce a continuous orthomosaic for each site. Image analysis for the Red, Green and Blue (RGB) colour channel was conducted in ArcGIS Pro Version 3.0.3. At each of the water sampling points, an area of $1m^2$ was plotted using the 'Buffer' tool. The average DN value for each sampling point was calculated using the 'Summarize Within' tool. For the orthomosaic, each pixel has a resolution of $0.0016m^2$, thus $1m^2$ occupies 625 pixels.

3.2.3.4. Calibration and validation of the Relationship between DN Values and SSC

The in-situ measurements of SSC from each sampling points were related with the respective digital numbers in the Red, Green and Blue band from the drone images to obtain a predictive equation. When fitting the trend line, polynomial equation with an order of 2 gave the strongest R^2 value in each colour band. In general, for all the colour bands, the trend line shows a positive relationship, whereby the Digital Number increases with the SSC. Among the three colour bands, the Red band has the strongest R^2 value of 0.7994 (Figure 3-19). This is then followed by the Green and Blue band with R^2 value of 0.6117 and 0.1985 respectively. Given that the Red band has the best R^2 value, its equation as described in Equation 3-8, was applied to all pixel Red band values to produce the SSC maps.

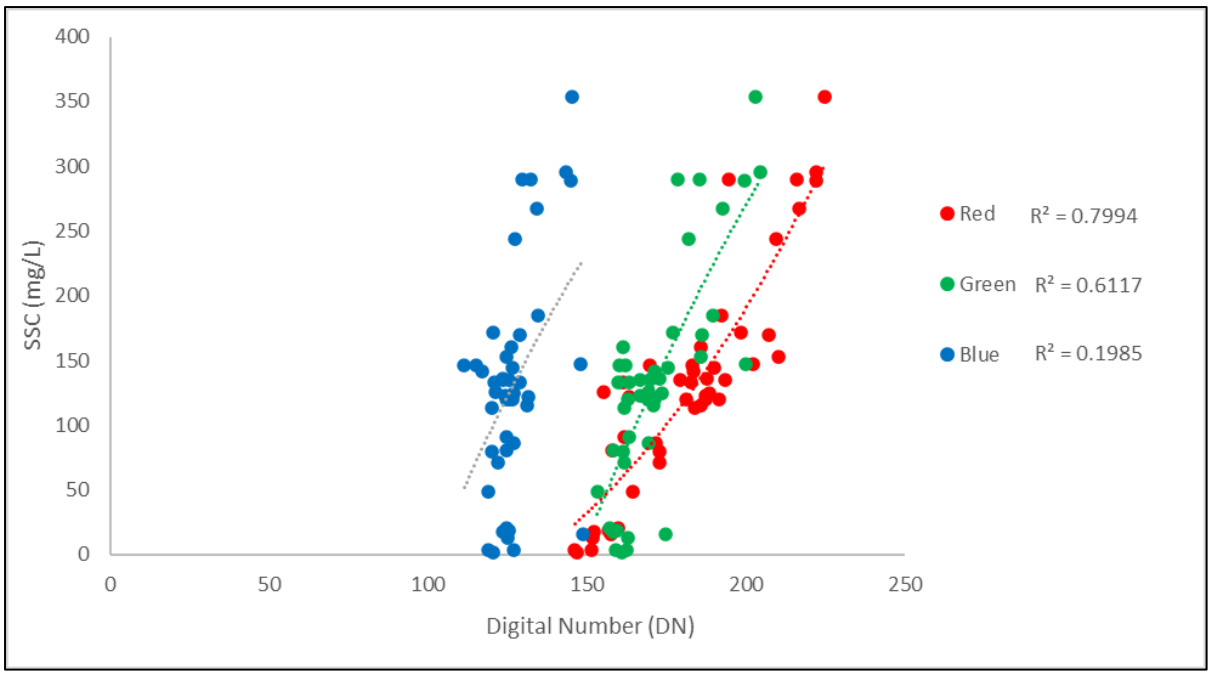

Figure 3-19: Calibration of SSC and DN values of each colour band

$$SSC = 0.0178(DN_{Red})^2 - 3.0723(DN_{Red}) + 92.756 \qquad \textit{(Equation 3-8)}$$

4. Results

4.1. Temporal patterns

Following the methods set out in Section 3.2.1., the discharge and suspended sediment concentration time-series for the period of February – December 2022 at Rh. Bawai A are presented in Figure 4-1. As tabulated in Table 4-1, the highest discharge was 3,412m^3/s in February, while the lowest discharge was 570m^3/s in July. Mean discharge for the period was 1,597$m^{3/}$s. There was little evidence of seasonality in flow – Feb and March had high flows, but these dropped over the period April to July, and were somewhat higher again between August and end of November.

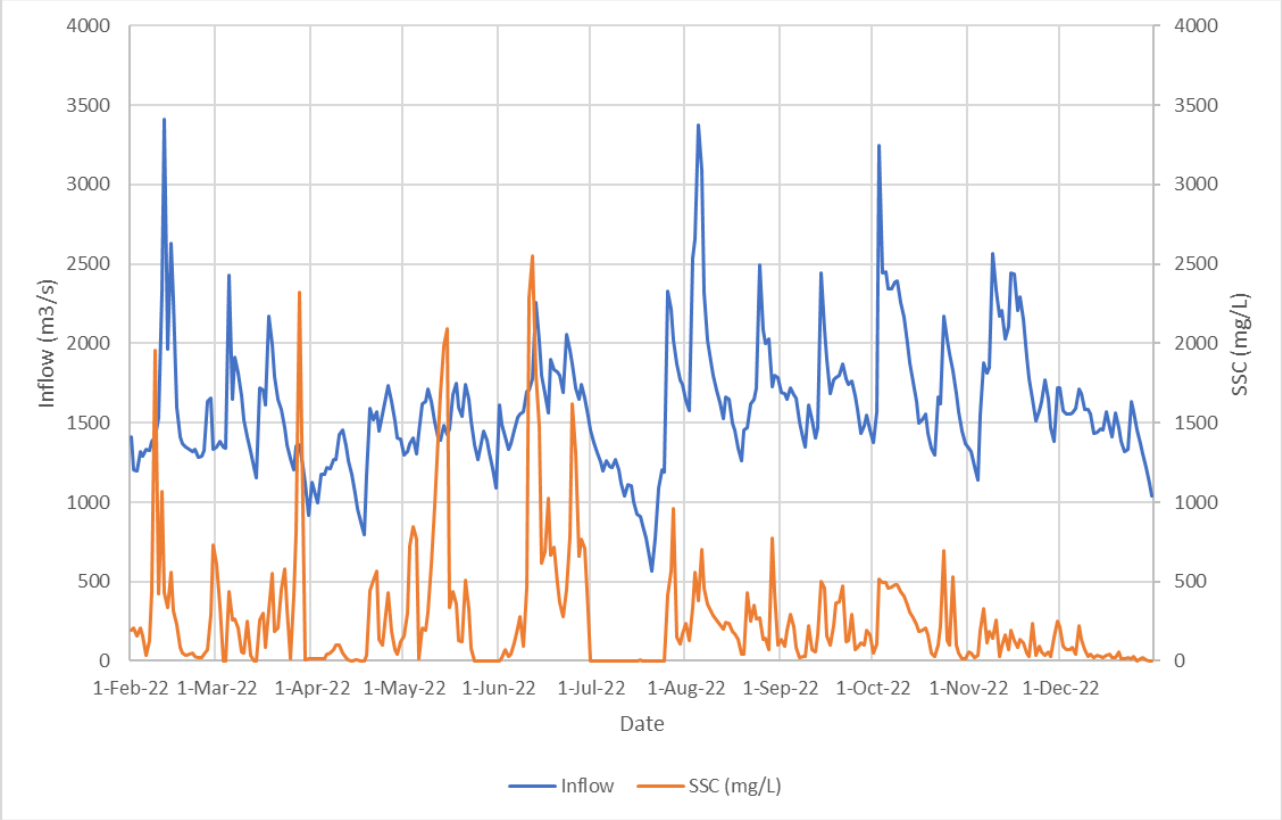

Figure 4-1: SSC and Inflow Time-Series

The total runoff for the study period was 46,070 million cubic metres (Mm^3) with a total suspended sediment load of 13,364,062 tonnes. Figure 4-2 shows the monthly distribution of water and suspended sediment yield at Baleh River, along with the corresponding mean

discharges and mean suspended sediment concentration for each month as presented in Table 4-1.

The zero and near-zero values of SSC observed in Figure 4-1 are due to the sensor being exposed to air when there are low river flows. These values (between 0 – 1mg/L) have been removed from the calculation daily and mean monthly SSC. It is also excluded from the minimum SSC as it is not the true value. Consequently, the estimate of total suspended sediment loads during periods where there are zero values would be underestimated of the true loads, and this is especially for end of May and most of July.

Table 4-1: Monthly discharge and suspended sediment data for the study period in Baleh River

Month	Q_{max} (m^3/s)	Q_{mean} (m^3/s)	Q_{min} (m^3/s)	Total Runoff (m^3)	SSC_{max} (mg/L)	SSC_{mean} (mg/L)	SSC_{min} (mg/L)	Total load (Ton)
February	3,413	1,580	1,199	3,823,004,683	1,960	285	10	1,268,073
March	2,426	1,516	919	4,061,731,198	2,321	409	8	1,364,389
April	1,731	1,301	797	3,372,343,101	569	135	6	458,338
May	1,751	1,461	1,087	3,912,683,141	2,094	655	4	1,858,327
June	2,254	1,702	1,335	4,410,903,211	2,553	674	5	3,270,403
July	2,332	1,259	570	3,372,568,194	962	459	1	428,226
August	3,376	1,886	1,261	5,052,577,660	776	279	12	1,540,555
September	2,441	1,671	1,350	4,330,955,576	502	186	11	860,243
October	3,243	1,877	1,294	5,026,413,959	696	181	4	1,535,900
November	2,565	1,836	1,141	4,760,007,919	332	112	10	571,141
December	1,718	1,474	1,036	3,946,825,805	222	54	1	208,466
Whole Period	3,413	1,597	570	46,070,014,447	2,553	312	1	13,364,062

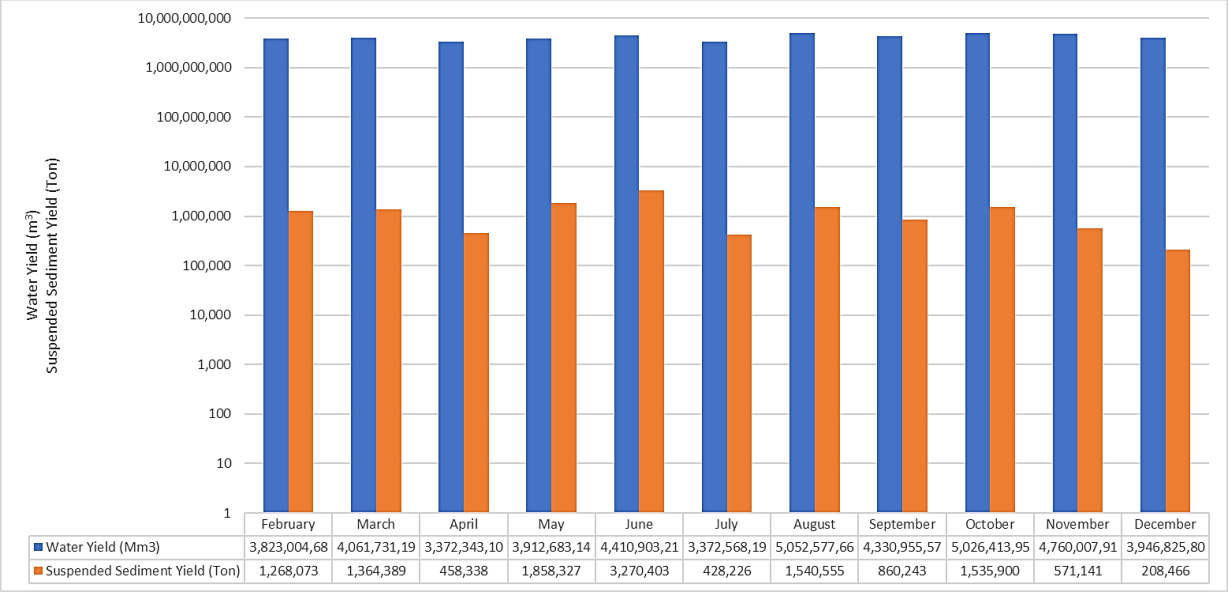

	February	March	April	May	June	July	August	September	October	November	December
Water Yield (Mm3)	3,823,004,68	4,061,731,19	3,372,343,10	3,912,683,14	4,410,903,21	3,372,568,19	5,052,577,66	4,330,955,57	5,026,413,95	4,760,007,91	3,946,825,80
Suspended Sediment Yield (Ton)	1,268,073	1,364,389	458,338	1,858,327	3,270,403	428,226	1,540,555	860,243	1,535,900	571,141	208,466

Figure 4-2: Monthly distribution of water and suspended sediment yield

In this study period, the wet months are identified to be from August to November, while the dry months are found to be from April to July. The suspended sediment concentration and suspended sediment load duration curve for the respective wet and dry periods, and whole year is illustrated in Figures 4-3 and 4-4.

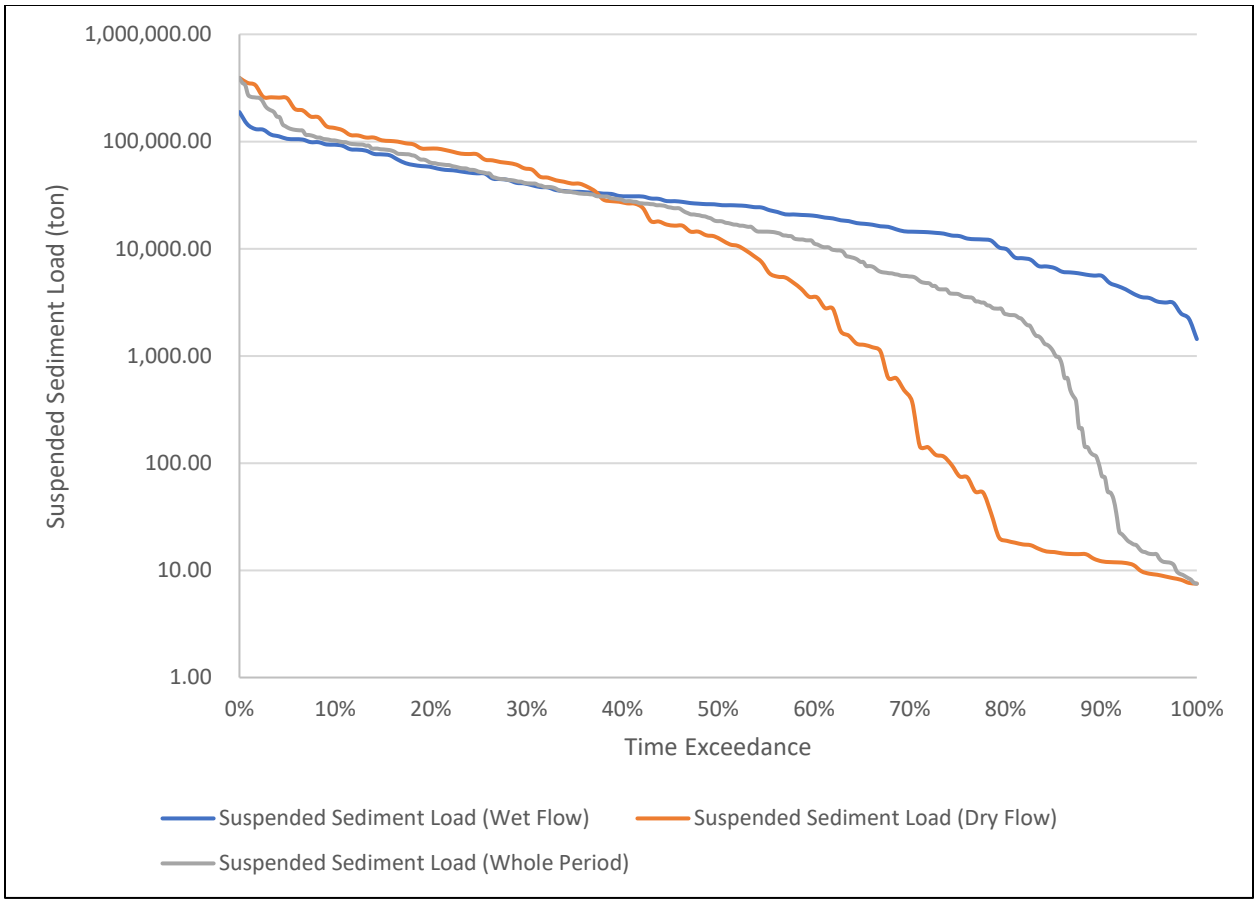

Figure 4-3: Suspended sediment load duration log curve for the respective entire period, wet period (August – November) and dry period (April – July)

Figure 4-3 shows duration statistics for suspended sediment loads based on daily load. Key percentile values are given in Table 4-2. It is clear that the major difference between the wet and dry periods occurs at the low load values / high time exceedance values (>40th percentile). For example, a daily suspended sediment load of 1,000 tonnes is exceeded for around 65% of the time in the dry period but 100 % of the time in the wetter period.

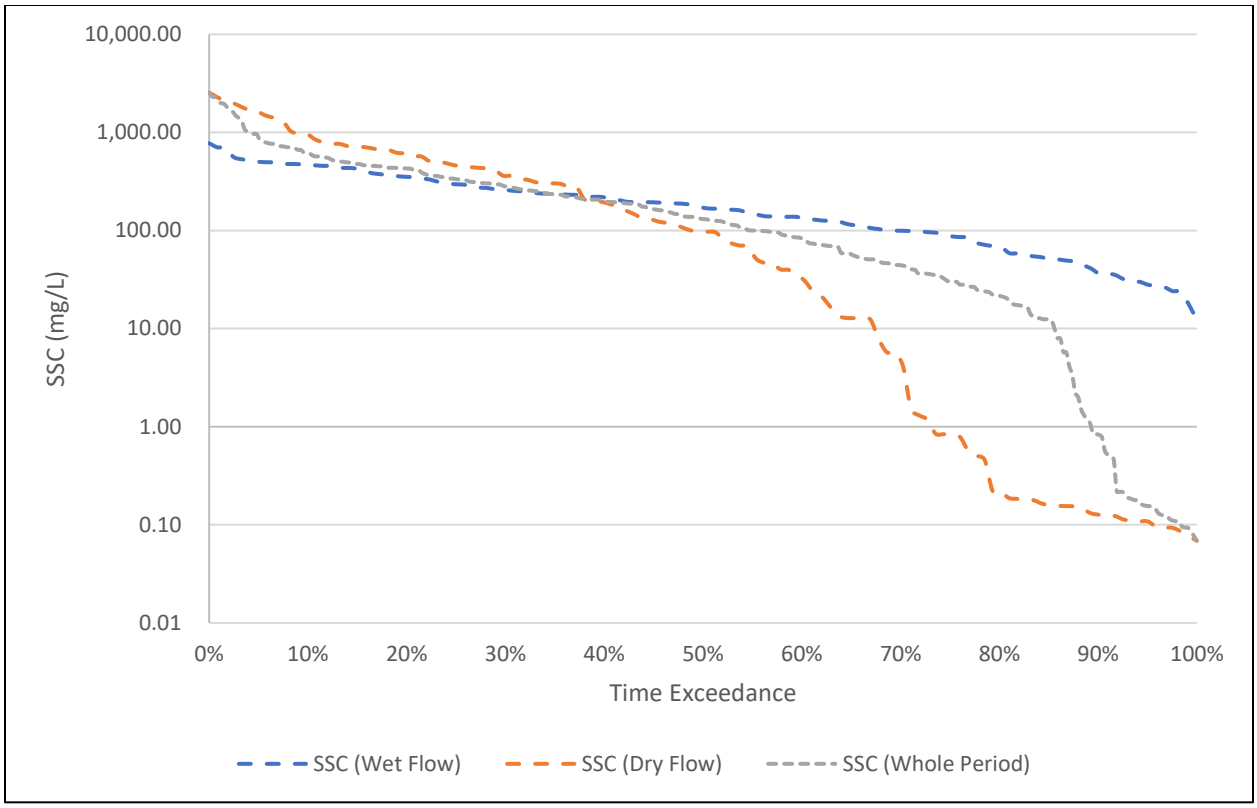

Figure 4-4: Suspended sediment load concentration log curve for the respective entire period, wet period (August – November) and dry period (April – July)

Figure 4-4 shows duration statistics for suspended sediment concentration based on daily data. The percentile values are shown in Table 4.2. Patterns are broadly similar to the load values, with the relative positions of the wet and dry period curves switching at an exceedance value of 40%. SSC of 700mg/L is exceeded for only 1% of the time in the wet season, but this concentration exceeded for 16% of the time in the dry period. Conversely, a concentration of 10mg/L is exceeded for around 70% of the time in the dry months, but 100% in the wet ones.

Table 4-2: Values of fine sediment loads and concentrations at various key percentile values

	10th percentile	50th percentile	90th percentile
Annual load curve (ton)	102,597.52	18,409.86	96.39
Dry Season load curve (ton)	133,889.72	13,068.04	12.13
Wet season load curve (ton)	93,468.33	25,967.04	5,579.90
Annual concentration curve (mg/L)	619.67	134.25	0.84
Dry season concentration curve (mg/L)	961.65	99.51	0.13
Wet season concentration curve (mg/L)	462.89	174.91	36.55

A Generalized Additive Model (GAM) model was fitted to determine the relationship between discharge and SSC. Using the mean daily discharge and mean daily SSC, the relationship is plotted in Figure 4.5. The plot shows that, as discharge increases, the SSC also increases. An inflection point is evident at approximately 2,000m^3/s, where the rate of increase in SSC is less pronounced compared to the discharge range between 1,500m^3/s to 2,000m^3/s.

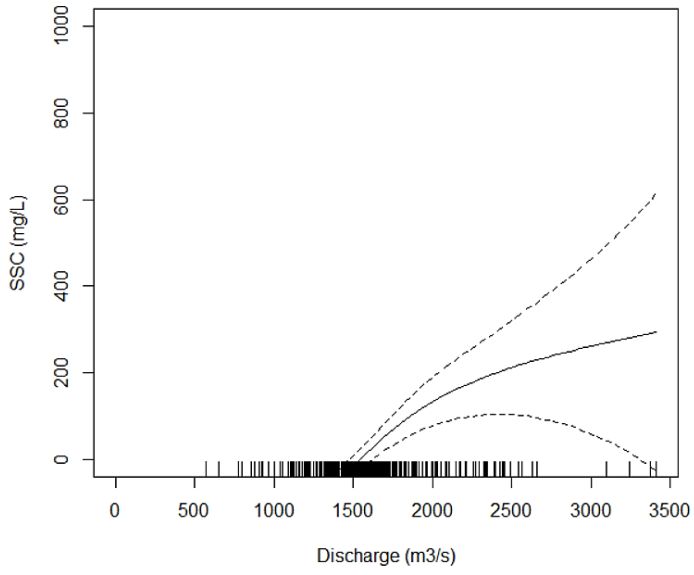

Figure 4-5: GAM analysis of Discharge vs SSC

4.2. Remote Sensing of SSC at River Scale (Satellite Image)

The SSC for Baleh River was computed using Equation 3-6, applied to the NDSSI values obtained from the satellite images; Figures 4-6, 4-8, and 4-10, show the SSC maps for the whole of the approximately 100km study section for July 2021, September 2022, and December 2020, representing days with dry, normal and wet flow conditions. Figures 4-7, 4-9, and 4-11 show selected subsections to illustrate more local patterns evident in the satellite image data. The resulting negative SSC values obtained from the satellite images (Figures 4-6 to 4-11) are from the conversion of NDSSI to SSC using Equation 3-6.

Following that, the longitudinal pattern of SSC along Baleh River was extracted from these remote sensing images; this is shown in Figure 4.12. For this plot, GAMs were fitted to smooth the longitudinal pattern. The unsmoothed data are shown in Figures 4-13, 4-14 and 4.15. The dotted vertical lines represent the locations of specific tributaries along the Baleh River, as well as the dam site.

It is clear that general longitudinal patterns depend on flow conditions. On the day with low flow ('dry' in Fig 4.12), there is a strong downstream increase, while no such overall trend is evident during the days with normal or high flows. On the low flow days, inputs from tributaries contribute sediment and increase SSC in the downstream direction, but on the other days, the patterns suggest that a combination of absolute lower sediment inputs and higher dilution mean that overall SSCs do not increase markedly downstream; indeed, at higher flows, concentrations drop at distances 20km to 60km.

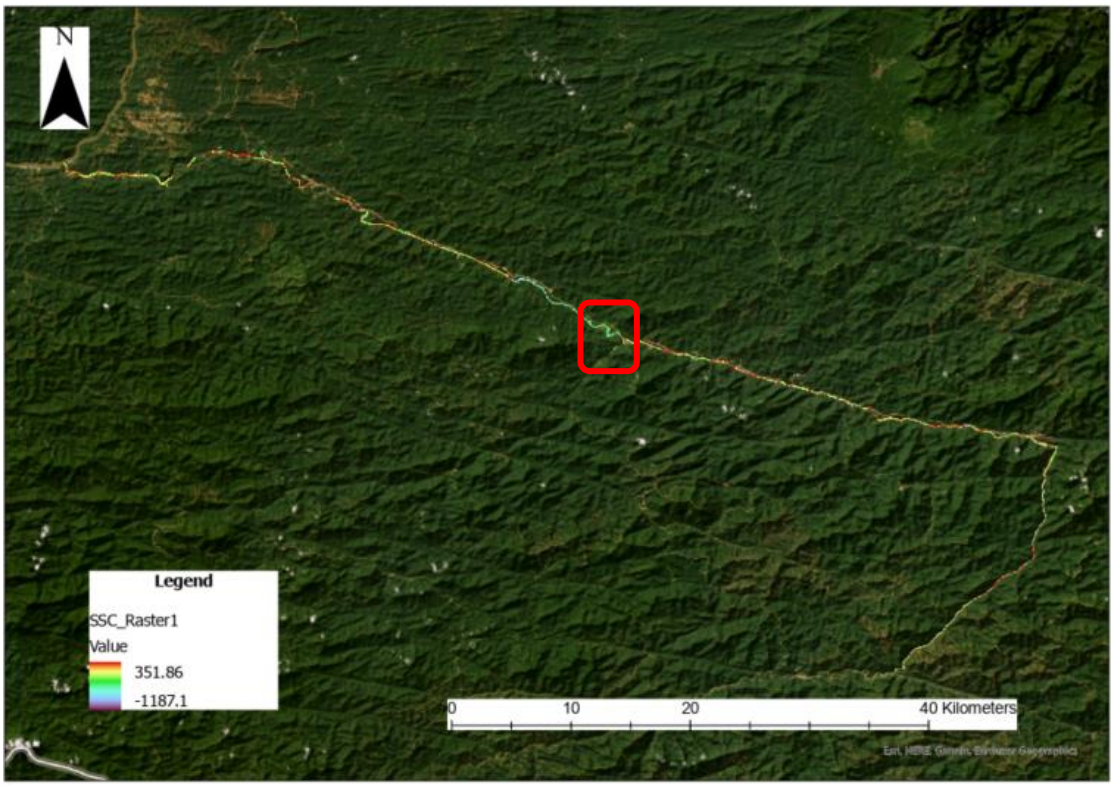

Figure 4-6: SSC map for Baleh River at dry flow. Red box indicates the blown-up area of Figure 4-7.

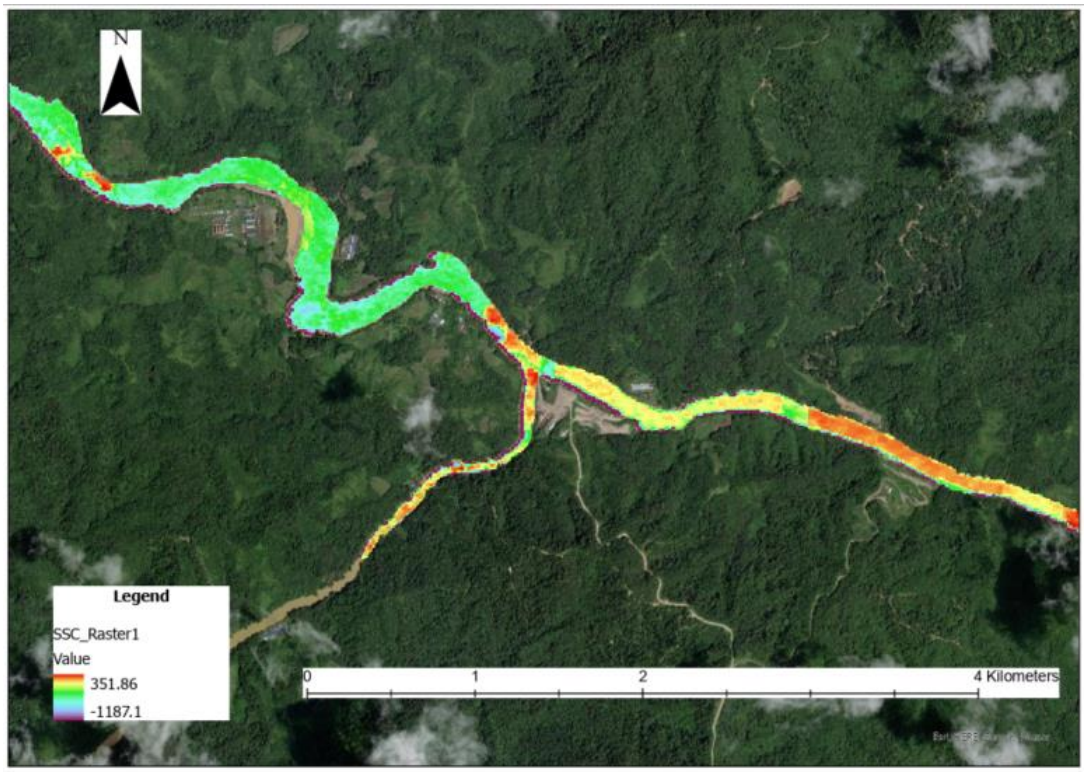

Figure 4-7: Magnified SSC map at dry flow

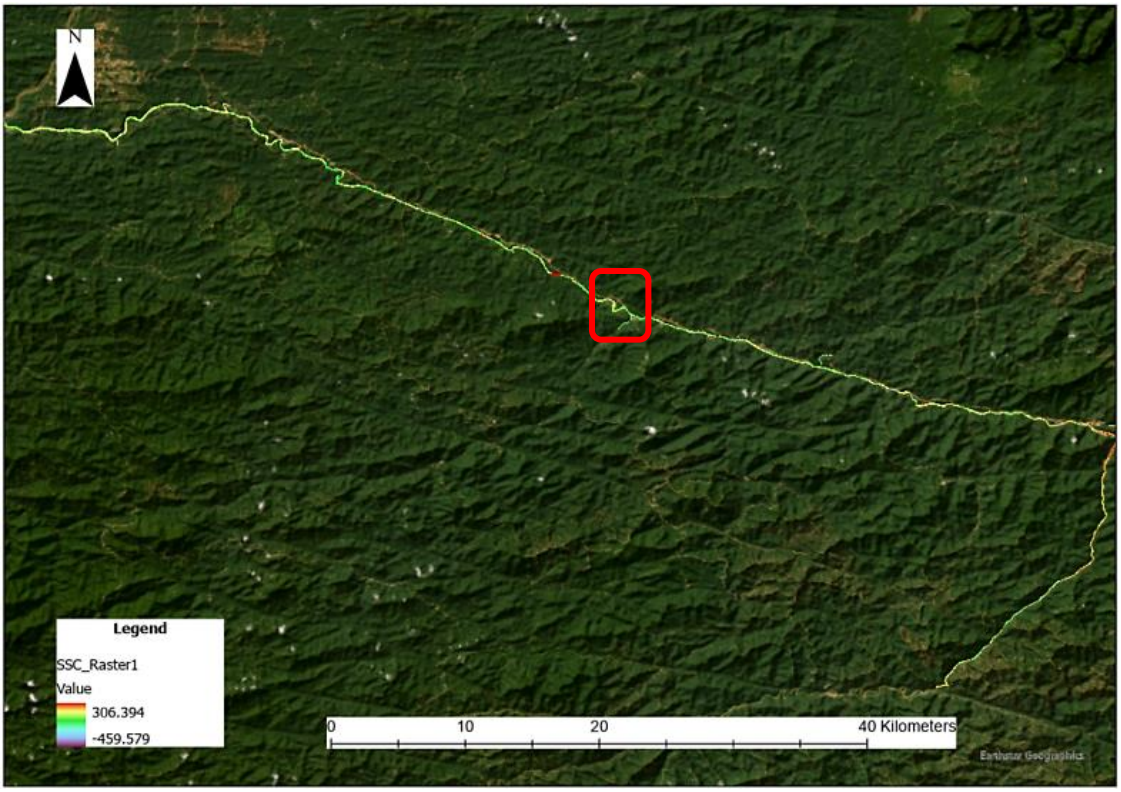

Figure 4-8: SSC map for Baleh River at normal flow. Red box indicates the blown-up area of Figure 4-9.

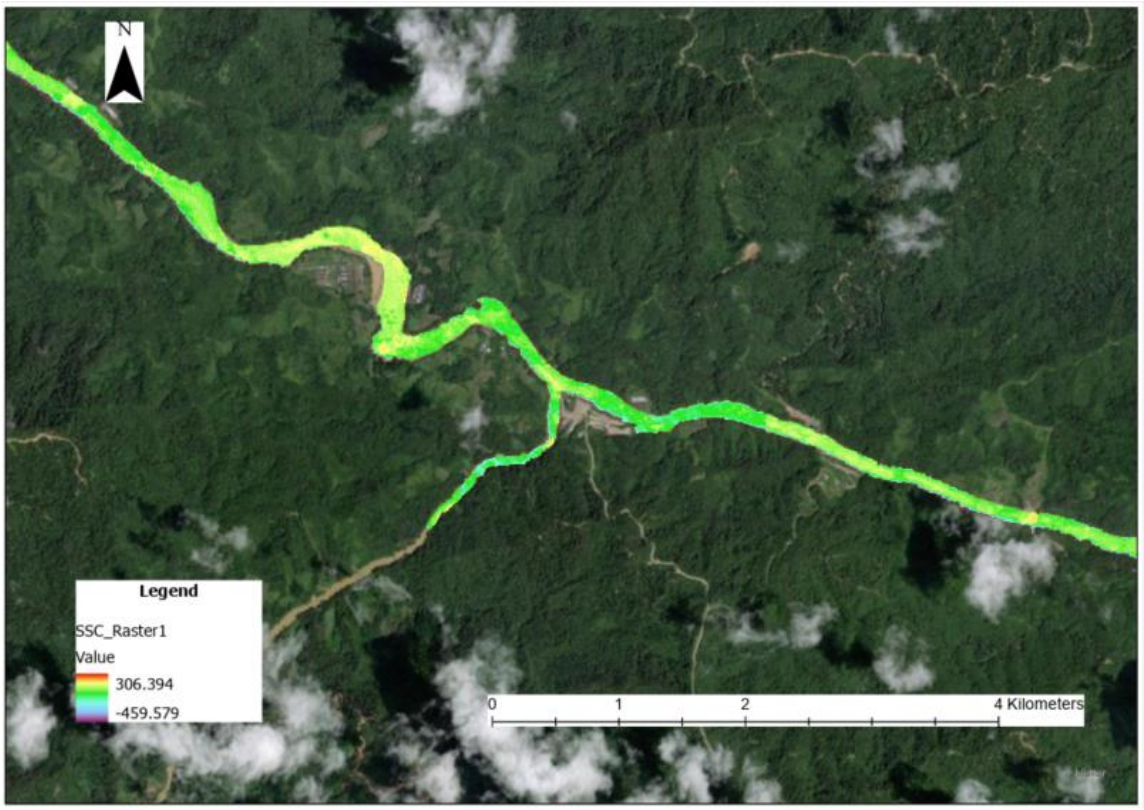

Figure 4-9: Magnified SSC map at normal flow

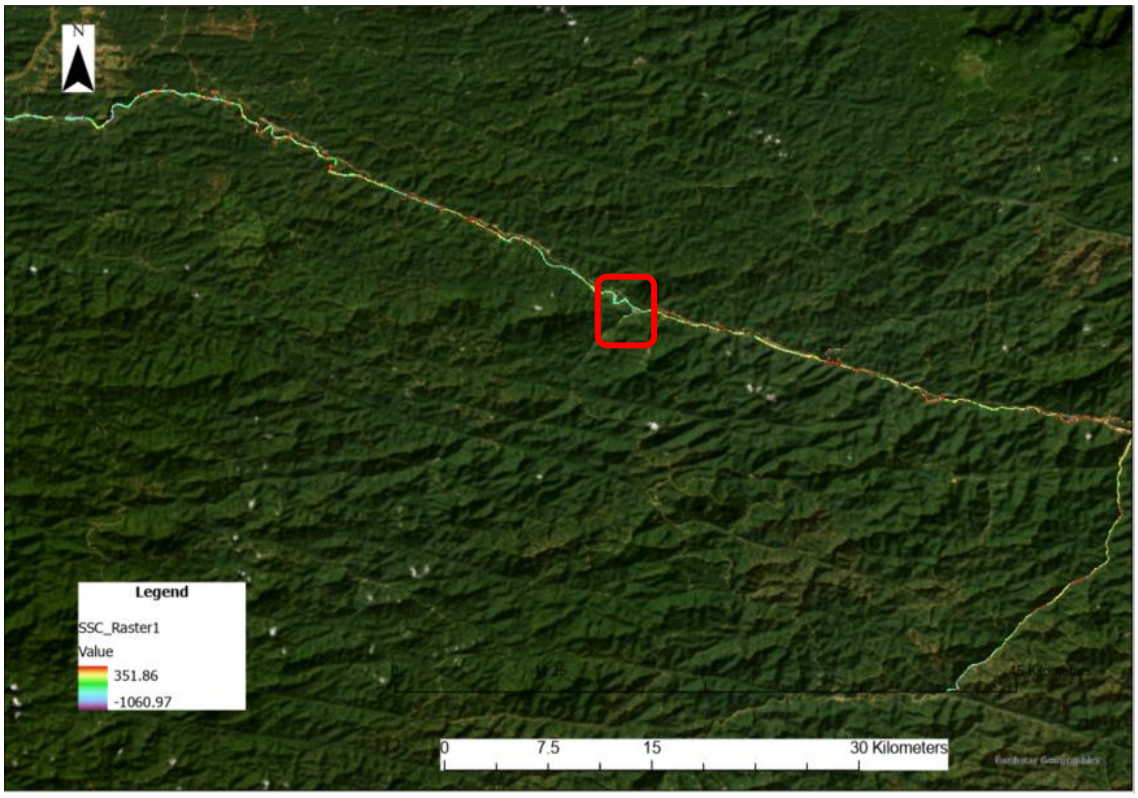

Figure 4-10: SSC map for Baleh River at wet flow. Red box indicates the blown-up area of Figure 4-11.

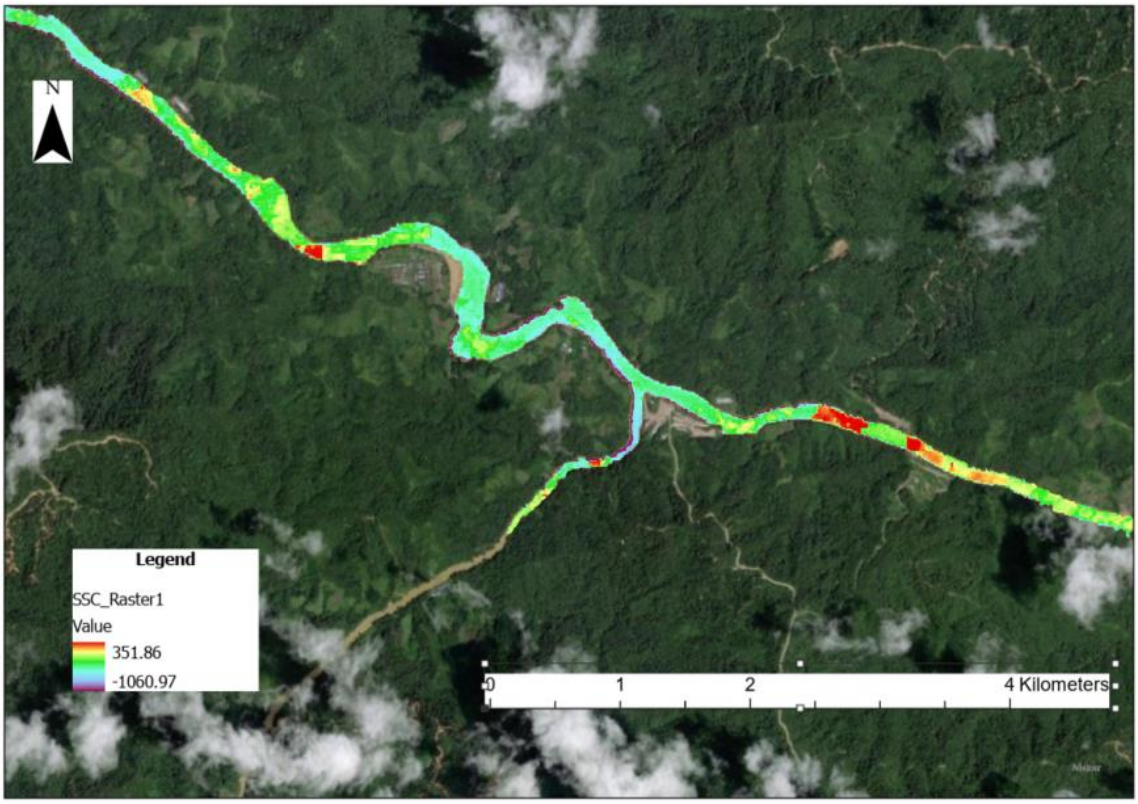

Figure 4-11: Magnified SSC map at wet flow

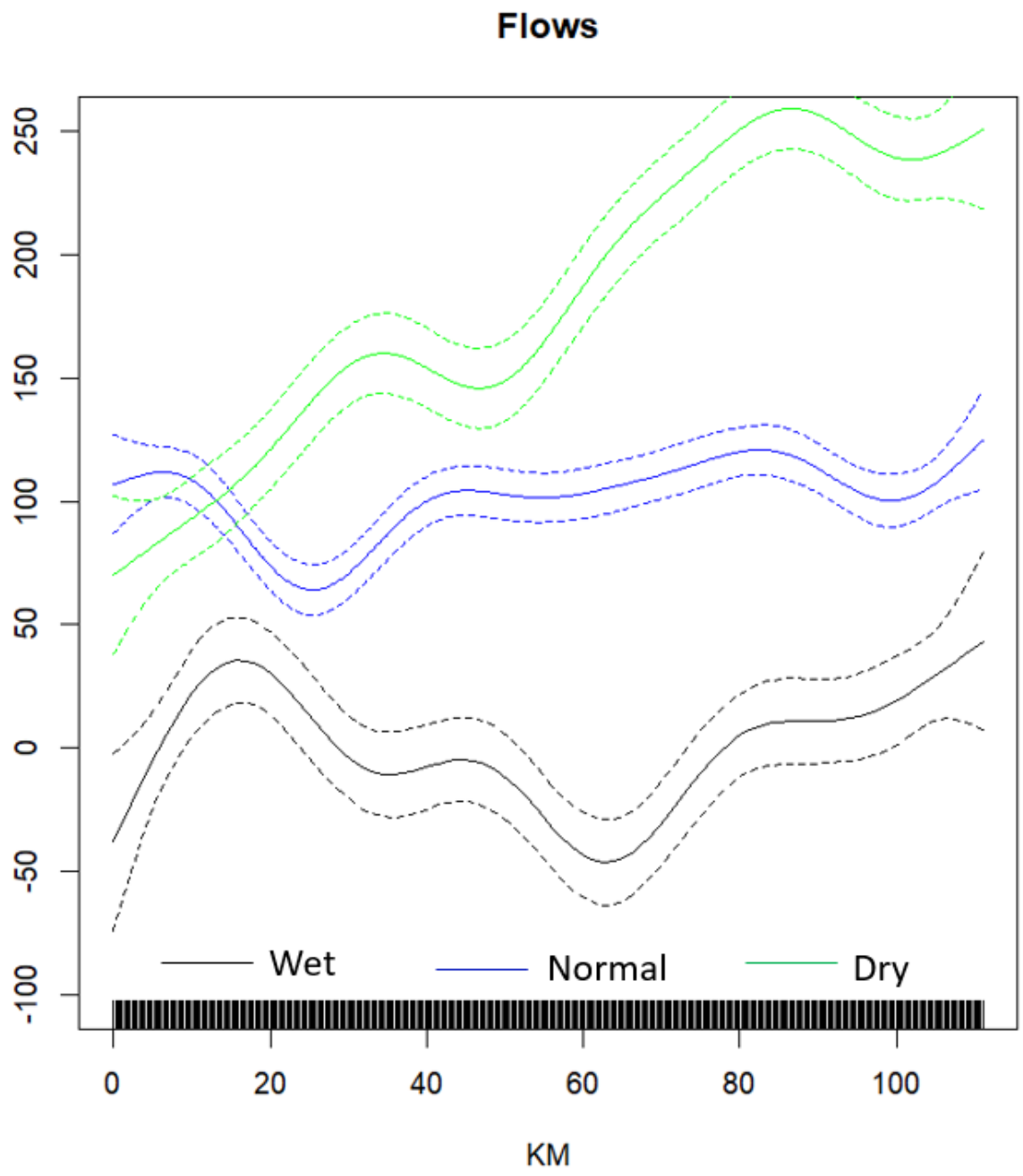

Figure 4-12: GAM analysis plot of the Baleh in wet, normal and dry conditions with 95% confidence intervals (0km starts at the upstream end of Baleh River, 22km upstream of Baleh Dam, and down towards the confluence with Rajang River)

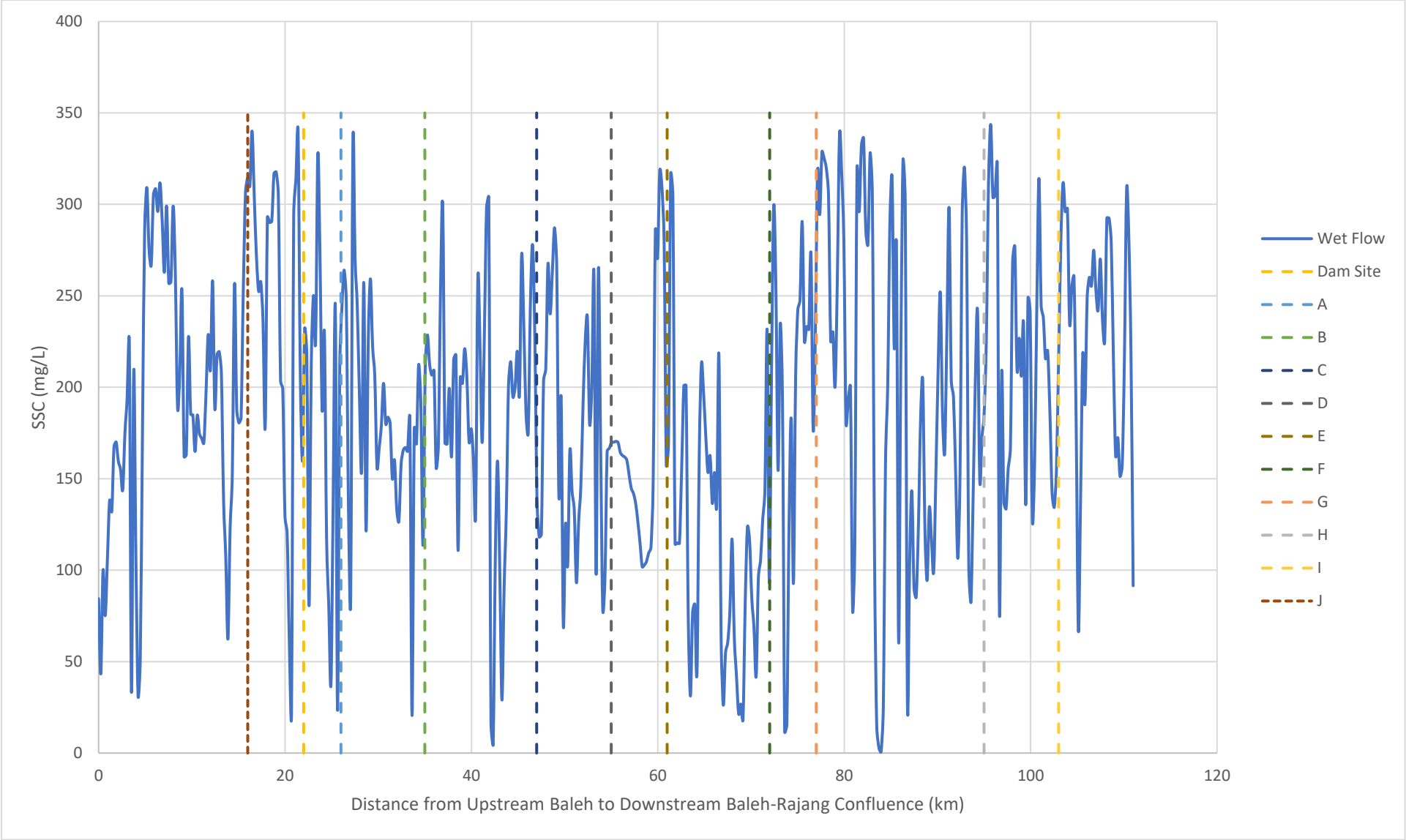

Figure 4-13: Longitudinal pattern of SSC along Baleh River from upstream to downstream for higher flow conditions

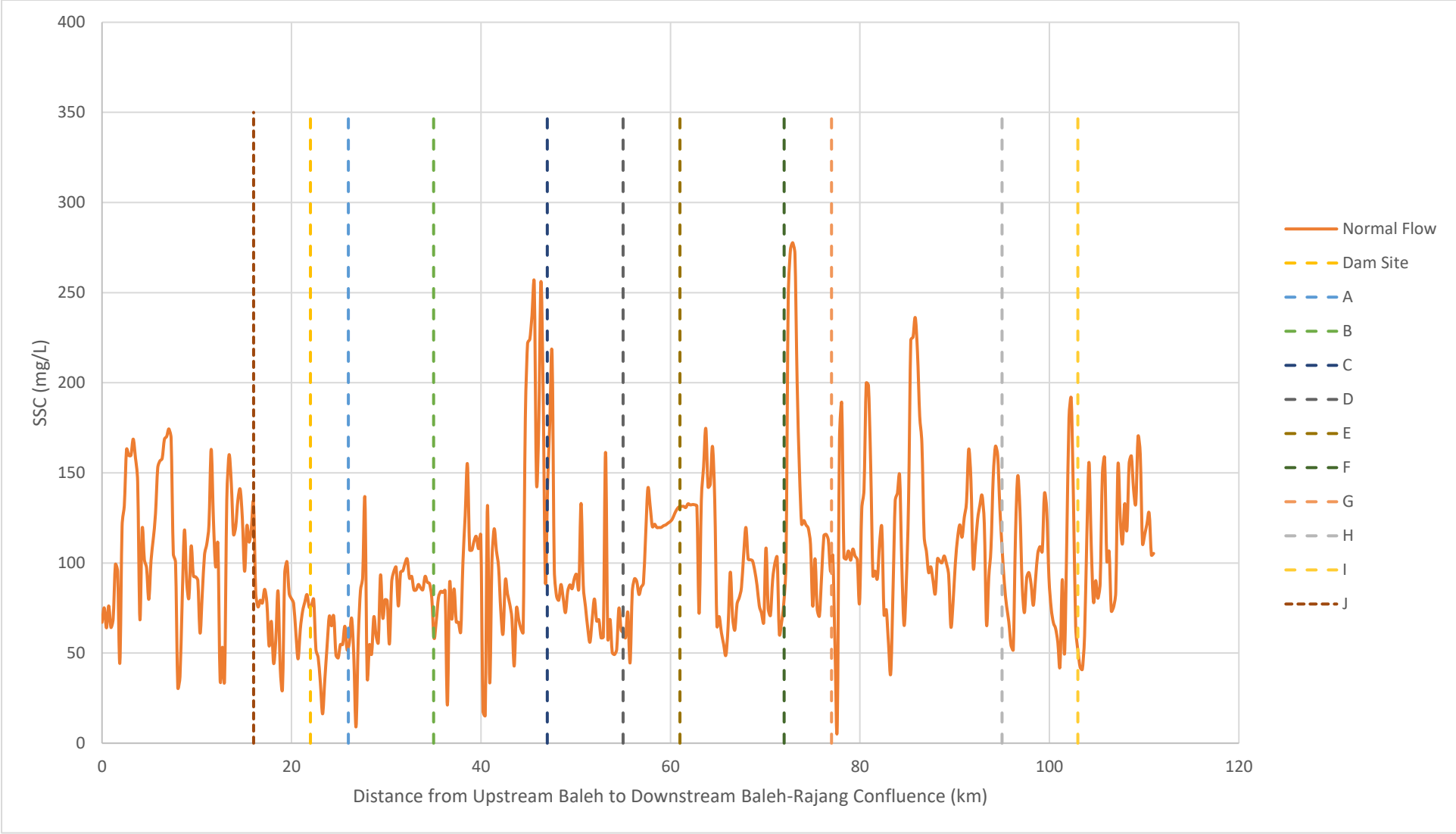

Figure 4-14: Longitudinal pattern of SSC along Baleh River from upstream to downstream for normal flow conditions

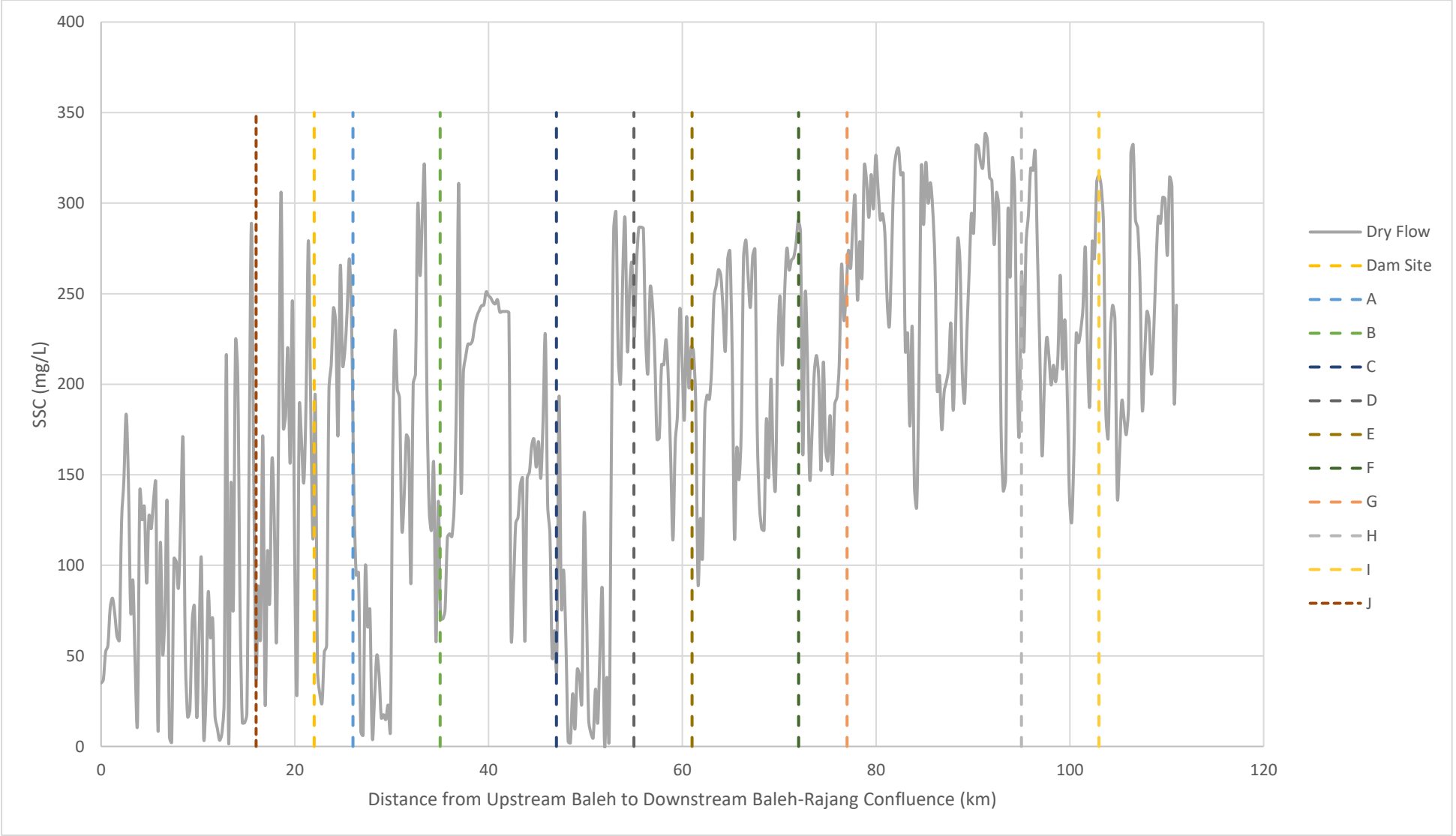

Figure 4-15: Longitudinal pattern of SSC along Baleh River from upstream to downstream for low flow conditions

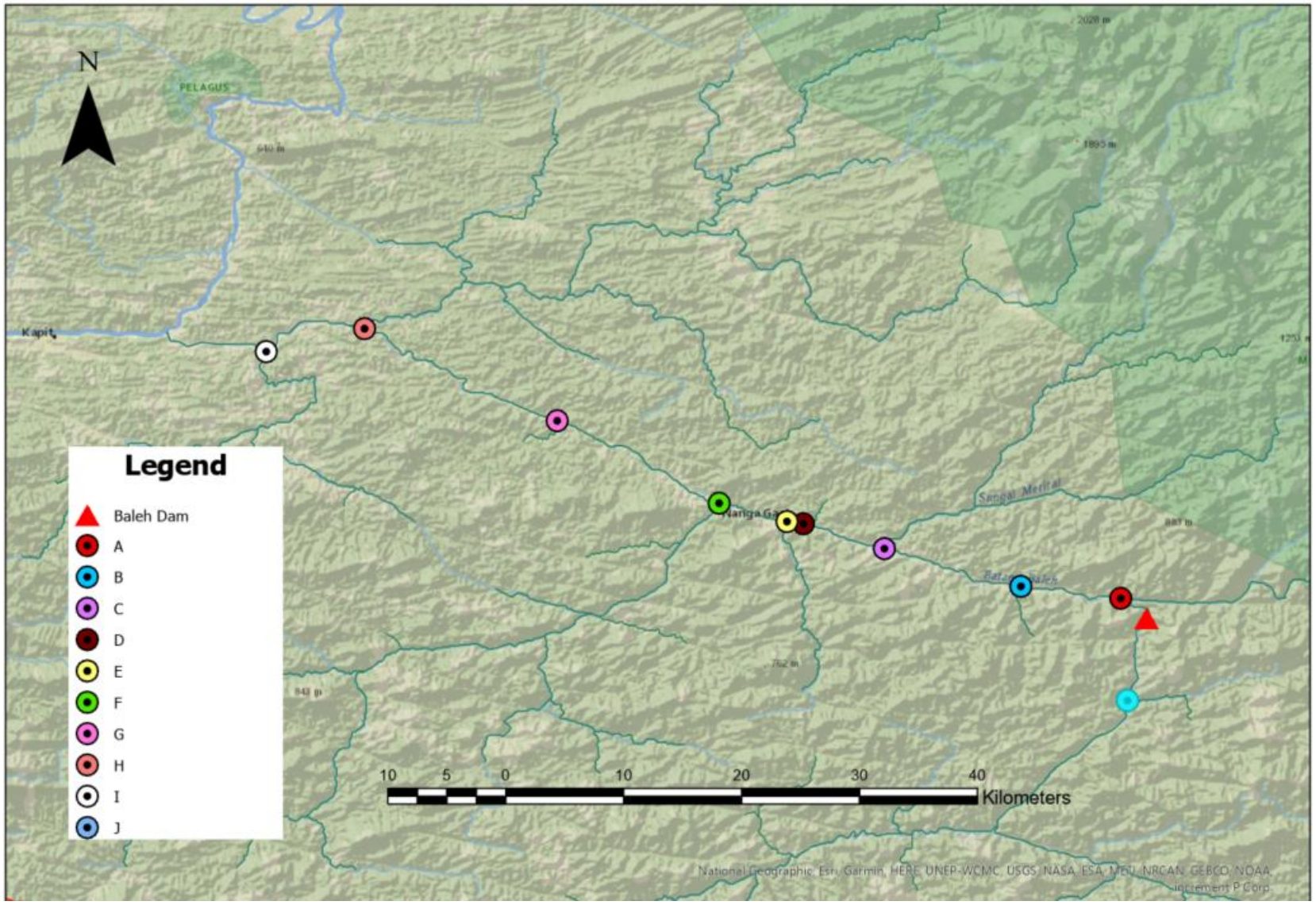

Figure 4-16: Locality of Dam Site and Tributaries of Baleh River, demarcated as A - J

From the results in Figures 4-13, 4-14 and 4-15, it is clear that there is considerable local variability associated with the effects of individual tributaries. However, this variability differs among tributaries with some causing reductions in mainstem SSC, while others cause increases, and this variation is observed across different flow conditions.

Tributary A increases the suspended sediment concentration during wet flows. There is a minor increase during normal flow conditions, but a reduction in suspended sediment concentration during low flows. In contrast, Tributary C brings an increase in the suspended sediment concentration at all flow conditions.

As for Tributary E, it increases the suspended sediment concentration during wet flow. During normal flow conditions, the suspended sediment concentration remains constant indicating that it does not increase or dilute the suspended sediment concentration. However, during dry flow conditions, the suspended sediment concentration is reduced.

Further downstream, nearer to the Baleh – Rajang confluence, Tributary H increases the suspended sediment concentration during wet flow. However, it reduces the suspended sediment concentration at normal flow and dry flow conditions. Similarly, at Tributary I, it displays the same behaviour as Tributary H.

4.3. Remote Sensing at Reach Scale (Drone Image)

Following Equation 3-8, the suspended sediment concentrations for the Putai and Merirai reaches are calculated and plotted in SSC maps as per Figures 4.17 to 4.19. These SSC maps are plotted on ArcGIS basemap. The SSC maps are produced from orthomosaics of three drone flights: March 2022, September 2022 and July 2023. In accordance with the seasonal pattern of Baleh as described by Chong et al. (2021), the orthomosaics from the aforementioned drone flights in March, September and July represent the wet, normal and dry flow conditions at Baleh respectively. They provide insights into how spatial patterns in tributary versus mainstem may change with flow conditions.

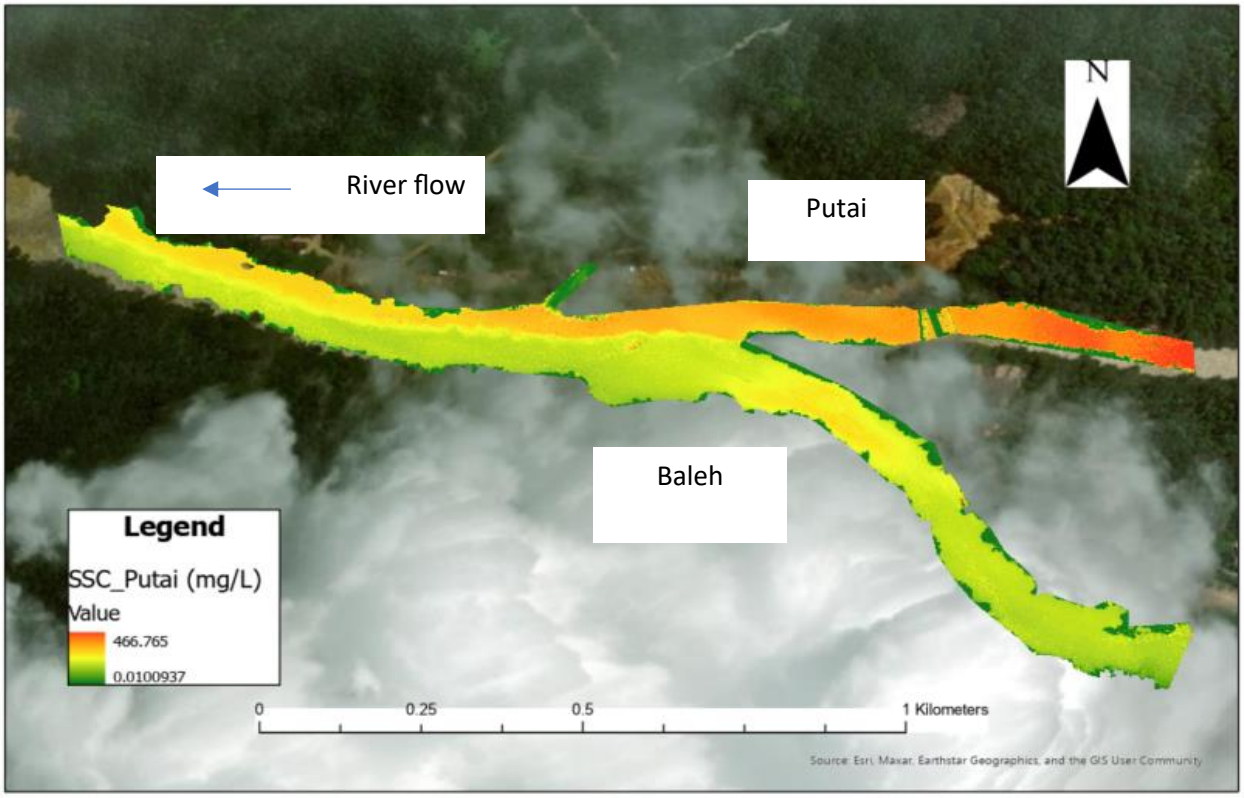

Figure 4-17: SSC Map of the Putai tributary during wet flow condition.

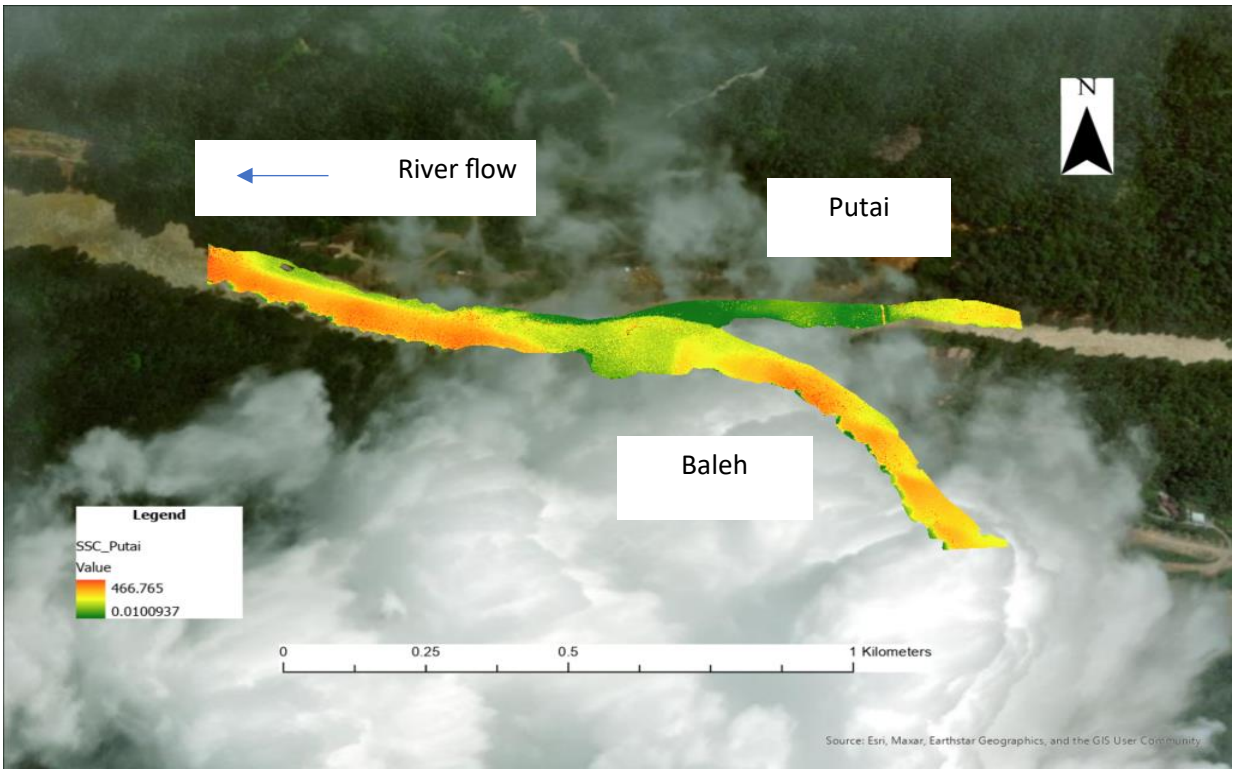

Figure 4-18: SSC Map of the Putai tributary at normal flow condition.

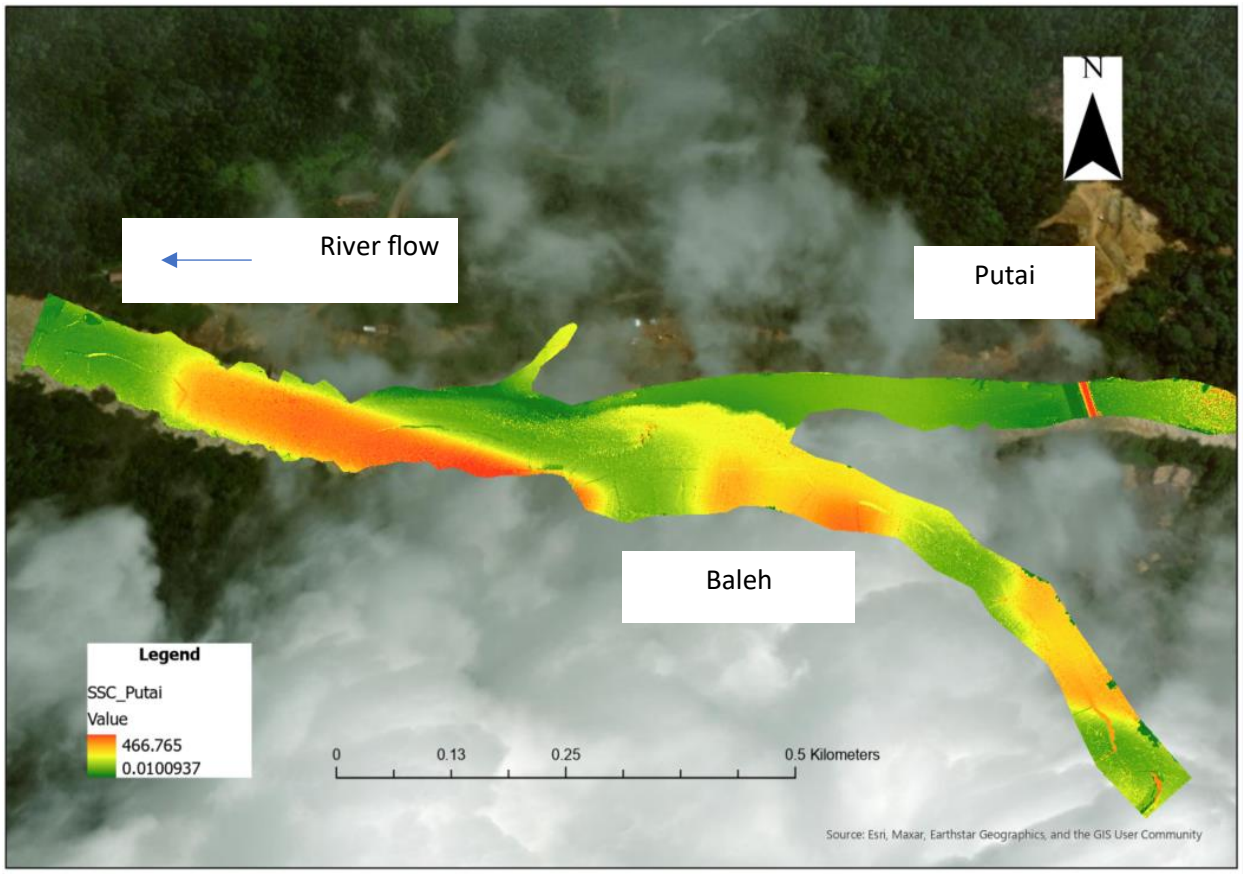

Figure 4-19: SSC Map of the Putai tributary at dry flow condition.

From Figures 4-17, 4-18 and 4-19, contrasts between SSC in the mainstem Baleh and the Putai tributary are evident. However, relative concentrations in the tributary and mainstem differ from day to day.

In Figure 4-17 (wet flow condition), the Putai is found to have higher SSC (ranging from 307mg/L – 460mg/L) than the Baleh River (SSC ranging from 150mg/L to 180mg/L), as indicated by the orange-coloured hue. Here, the SSC at the mixing zone ranges from 219mg/L up to 327mg/L as indicated by the yellow-orange hue and the mixing zone extends further downstream to the right bank of the Baleh. There is also an observed demarcation of SSC from the Putai and the Baleh as indicated by a yellow line which separates the SSC from Putai (orange hue) and the Baleh (green hue).

In Figure 4-18 (normal flow condition), the Putai is observed to have a range of SSC from 10mg/L to 178mg/L. It can be observed here that the SSC at Putai increases as it goes further upstream as shown from the transition of green to yellow hue. The Baleh on the other hand, has SSC ranging from 170mg/L to 250mg/L as indicated by the orange hue. Here, the mixing zone is identified by the yellowish-green hue at the confluence area, and the SSC here ranges from 113mg/L to 210mg/L. It can be observed that the mixing zone extends further downstream at the right bank of Baleh as indicated by the yellowish-green hue.

As for Figure 4-19 (dry flow condition), the SSC in Putai is lower than that in the Baleh, with Putai's SSC ranging from 37mg/L – 62mg/L, as indicated by the green hue. Here, the Baleh's SSC ranges from 46mg/L to 292mg/L. Here, the mixing zone is indicated by the yellow hue at the mixing zone at the confluence area, and the SSC ranges from 41mg/L to 182mg/L.

The key points from the drone-based images are that sometimes the Putai is relatively clear and acts to dilute SSCs within the Baleh at normal and dry flow conditions, but other times, when there is high flow, it contributes significant amounts of sediment to the mainstem. Whatever the circumstances, it creates a highly heterogeneous environment in the vicinity of the confluence. The water and sediment from the Putai tend to remain close to the true right bank, and at high flows, it is evident as a long 'plume' of red along the bankside. Mixing is much more evident at the other flows when this plume is less clear and extends for a shorter distance.

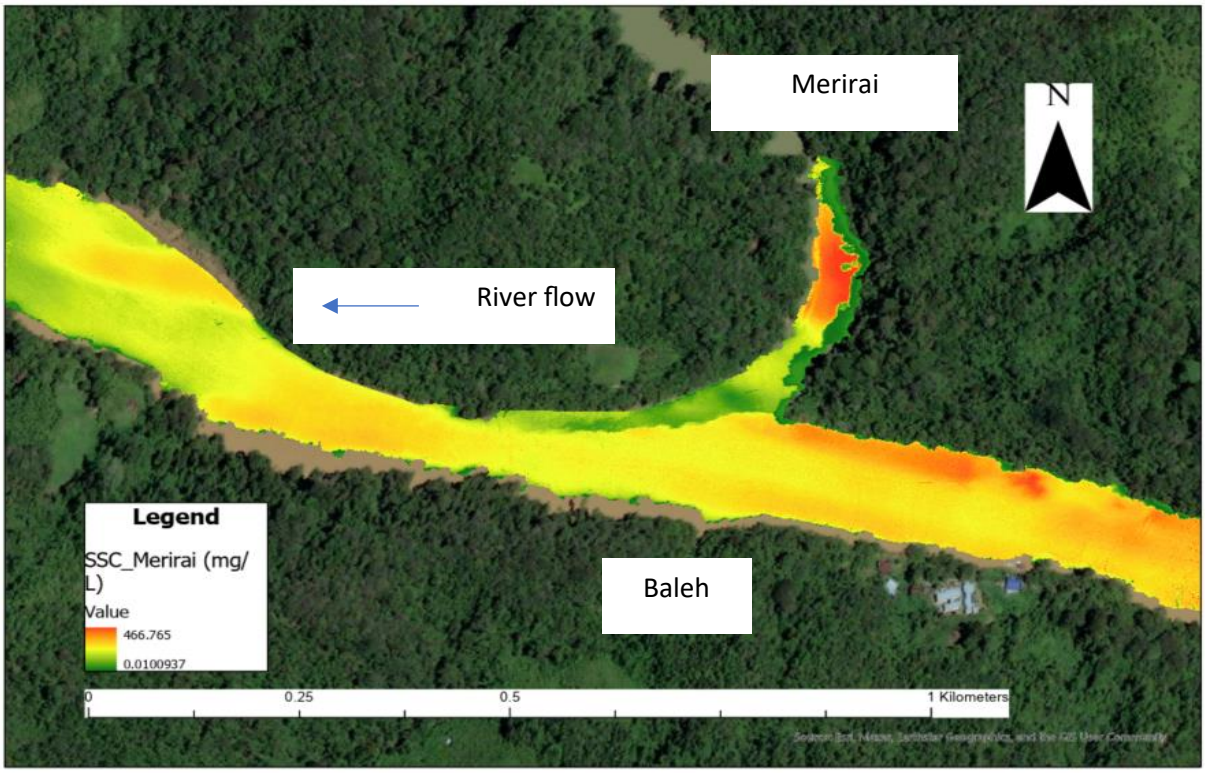

Figure 4-20: SSC Map of Merirai tributary at wet flow condition.

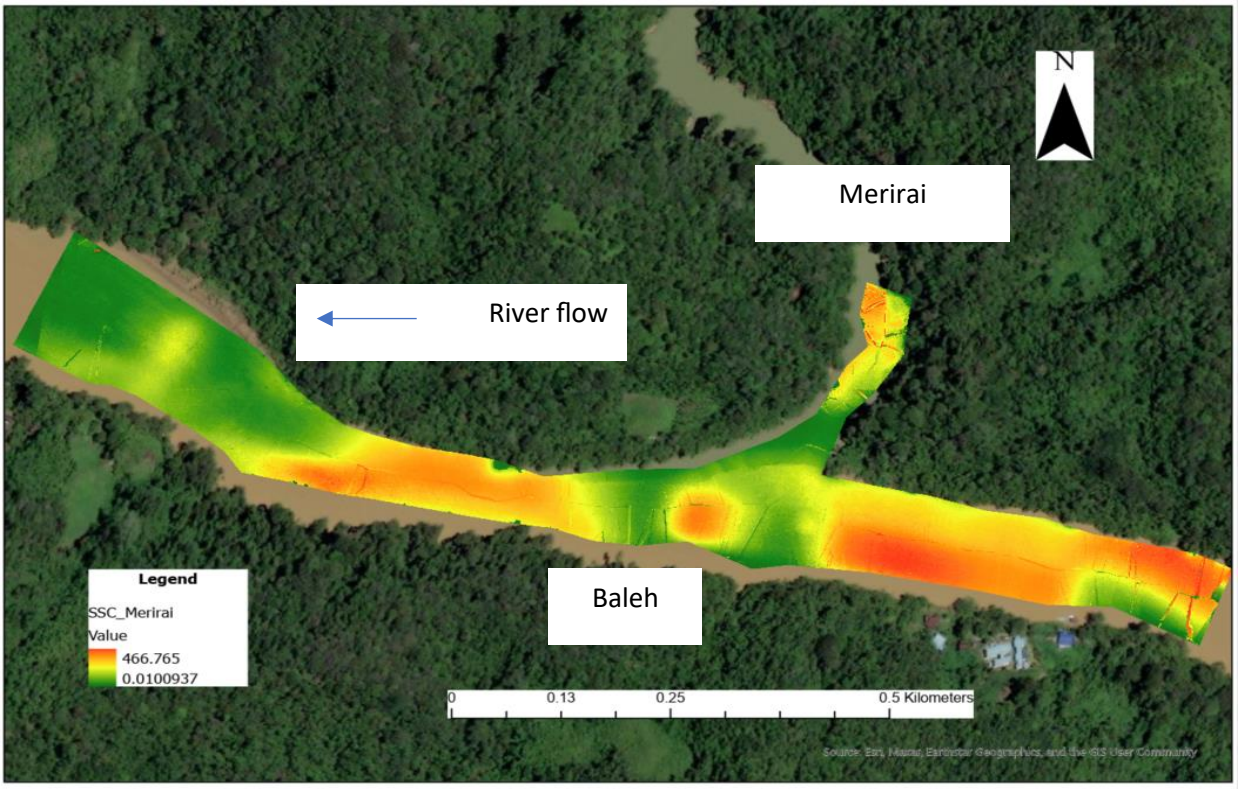

Figure 4-21: SSC Map of Merirai tributary at dry flow condition.

Around the confluence with the Merirai tributary, patterns in SSC are generally very complex and patchy. They are clearest under wet flow conditions (Figure 4-20), when the Baleh flow is relatively high. Here, Baleh is observed to have SSC that ranges from 45mg/L to 270mg/L. On the other hand, the Merirai's SSC ranges from 39mg/L to 280mg/L with the higher SSC at the upstream end of the Merirai. The mixing zone's SSC ranges from 96mg/L to 140mg/L but this zone is spatially limited; it appears very strongly demarcated, with strong contrast between the lower SSCs from Merirai water and higher SSC in the Baleh. This strong demarcation was very evident in the field, so the images represent very well what was evident in life. The Baleh flows were quite high but the Merirai was rather low, and so was not able to push out into the Baleh; hence there was little mixing until at least 0.25km downstream.

At dry flow conditions, as indicated in Figure 4-21, the pattern is very different. Upstream and downstream of the Merirai confluence, the Baleh has relatively high SSC. However, immediately outside of the Merirai's entry point, SSCs in Baleh are lower. This suggests mixing, which not only takes place on the surface, but within the water column as well. This process of mixing in 3D is very complex. However, a red patch is noticeable in the middle of this mixing area, and it is likely to be caused by sun-glare during the drone photo acquisition process. Attempts were made to remove the sun-glare during the photo post-processing stage, but by doing so, the image would not reflect the true colour, and this would greatly affect its digital number. Hence, the images were maintained as is to ensure no data is being manipulated.

Overall, the orthomosaic from the drone images provides high resolution spatial variation of suspended sediment concentration in rivers and the orthomosaic provides a distinct illustration of the tributaries influences on SSCs in the main river. Compared to the satellite images, the drone images provide higher resolution. In this case, the drone used was able to provide high resolution of up to 5cm, whereas the Sentinel data only had a resolution of 10m, much coarser than the drone.

For visualization, Figures 4-22 and 4-23 illustrate the differences in spatial variation of SSC from satellite and drone image of the Putai confluence during wet flow. The SSC map from satellite image also has lower resolution, as evident from the pixelation, in contrast to the drone image,

which displays a smoother image in the map. Due to resolution, the two scales of analyses reveal different levels of detail; this is especially evident in relation to the plume of high SSC water along the right bank of the Baleh downstream from the confluence, which is visible in the drone image but not the satellite.

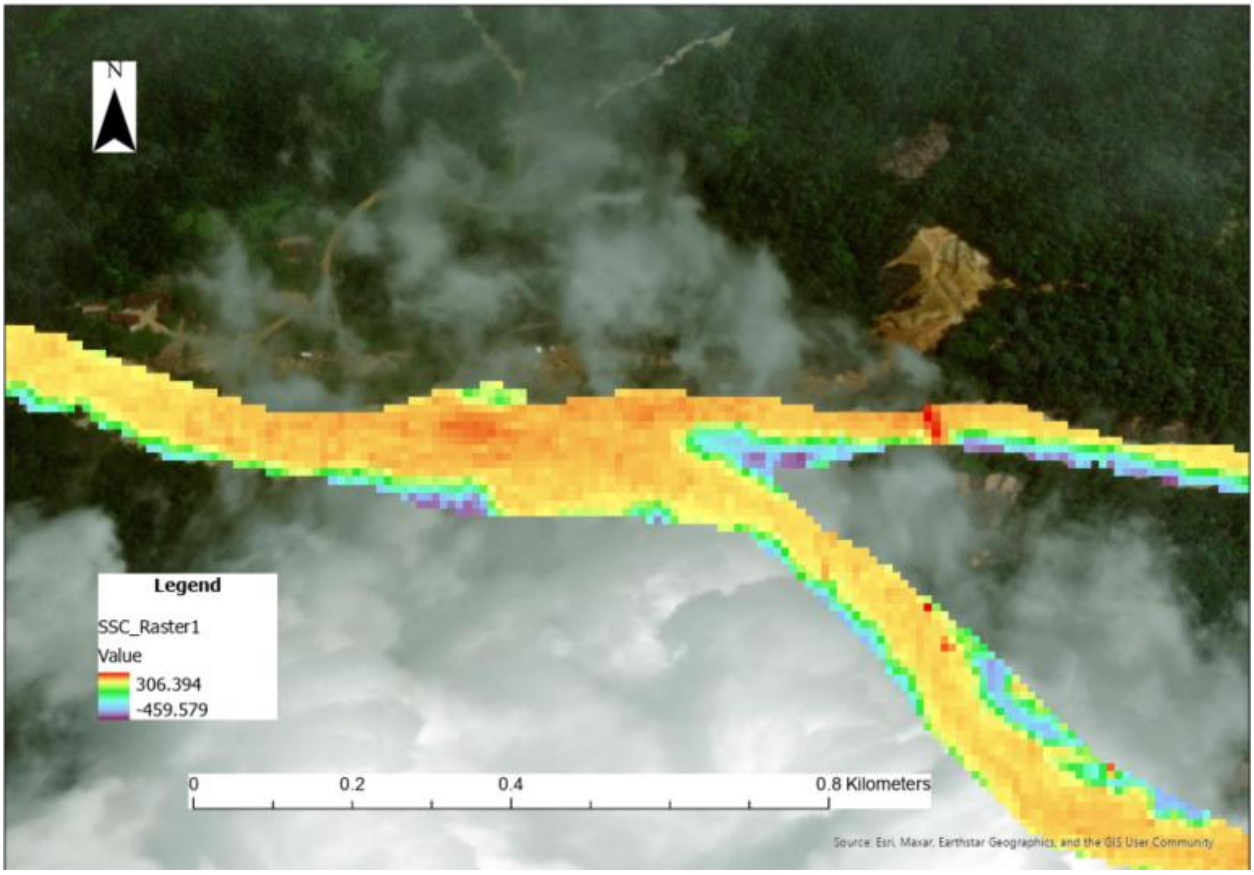

Figure 4-22: SSC Map of Putai Tributary using Satellite Image Source

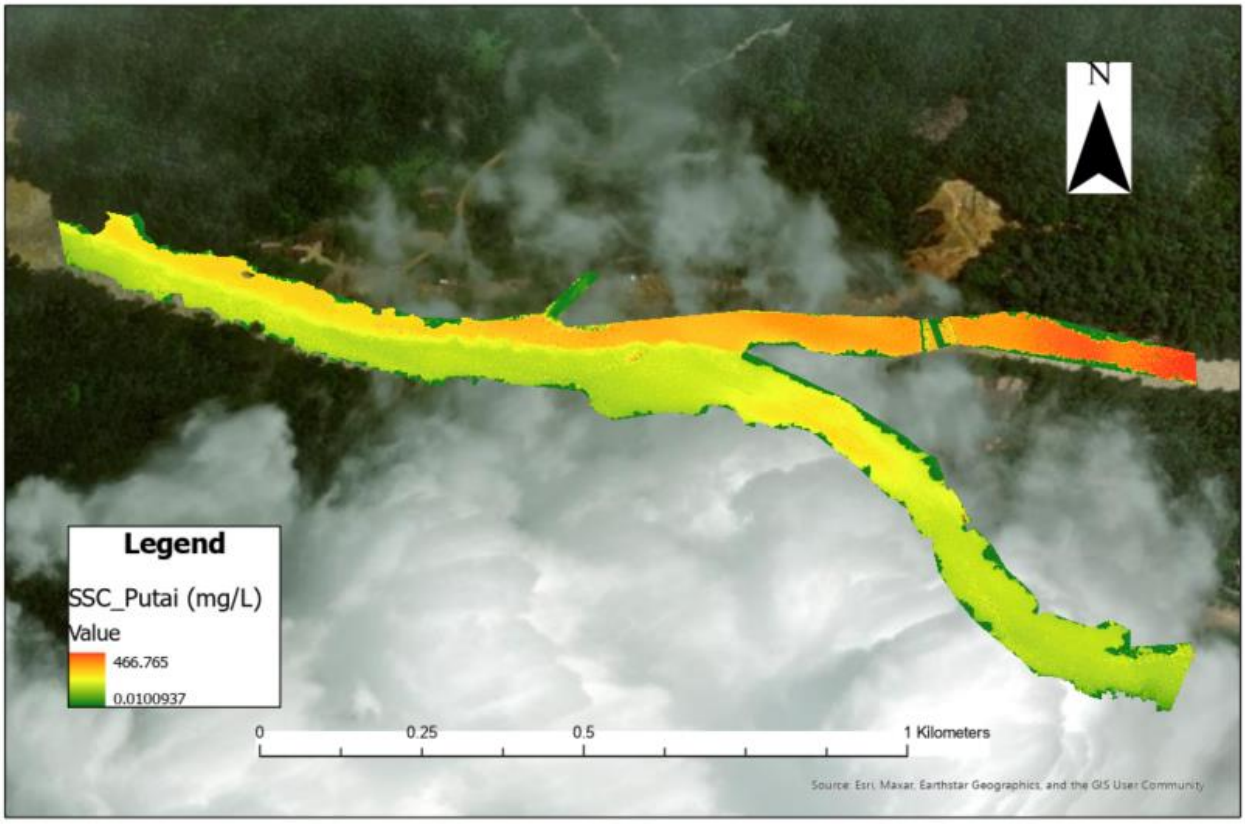

Figure 4-23: SSC Map of Putai tributary using Drone Image Source.

To illustrate the degree of resolution and how that translates to the variation of SSC captured more quantitatively, Figure 4-24 shows the ranges of SSC for each of the pixels across respective images for both the Putai and Merirai confluence areas. Figure 4-24 indicates that the drone images can capture a wider range of SSCs compared to the satellite images. For example, at Putai, the interquartile range for satellite image is about 22mg/L, whereas for the drone, the interquartile range is 133mg/L. At Merirai, the interquartile range for SSC captured by the drones is 133mg/L. In comparison with that of the SSC captured by the satellite, the range is only about 18mg/L and 17mg/L respectively.

From Figure 4-24, it can be deduced that the orthomosaic from drone images provides a better insight into local spatial variation of SSC compared to that from the satellite images. There are outliers from the drone images for SSCs above 354mg/L and these high SSCs are likely to be caused by the sun-glares in the drone images, resulting to high estimations of SSC. On the other

hand, the SSC outliers from the satellite image at Putai (below 99mg/L) are due to the shadow of trees on the river, as captured by the satellite image.

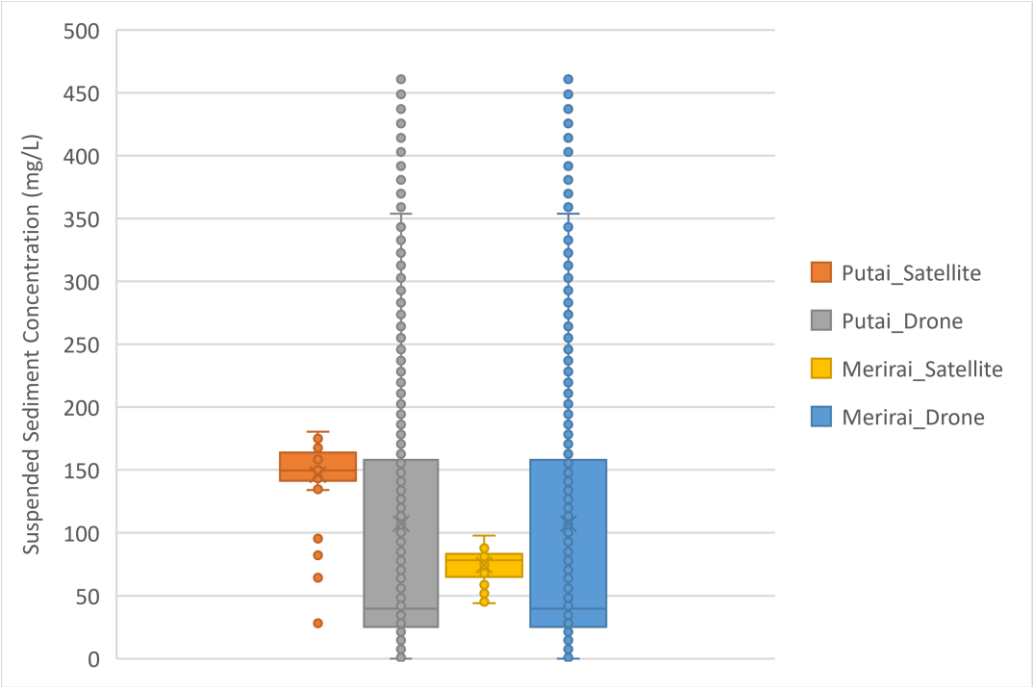

Figure 4-24: Box and Whisker Plot of SSC for Satellite versus Drone Image at Each Site.

5. Discussion

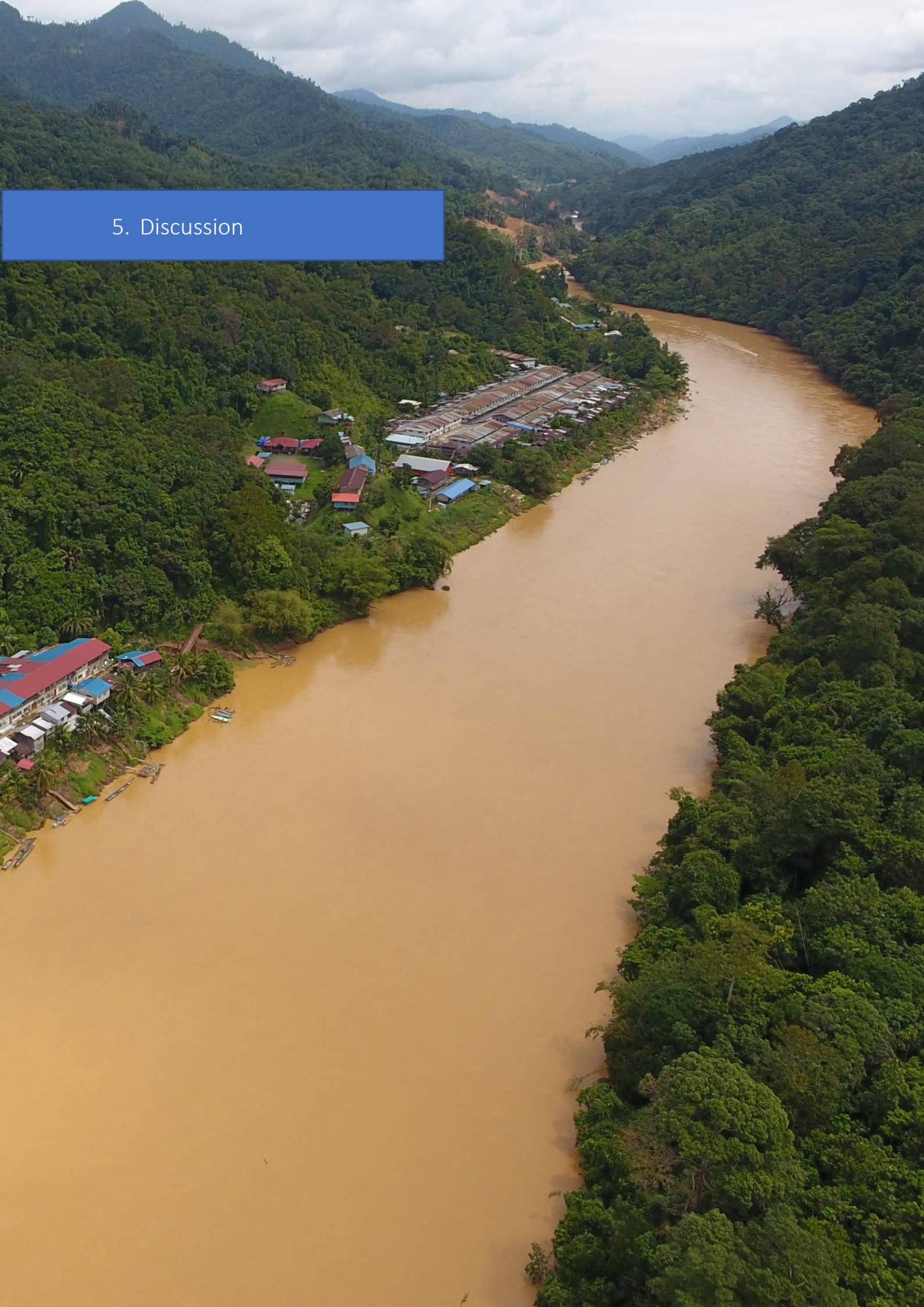

5.1. Background

This project focused on establishing baseline conditions of fine sediment in the Baleh River prior to damming. As detailed in the literature review, in the tropics, high sediment loads are contributed by erodible soils and high rainfall-runoff volume (USGS, 2018). The relationship between flows and SSC is complex (Lloyd et al., 2016, Mukundan et al., 2013) but in general flow exerts an important control on the fine sediment concentrations and loads. Both are likely to be altered in the Baleh due to the dam. Construction of Baleh Dam is well underway, but it is a large project and is not scheduled for completion for at least another four years. This provides a window within which a number of projects are underway, including the work presented in this thesis.

The current work provides information on pre-damming conditions, such that it is possible to assess whether the changes that have been reported elsewhere following dam closure become evident in the Baleh; e.g. the Manwan Dam in Mekong has caused a decline in the sediment load (Liu et al., 2013), with Lu and Siew (2006) reporting a 40% reduction in monthly SSC in the Lower Mekong River, and the annual sediment flux reduced by half after the completion of Manwan Dam (Kummu and Varis, 2007).

The following section outlines the main findings related to each of the project's objectives. It stresses similarities and differences with what has been reported in the literature in terms of loads, SSC, and spatiotemporal dynamics.

5.2. Key Findings

Objective 1: To estimate the annual fine sediment load of the Baleh River and assess monthly and seasonal patterns.

From this study, the annual fine sediment in Baleh is estimated to be 14.6 million tonnes/year. Monthly loads varied markedly, with June and December having the highest and lowest sediment loads of 3.3 million tonnes and 0.2 million tonnes, respectively. The median annual concentration was 134mg/L, with a 10^{th} percentile value of around 620mg/L and a 90^{th} percentile of around 0.9mg/L.

The study year was rather unusual in terms of seasonal patterns, with hardly any difference in river discharge between the supposed dry and wet seasons. In the study year, the wet months were found to be August to November, and the dry months were found to be April to July. These two periods had different fine sediment loads and concentrations, especially at the extremes. In the dry period, the 10th percentile SSCs were 426mg/L in the wetter months but 961mg/L in the dryierones, while the 10th percentiles were 0.13mg/L in the dry months but 36mg/L in the wetter months. In general, SSC increased with discharge (as per Figure 4-5) but the relationship was non-linear.

Objective 2: To assess longitudinal patterns of SSC along the Baleh, from the dam site to its confluence with the main Rajang River, identifying the riverscale patterns especially the influence of tributaries in altering mainstem Baleh's SSC.

This study was able to assess changes in SSC continuously over a distance of approximately 100km using satellite images. Sediment index values were computed from images that extended from around 20km upstream from the dam site to the Baleh's confluence with the Rajang. Longitudinal patterns were highly dependent on flow. Images were analysed for relatively high, moderate and lower discharge. Clear, consistent downstream increases were only evident during periods of lower flows. This appears to be the result of temporally variable effects of tributaries across this large basin, which sometimes deliver their flow with higher SSCs than the mainstem river, but sometimes lower.

Objective 3: To assess patterns of SSC mixing around confluence zones and they vary with flow.

The confluence of Putai and Merirai was analyzed at river reach scale to investigate the spatiotemporal pattern of SSC and how they vary with flow conditions. The study found that Putai is typically relatively clear and acts to dilute SSC within the Baleh at normal and dry flow conditions. However, when there is high flow in this tributary, it contributes significant amount of sediment to the mainstem Baleh. As for the Merirai, it dilutes the SSC at the Baleh at all flow conditions.

From the drone based images, it is found that in any flow conditions, there is a highly heterogenous concentrated sediment environment in the vicinity of these confluences. In

particular, there appears to be little mixing, resulting in contrasting zones of clear and highly turbid water. Concentrations can vary markedly across short distances.

5.3. Discussion and conclusions

5.3.1. Fine Sediment Load at the Baleh River

In total, throughout the study period from February 2022 – December 2022, the total sediment load delivered from the Baleh to the Rajang River was 13,364,062 tonnes, equivalent to about 14.6 million tonnes/year. This rate is comparable to the Indian river of Mahanadi (15.7 million tonnes/year) (Subramanian, 1993), the American river of Brazos (16 million tonnes/year) and the Po River in Italy (15 million tonnes/year) ((Milliman and Meade, 1983).

The wet months during this study period were Identified to be from August to November, while the dry months were from April to July. The highest sediment load was found to be in the month of June with a total 3.3 million tonnes, while the lowest sediment load to be in the month of December at 0.2 million tonnes. During the wet months of August to November, the total sediment load was 4.5 million tonnes, while during the dry months of April to July, the it was 6 million tonnes. On average per month, these two periods show minimal difference. Despite sediment loads typically being higher in the wet months, a study published by Xia (2010) found that the Skunk River in Iowa, USA, transported more suspended sediment loads in the dry years and concluded that it is due to the difference in climate compared to the past.

In the Baleh, any true differences between wet and dry seasons are likely to be obscured by ongoing infrastructure development. A new road is being constructed along the line of the river, and this crosses all tributaries between the flow gauging station at Teluk Buing and the dam site. This involves bridge crossings being built across tributaries and the cutting of road culverts along hillslopes close to the river. These constructions are happening in an ongoing fashion and are likely to be contributing to creation of major new local sources of fine sediment entering the river in a temporal sequence that is out of phase with normal flow and associated runoff patterns.

5.3.2. Longitudinal Patterns of SSC along the Baleh at River Scale

The Baleh is already quite turbid by the time it reaches the dam site (up to around 500mg/L), indicating the effects of forest clearance upstream. On some days, tributaries such as the Putai deliver clean water (less than 1mg/L; Fig 4.14) but on other days, they deliver more than 400mg/L. The effects of these temporally variable inputs are that downstream patterns along the mainstem are locally variable, with some sudden increases and some sudden decrease as different tributaries discharge their water.

A Generalized Additive Model (GAM) analysis was conducted to simplify this complex relationship and its results are plotted in Figure 4-12, where the y-axis indicates the SSC in mg/L and the x-axis indicates the distance in kilometres from point at which the river is too narrow to extract data from satellite images. These smoothed curves illustrate that only on some days, when mainstem flows are low, there is clear downstream increase in SSC along the 100km length. The lack of downstream trend under other flow conditions likely reflects locally variable flow volumes and sediment load across this large catchment, where localised rainfall may be driving quite different processes in tributaries.

On days with higher flow, SSCs dropped along much of the middle part of the river. This bears resemblance to research findings in China where tributaries of the Yellow River have been shown to contribute to a dilution of SSC in the mainstem Yellow River (Xu, 2014). Furthermore, these findings in Baleh align with similar observations made in the Orinoco River in South America (Stallard, 1987), and in the Hwang and Nakdong Rivers in South Korea (Kwon et al., 2023).

5.3.3. Spatiotemporal Patterns of SSC around Confluence Zones

By using the orthomosaic from drone images, the spatial variation in SSC can be observed at 5cm resolution. With this high resolution, the variation in SSC is clearly distinct and the influence of tributaries on the main river is obvious.

Based on the results, the Putai acts as both contributor and dilutor of SSC to the main Baleh River. At high flow conditions, the Putai delivers high SSC to the Baleh river, about twice the

amount of SSC at the Baleh River. At dry and normal flow conditions, the Putai has less SSC, diluting the SSC of Baleh at the mixing zone. At this confluence, the mixing zone extends further downstream toward the right bank of the Baleh.

At the Merirai, in all flow conditions, the Merirai is found to dilute the SSC as evidenced by its patterns at the mixing zone. Based on the results, the Merirai delivers about one-third to one-fourth the SSC of the Baleh. Similar to the Putai, the mixing zone at Merirai is also indicated by the yellow hue, indicating the gradual transition between the SSCs of both rivers.

The orthomosaic from drone images have proven to provide higher resolution of spatial variation compared to those from satellite images. These are suitable for assessing the spatial variations of SSC at a finer scale, in areas like confluences, small or medium sized rivers (Hemmelder et al., 2018, Hodge, 2014, Larson et al., 2018). As for the satellite images, they are more suited for assessing the spatial variation of SSC at larger scales, in larger water bodies like lakes and coastal areas, where their resolution (>10m) is less problematic (Choo et al., 2022, Ody et al., 2022). The comparisons shown in Figures 4-22 and 4-23 indicate that the satellite images are not able to detect even quite marked local contrasts. Such contrasts may be important ecologically, so at this scale drone-based surveys offer clear advantages.

In general, the SSC estimates from the satellite images were lower than those for the drones. The respective dates were not the same but separated by a maximum of 2 days. This may partly explain the difference, but most likely, it is due to the smaller sample size (few pixels across the same area) and errors related to the low R^2 value of the NDSSI index (0.35).

5.4. Implications for Management and conservation

It is a fact that dams are major barriers to sediment transport and many papers have asserted that dams reduce the suspended sediment loads and concentration downstream of the dam (Alexandra, 2021, Lu et al., 2015, Pacini et al., 2013, Schellenberg et al., 2017, Vörösmarty et al., 2003, Wohl et al., 2015). With the completion of Baleh Dam, we can anticipate the same thing to happen, where SSCs and suspended sediment load would be reduced. In the Mississippi River, USA, Meade and Parker (1985) reported that the major cascading dams in its river system have reduced the suspended sediment loads by 70%. Powell (2002) also

reported that 90% of the suspended sediment in the Colorado river is trapped behind the Glen Canyon Dam in Lake Powell. In Mekong, Lu and Siew (2006) reported a 40% reduction in monthly SSC at the Lower Mekong River. Lum (2021) estimated that around 97% of all sediment will be trapped by the Baleh dam, based on Soil and Water Assessment Tool (SWAT) simulations. This will lead to sediment starvation downstream and would lead to "hungry water" effect in the downstream reaches (Batalla, 2003), with bed and bank scour likely. The erosion, together with tributary inputs, may quicky result in increased SSCs. The high drainage density of tropical rivers such as the Baleh may mean that the downstream extent of re-adjustment is less than temperate systems, due to large numbers of tributaries discharging their flow and water. Monitoring after dam completion is needed to assess this.

A lot will depend on flow magnitudes, especially during the lengthy filling stage. It may take 2 years after dam closure for the lake to fill to operational level (SEB pers comm). Discharges during this period will be low (only 250m^3/s at the dam site). While this may limit hungry water effects, it may have other consequences for bed conditions; for instance, fine sediment input from tributaries may settle on the bed of the mainstem Baleh rather than being conveyed downstream, due to low velocities and competence. Again, monitoring is needed.

During the construction of the Baleh Dam, it is observed that a comprehensive road network and bridges have been built to provide access to the dam. The construction of these roads and bridges will continue contribute more fine sediment to the Baleh River. Chong (unpublished PhD thesis) modelled the effects of roads on connectivity across the basin. She found that while the roads can indeed have localised effects on connectivity in the Baleh, the increases brought by the roads were more than cancelled out by the effect of the dam itself. It is possible that, as observed elsewhere, roads create access for illegal and uncontrolled forest clearance. This will affect sediment inputs. Thus, a complex series of changes may alter the Baleh's future fine sediment budget.

5.5. Recommendations

It is highly recommended to continue monitoring the suspended sediment loads and SSC in the Baleh, to assess the changes on both parameters, post-dam. Aside from the current

methods of data collection, it would be helpful to install additional turbidity loggers, with rainfall and water level sensors within the catchment to get a better estimation on the suspended sediment loads and sediment transport across the Baleh River System. A critical location would be the dam site itself and upstream of the dam, to develop sediment load estimates for the section between upstream of the dam and Putai confluence. Bathymetry surveys should also be conducted to determine any changes in the riverbed levels at selected sites, prior to post damming. This can be done using ADCPs or sonar.

Aside from the monitoring works, sediment replenishment strategy should be considered, to compensate sediment deficits downstream and improve habitat quality and ecological functions. Periodic flushing flows may be needed, depending on changes to fine sediment deposited on the bed (Serra et al., 2022). There are several more years before the dam is closed and this provides a window for further data collection, modelling and assessment of likely downstream changes.

The potential for dam impacts should be conveyed to relevant authorities, most notably the Malaysian Department of Irrigation and Drainage. This is particularly important in Malaysia, since few comprehensive assessments of dam impacts have been made public and where currently there is no widespread adoption of integrated river basin planning.

6. Conclusion

This thesis is a rare example of a fluvial geomorphic assessment in tropical south-east Asian river. It is important in providing some fundamental baseline data prior to damming of this important, large river, as well as adding to the limited literature of fine sediment loads of rivers in this region.

Estimates suggest that the Baleh river releases about 14.6 million tonnes of suspended sediment load per year into the Rajang River. The highest sediment load was found to be in the month of June with a total 3.3 million tonnes, while the lowest sediment load is found to be in the month of December, at 0.2 million tonnes. During the wet period of August to November, the total sediment load is 4.5 million tonnes while during the dry period, from April to July, the total sediment load is 6 million tonnes.

Consistent with the high amount of suspended sediment load in the dry flow conditions, the longitudinal pattern of the suspended sediment concentration along the Baleh river is the strongest during dry flow conditions. Nevertheless, the tributaries along the Baleh River both contribute and dilute the suspended sediment concentration along the mainstem, depending on localised rainfall, land use changes and prevailing mainstem flows. Downstream patterns are not always clear.

Remote sensing has been proven to be useful in assessing Baleh's suspended sediment concentration. Given that Baleh is remote and large, remote sensing has provided insight into the spatial patterns of suspended sediment concentration along the Baleh and its confluences. Satellite data was able to show the pattern of suspended sediment concentration along the entire Baleh river stretch. However, it is clear that calibration and validation data sets are absolutely critical to reduce the errors associated with this remote sensing approach. On a more local scale, the drone images were able to illustrate the pattern suspended sediment concentration at the confluences, giving a better picture at how tributaries influence the suspended sediment concentration at the main Baleh River. Through the drone images, we were able to discern the patterns of mixing of the suspended sediment between the tributary and the mainstem of Baleh River. It is clear that these tributary zones are spatially heterogeneous, in terms of SSCs, and so present very contrasting local conditions that animals need to be able to tolerate. An animal moving only a few meters might experience major changes in water turbidity and clarity change habitat from being usable to unusable.

As the Baleh is found to have high suspended sediment load and concentration during the dry flow conditions, it is important for the dam operators to release adequate flows during the dry season once Baleh HEP is in operation. More importantly, it is recommended for the dam operators to have a reservoir sediment management in place to help deal with issues of sediment starvation. However, this is complicated, since ongoing changes related to road construction and land clearance are already changing the river's suspended sediment load. Monitoring is needed at a matter of priority.

7. References

ALEXANDRA, C.-N. 2021. *How to reconcile dams and sediment transport?, Encyclopedia of the Environment* [Online]. France: Association des Encyclopédies de l'Environnement et de l'Énergie. Available: https://www.encyclopedie-environnement.org/en/water/how-reconcile-dams-sediment-transport/#:~:text=In%20absolute%20terms%2C%20the%20establishment,hydrological%20functioning%20of%20the%20river. [Accessed 02/07/2019 2019].

ALI, D. D. A. R. M. 2017. Erosion & Sedimentation. *In:* MALAYSIA, A. O. S. (ed.). Kuala Lumpur: Academy of Sciences Malaysia.

AMERICAN PUBLIC HEALTH ASSOCIATION 2012. Standard Methods for the Examination of Water and Wastewater, 22nd Edition. *In:* RICE, E. W., BAIRD, R.B., EATON, A.D., CLESCERI, L.S (ed.). American Water Works Association.

ANCEY, C. 2020. Bedload transport: a walk between randomness and determinism. Part 1. The state of the art. *Journal of Hydraulic Research,* 58**,** 1-17.

AUGUSTYN, A., ZEIDAN, A., ZELAZKO, A., ELDRIDGE, A., MCKENNA, A., TIKKANEN, A., GADZIKOWSKI, A., SCHREIBER, B. A., DUIGNAN, B., MAHAJAN, D., PROMEET, D., GOLDSTEIN, E., RODRIGUEZ, E., GREGERSEN, E., SHUKLA, G., LIESANGTHEM, G., LOTHA, G., YOUNG, G., BOLZON, H., LUEBERING, J. E., WALLENFELDT, J., HIBLER, J., RAFFERTY, J. P., GUPTA, K., ROGERS, K., CHMIELEWSKI, K., MANCHANDA, K., HEINTZ, K., CHAVERIAT, L., DIXON, L., MATTHIAS, M., PETRUZZELLO, M., RAY, M., METYCH, M., BAUER, P., RILEY, P., PIYUSH BHATHYA, VASICH, S., HOLLAR, S., SINGH, S., GUPTA, S., SEDDON, S., BRITANNICA, T. I. A. O. E., SETIA, V. & EDITORS, W. D. 1998. Erosion. *In:* ADAM AUGUSTYN, A. Z., ALICJA ZELAZKO, ALISON ELDRIDGE, AMY MCKENNA, AMY TIKKANEN, ANN GADZIKOWSKI, BARBARA A. SCHREIBER, BRIAN DUIGNAN, DEEPTI MAHAJAN, DUTTA PROMEET, EMILY GOLDSTEIN, EMILY RODRIGUEZ, ERIK GREGERSEN, GAURAV SHUKLA, GITA LIESANGTHEM, GLORIA LOTHA, GRACE YOUNG, HENRY BOLZON, J.E. LUEBERING, JEFF WALLENFELDT, JOAN HIBLER, JOHN P. RAFFERTY, KANCHAN GUPTA, KARA ROGERS, KENNY CHMIELEWSKI, KOKILA MANCHANDA, KURT HEINTZ, LAURA CHAVERIAT, LETRICIA DIXON, MEG MATTHIAS, MELISSA PETRUZZELLO, MICHAEL RAY, MICHELE METYCH, PATRICIA BAUER, PATRICK RILEY, PIYUSH BHATHYA, SHEILA VASICH, SHERMAN HOLLAR, SHIVETA SINGH, SHWETA GUPTA, STEPHEN SEDDON, THE INFORMATION ARCHITECTS OF ENCYCLOPAEDIA BRITANNICA, VEENU SETIA, AND WORLD DATA EDITORS. (ed.) *Encyclopedia Brittanica.*

AUTHORITY, M.-D. B. 2019. Murray-Darling Basin Sediment Management Strategy.

AZIZ, A., ESSAM, Y., AHMED, A. N., HUANG, Y. F. & EL-SHAFIE, A. 2021. An assessment of sedimentation in Terengganu River, Malaysia using satellite imagery. *Ain Shams Engineering Journal,* 12**,** 3429-3438.

BAGNOLD, R. A. 1973. The nature of saltation and of 'bed-load' transport in water. *Proceedings of the Royal Society London A,* 332**,** 473-504.

BANK, T. W. 2021. *For Mekong Delta Farmers, Diversification is the Key to Climate Resilience* [Online]. Available: https://www.worldbank.org/en/news/feature/2021/10/21/for-mekong-delta-farmers-diversification-is-the-key-to-climate-resilience [Accessed].

BANNIGAN, D. N. A. 2013. Baleh Hydroelectric Project, Hydrology Review and Update. Malaysia.

BASSON, G. Hydropower Dams and Fluvial Morphological Impacts - An African Perspective. Sotuh Africa.

BATALLA, R. J. 2003. Sediment deficit in rivers caused by dams and instream gravel mining. A review with examples from NE Spain. *Cuaternario y geomorfología: Revista de la Sociedad Española de Geomorfología y Asociación Española para el Estudio del Cuaternario, ISSN 0214-1744, Vol. 17, Nº. 3-4, 2003, pags. 79-91,* 17.

BECK, J. S., BASSON, G.R. 2003. *The hydraulics of the impacts of dam development on the river morphology,* South Africa, Department of Civil Engineering, University of Stellenbosch.

BERNHARDT, E. S., PALMER, M. A., ALLAN, J. D., ALEXANDER, G., FULTON, J. A., & TOWNSEND, C. R. 2005. *Riverine Ecosystem Services and Their Management: A Synthesis*

BOARD, C. R. W. Q. C. 2023. Colorado River Delta Sediment Management Plan.

BORNEO POST, C., IRENE. 2022. Construction of Baleh Hydroelectric Project reaches 33 pct completion. *The Borneo Post*.

BURGESS, O. T., PINE III, W. E. & WALSH, S. J. 2013. IMPORTANCE OF FLOODPLAIN CONNECTIVITY TO FISH POPULATIONS IN THE APALACHICOLA RIVER, FLORIDA. *River Research and Applications,* 29**,** 718-733.

CARLING, P. A. 1995. *The Suspended Load of Rivers*, Wiley.

CHANSON, H. 2004. 6 - Introduction to sediment transport in open channels. *In:* CHANSON, H. (ed.) *Hydraulics of Open Channel Flow (Second Edition).* Oxford: Butterworth-Heinemann.

CHONG, X. Y. 2023. *Developing Environmental Flows for the Baleh River - Hydrological and Geomorphological Processes in the Baleh Catchment Prior to Damming.* University of Nottingham Malaysia.

CHONG, X. Y., GIBBINS, C. N., VERICAT, D., BATALLA, R. J., TEO, F. Y. & LEE, K. S. P. 2021. A framework for Hydrological characterisation to support Functional Flows (HyFFlow): Application to a tropical river. *Journal of Hydrology: Regional Studies,* 36**,** 100838.

CHOO, J., CHERUKURU, N., LEHMANN, E., PAGET, M., MUJAHID, A., MARTIN, P. & MÜLLER, M. 2022. Spatial and temporal dynamics of suspended sediment concentrations in coastal waters of the South China Sea, off Sarawak, Borneo: ocean colour remote sensing observations and analysis. *Biogeosciences,* 19**,** 5837-5857.

CINCO-CASTRO, S., HERRERA-SILVEIRA, J. & COMÍN, F. 2022. Sedimentation as a Support Ecosystem Service in Different Ecological Types of Mangroves. *Frontiers in Forests and Global Change,* 5.

COLLINS, A. L. & ZHANG, Y. 2016. Exceedance of modern 'background' fine-grained sediment delivery to rivers due to current agricultural land use and uptake of water pollution mitigation options across England and Wales. *Environmental Science & Policy,* 61**,** 61-73.

COLLINSON, J. 2005. SEDIMENTARY PROCESSES | Depositional Sedimentary Structures. *In:* SELLEY, R. C., COCKS, L. R. M. & PLIMER, I. R. (eds.) *Encyclopedia of Geology.* Oxford: Elsevier.

CSIRO 2018. Murray-Darling Basin Sediment Management.

CUI, L., LI, G., LIAO, H., OUYANG, N., LI, X. & LIU, D. 2022. Remote Sensing of Coastal Wetland Degradation Using the Landscape Directional Succession Model. *Remote Sensing* [Online], 14.

CZUBA, J. A., MAGIRL, C. S., CZUBA, C. R., GROSSMAN, E. E., CURRAN, C. A., GENDASZEK, A. S. & DINICOLA, R. S. 2011. Sediment load from major rivers into Puget Sound and its adjacent waters. *Fact Sheet.* Reston, VA.

EPA, U. S. E. P. A. 2005. Sediment Pollution.

FONDRIEST ENVIRONMENTAL, I. 2014. *Sediment Transport and Deposition* [Online]. Available: https://www.fondriest.com/environmental-measurements/parameters/hydrology/sediment-transport-deposition/ > [Accessed].

GAVEAU, D. L. A., SLOAN, S., MOLIDENA, E., YAEN, H., SHEIL, D., ABRAM, N. K., ANCRENAZ, M., NASI, R., QUINONES, M., WIELAARD, N. & MEIJAARD, E. 2014. Four Decades of Forest Persistence, Clearance and Logging on Borneo. *PLOS ONE,* 9**,** e101654.

GILBERT, G. K. & MURPHY, E. C. 1914. The Transportation of Debris by Running Water. *Professional Paper.* - ed.

GIOSAN, L., SYVITSKI, J., CONSTANTINESCU, S. & DAY, J. 2014. Climate change: Protect the world's deltas. *Nature,* 516**,** 31-33.

GRAY, A. B., & GARTNER, J.W. 2009. Continuous Sediment Monitoring in Rivers. *Journal of Hydraulic Engineering,* 135**,** 927-939.

HADDADCHI, A. 2017. Review of Suspended Sediment Measurement Techniques. NIWA.

HÅKANSON, L. 2006. The relationship between salinity, suspended particulate matter and water clarity in aquatic systems. *Ecological Research,* 21**,** 75-90.

HASSAN, M. A., VOEPEL, H., SCHUMER, R., PARKER, G. & FRACCAROLLO, L. 2013. Displacement characteristics of coarse fluvial bed sediment. *J. Geophys. Res. Earth Surf,* 118**,** 155-165.

HAUER, C., LEITNER, P., UNFER, G., PULG, U., HABERSACK, H. & GRAF, W. 2018. The Role of Sediment and Sediment Dynamics in the Aquatic Environment. *Riverine Ecosystem Management.*

HAUER, F. 2015. The Role of Sediment and Sediment Dynamics in the Aquatic Environment. *Oxford Unviersity Press***,** 155-180.

HEMMELDER, S., MARRA, W., MARKIES, H. & DE JONG, S. 2018. Monitoring river morphology & bank erosion using UAV imagery – A case study of the river Buëch, Hautes-Alpes, France. *International Journal of Applied Earth Observation and Geoinformation,* 73**,** 428-437.

HESTER, E. T., & DOYLE, M. W. 2008. Challenge in Continuous Monitoring and Adaptive Management of River Systems. *Journal of the American Water Resources Association,* 44**,** 382-398.

HODGE, R., A., & AUSTIN, M. J., 2014. *A Review of Spatial Data Analysis Methods for Hydrological Applications*.

HOLEMAN, J. N. 1968. The Sediment Yield of Major Rivers of the World. *Water Resources Research,* 4**,** 737-747.

HOROWITZ, A. J. 2008. Determining annual suspended sediment and sediment-associated trace element and nutrient fluxes. *Science of The Total Environment,* 400**,** 315-343.

HOSSAIN, A. K. M., JIA, Y. & CHAO, X. 2010. *Development of Remote Sensing Based Index for Estimating/Mapping Suspended Sediment Concentration in River and Lake Environments*.

HUI, T. R., PARK, E., LOC, H. H. & TIEN, P. D. 2022. Long-term hydrological alterations and the agricultural landscapes in the Mekong Delta: Insights from remote sensing and national statistics. *Environmental Challenges,* 7**,** 100454.

INTERNATIONAL HYDOPOWER ASSOCIATION, I. 2020. *How-To Guide: Hydropower Downstream Flow Regimes,* London, IHA.
KEMP, P., SEAR, D., COLLINS, A., NADEN, P. & JONES, I. 2011. The impacts of fine sediment on riverine fish. *Hydrological Processes,* 25**,** 1800-1821.
KONDOLF, G. M. 1997. Hungry water: Effects of dams and gravel mining on river channels. *ENVIRON. MANAGE.,* 21**,** 533-551.
KONDOLF, G. M. & WOLMAN, M. G. 1993. The sizes of salmonid spawning gravels. *Water Resources Research,* 29**,** 2275-2285.
KUMMU, M. & VARIS, O. 2007. Sediment-related impacts due to upstream reservoir trapping, the Lower Mekong River. *Geomorphology,* 85**,** 275-293.
KWON, S., SEO, I. W. & LYU, S. 2023. Investigating mixing patterns of suspended sediment in a river confluence using high-resolution hyperspectral imagery. *Journal of Hydrology,* 620**,** 129505.
LANGENDOEN, E. J., & SIMON, A. 2014. *Continuous Monitoring of Suspended Sediment Concentration and Turbidity in Surface Waters*.
LARSON, M., ANITA, S. M., VINCENT, R. & EVANS, J. 2018. Multi-depth suspended sediment estimation using high-resolution remote-sensing UAV in Maumee River, Ohio. *International Journal of Remote Sensing,* 39**,** 1-18.
LEMMA, H., NYSSEN, J., FRANKL, A., POESEN, J., ADGO, E. & BILLI, P. 2019. Bedload transport measurements in the Gilgel Abay River, Lake Tana Basin, Ethiopia. *Journal of Hydrology,* 577**,** 123968.
LENZI, M. A., MAO, L. & COMITI, F. 2006. Effective discharge for sediment transport in a mountain river: Computational approaches and geomorphic effectiveness. *Journal of Hydrology,* 326**,** 257-276.
LEOPOLD, L. B., WOLMAN, M.G., & MILLER, J.P. 1964. *Fluvial Pocesses in Geomorphology,* New York, Freeman and Company.
LING, T.-Y., SOO, C.-L., SIVALINGAM, J.-R., NYANTI, L., SIM, S.-F. & GRINANG, J. 2016. Assessment of the Water and Sediment Quality of Tropical Forest Streams in Upper Reaches of the Baleh River, Sarawak, Malaysia, Subjected to Logging Activities. *Journal of Chemistry,* 2016**,** 8503931.
LIU, C., HE, Y., DES WALLING, E. & WANG, J. 2013. Changes in the sediment load of the Lancang-Mekong River over the period 1965–2003. *Science China Technological Sciences,* 56**,** 843-852.
LLOYD, C. E. M., FREER, J. E., JOHNES, P. J. & COLLINS, A. L. 2016. Using hysteresis analysis of high-resolution water quality monitoring data, including uncertainty, to infer controls on nutrient and sediment transfer in catchments. *Science of The Total Environment,* 543**,** 388-404.
LU, X. X., OEURNG, C., LE, T. P. Q. & THUY, D. T. 2015. Sediment budget as affected by construction of a sequence of dams in the lower Red River, Viet Nam. *Geomorphology,* 248**,** 125-133.
LU, X. X. & SIEW, R. Y. 2006. Water discharge and sediment flux changes over the past decades in the Lower Mekong River: possible impacts of the Chinese dams. *Hydrol. Earth Syst. Sci.,* 10**,** 181-195.
LUM, Z. X. Y. 2023. The interactive effects of climate, land cover change and damming on the flow regime and fine sediment dynamics of a tropical river.
MCCARTNEY, M., SULLIVAN, C. & ACREMAN, M. 2001. Ecosystem Impacts of Large Dams. *School of Arts and Social Sciences Papers*.

MEADE, R. & PARKER, R. 1985. Sediment in rivers of the United States. *US Geological Survey Water-Supply Paper,* 2275**,** 49-60.
MILLIMAN, J. & MEADE, R. R. 1983. World-wide Delivery of River Sediment to the Oceans. *Journal of Geology,* 91**,** 1-21.
MILNER, N. J., ELLIOTT, J. M., ARMSTRONG, J. D., GARDINER, R., WELTON, J. S. & LADLE, M. 2003. The natural control of salmon and trout populations in streams. *Fisheries Research,* 62**,** 111-125.
MONTGOMERY, D. R. & BUFFINGTON, J. M. 1997. Channel-reach morphology in mountain drainage basins. *GSA Bulletin,* 109**,** 596-611.
MRC, M. R. C. 2019. Mekong Sediment from the MRC Council Study.
MUKUNDAN, R., PIERSON, D. C., SCHNEIDERMAN, E. M., O'DONNELL, D. M., PRADHANANG, S. M., ZION, M. S. & MATONSE, A. H. 2013. Factors affecting storm event turbidity in a New York City water supply stream. *CATENA,* 107**,** 80-88.
NADAL-ROMERO, E., REGÜÉS, D. & LATRON, J. 2008. Relationships among rainfall, runoff, and suspended sediment in a small catchment with badlands. *CATENA,* 74**,** 127-136.
NADEN, P. S. 2010. The Fine-Sediment Cascade. *In:* TIMOTHY BURT, R. A. (ed.) *Sediment Cascades: An Integrated Approach.* John Wiley & Sons, Ltd.
NIÑO, Y., GARCÍA, M. & AYALA, L. 1994. Gravel saltation: 1. Experiments. *Water Resources Research,* 30**,** 1907-1914.
ODY, A., DOXARAN, D., VERNEY, R., BOURRIN, F., MORIN, G. P., PAIRAUD, I. & GANGLOFF, A. 2022. Ocean Color Remote Sensing of Suspended Sediments along a Continuum from Rivers to River Plumes: Concentration, Transport, Fluxes and Dynamics. *Remote Sensing* [Online], 14.
OWENS, BATALLA, R. J., COLLINS, A. J., GOMEZ, B., HICKS, D. M., HOROWITZ, A. J., KONDOLF, G. M., MARDEN, M., PAGE, M. J., PEACOCK, D. H., PETTICREW, E. L., SALOMONS, W. & TRUSTRUM, N. A. 2005. Fine-grained sediment in river systems: environmental significance and management issues. *River Research and Applications,* 21**,** 693-717.
PACINI, N., DONABAUM, K., HENRY DE VILLENEUVE, P., KONECNY, R., PINESCHI, G., POCHON, Y., SALERNO, F., SCHWAIGER, K., TARTARI, G., WOLFRAM, G. & ZIERITZ, I. 2013. Water-quality management in a vulnerable large river: the Nile in Egypt. *International Journal of River Basin Management,* 11**,** 205-219.
PANIN, A. Land-ocean sediment transfer in palaeotimes, and implications for present-day natural fluvial fluxes. 2004 Moscow. IAHS Publication, 115-124.
PIQUÉ, G., LÓPEZ-TARAZÓN, J. A. & BATALLA, R. J. 2014. Variability of in-channel sediment storage in a river draining highly erodible areas (the Isábena, Ebro Basin). *Journal of Soils and Sediments,* 14**,** 2031-2044.
PONCE, D. V. M. 2014. Engineering Hydrology: Principles and Practices. *Chapter 13: Sediment in the Hydrologic Cycle.*
POWELL, K. 2002. Grand Canyon: open the floodgates! *Nature,* 420**,** 356-359.
POWER, M. E., DIETRICH, W. E. & FINLAY, J. C. 1996. Dams and downstream aquatic biodiversity: Potential food web consequences of hydrologic and geomorphic change. *Environmental Management,* 20**,** 887-895.
PROTEUS. 2023. *Proteus Instruments User Manual*. United Kingdom patent application.
PUSCH, M., & MUHAR, S. 2008. Importance of Coarse-Grained Sediments for Macroinvertebrate Communities in Lowland Rivers. *Journal of the North Americal Benthological Society,* 27(1)**,** 47-58.

SARAWAK ENERGY BERHAD, S. 2019. *Baleh Hydroelectric Project* [Online]. Available: https://www.sarawakenergy.com/baleh-hep [Accessed].
SCHELLENBERG, G., DONELLY, C. R., HOLDER, C. & AHSAN, R. 2017. Dealing with Sediment: Effects on Dams and Hydropower Generation. *Hydro Review,* 25.
SERRA, T., SOLER, M., BARCELONA, A. & COLOMER, J. 2022. Suspended sediment transport and deposition in sediment-replenished artificial floods in Mediterranean rivers. *Journal of Hydrology,* 609**,** 127756.
SHAFFER, J. 2017. It's Not Just Dirt: Impacts of Sediment Pollution. *Mountain Watershed Association* [Online]. Available from: https://www.mtwatershed.com/2016/11/05/its-not-just-dirt-impacts-of-sediment-pollution/.
SOUKHAPHON, A., BAIRD, I. G. & HOGAN, Z. S. 2021. The Impacts of Hydropower Dams in the Mekong River Basin: A Review. *Water,* 13.
STALLARD, R. F. 1987. Cross-channel mixing and its effect on sedimentation in the Orinoco River. *Water Resources Research,* 23**,** 1977-1986.
STAUB, J. R., AND GASTALDO, R.A. 2000. Seasonal sediment transport and deposition in the Rajang River delta, Sarawak, East Malaysia. *Sedimentary Geology,* 133(3-4)**,** 249-264.
SUBRAMANIAN, V. 1993. Sediment load of Indian rivers. *Current Science,* 64**,** 928-930.
SYVITSKI, J. P. M., VÖRÖSMARTY, C. J., KETTNER, A. J. & GREEN, P. 2005. Impact of Humans on the Flux of Terrestrial Sediment to the Global Coastal Ocean. *Science,* 308**,** 376.
TENA, A. & BATALLA, R. J. 2013. The sediment budget of a large river regulated by dams (The lower River Ebro, NE Spain). *Journal of Soils and Sediments,* 13**,** 966-980.
THAPA, B. B., & GYAWALI, D. 2011. Impact of Land Use Change on Sediment Yield in the Koshi River Basin, Nepal. *Journal of Hydrology,* 397 (1-2)**,** 12-21.
THI HA, D., OUILLON, S. & VAN VINH, G. 2018. Water and Suspended Sediment Budgets in the Lower Mekong from High-Frequency Measurements (2009–2016). *Water* [Online], 10.
TIE, Y. L. 1982. *Soil Classification in Sarawak,* Kuching, Soils Division, Deppartment of Agriculture.
USBR, U. B. O. R. 2019. Colorado River Sediment Management.
USBR, U. B. O. R. 2023. *Colorado River Sediment Management* [Online]. Available: https://www.usbr.gov/water/research/projects/colorado/sediment/ [Accessed].
USDA, U. S. D. O. A. 1993. Soil Survey Manual. *In:* SERVICE, S. C. (ed.).
USGS. 2018. *Sediment and Suspended Sediment* [Online]. Available: https://www.usgs.gov/special-topics/water-science-school/science/sediment-and-suspended-sediment#:~:text=Fast%2Dmoving%20water%20can%20pick,during%20a%20low%2Dflow%20period. [Accessed].
VANNOTE, R. L., MINSHALL, G. W., CUMMINS, K. W., SEDELL, J. R. & CUSHING, C. E. 1980. The River Continuum Concept. *Canadian Journal of Fisheries and Aquatic Sciences,* 37**,** 130-137.
VOLKE, M. A., SCOTT, M. L., JOHNSON, W. C. & DIXON, M. D. 2015. The Ecological Significance of Emerging Deltas in Regulated Rivers. *BioScience,* 65**,** 598-611.
VÖRÖSMARTY, C. J., MEYBECK, M., FEKETE, B., SHARMA, K., GREEN, P. & SYVITSKI, J. P. M. 2003. Anthropogenic sediment retention: major global impact from registered river impoundments. *Global and Planetary Change,* 39**,** 169-190.

WAGNER, R. J., BOULGER, R.W., OBLINGER, C. J., & SMITH, B.A. 2006. *Guidelines and Standard Procedures for Continuous Water Quality Monitors: Station Operation, Record Computation, and Data Reporting,* Virginia.

WALLACE, J. B., & GREGORY, S. V., . The Role of Fine Sediment in Stream Ecosystems. American Fisheries Society Symposium, 2002. 59-72.

WALLING, D. & COLLINS, A. 2016. River science: Research and management for the 21st Century (Chapter 3). *ChichesterFine Sediment Transport and Management; Wiley-Blackwell: Chichester, UK***,** 37-60.

WALLING, D. E. 2006. Human impact on land–ocean sediment transfer by the world's rivers. *Geomorphology,* 79**,** 192-216.

WANG, Y., ZHANG, J., ZHOU, Y., & ZHANG, Y. 2016. Impacts of Human Activities on Sediment Yield: A Case Study of the Yellow River Basin, China. *Science of the Total Environment,* 542**,** 1062-1070.

WENTWORTH, C. K. 1922. A Scale of Grade and Class Terms for Clastic Sediments. *The Journal of Geology***,** 377-392.

WHEATON, J. M., BRASINGTON, J., DARBY, S. E., & SEAR, D. A. 2010. *Accounting for Uncertainty in DEMs from Repeat Topographic Surveys: Improved Sediment Budgets*.

WILCOCK, P., PITLICK, J. & CUI, Y. 2009. Sediment Transport Primer Estimating Bed-Material Transport in Gravel-Bed Rivers.

WILLIAMS, G. P. & WOLMAN, M. G. 1984. Downstream effects of dams on alluvial rivers. *Professional Paper.* - ed.

WOHL, E., BLEDSOE, B., JACOBSON, R., POFF, N., RATHBURN, S., WALTERS, D. & WILCOX, A. 2015. The Natural Sediment Regime in Rivers: Broadening the Foundation for Ecosystem Management. *BioScience,* 65.

WOOD, P. J. & ARMITAGE, P. D. 1997. Biological Effects of Fine Sediment in the Lotic Environment. *Environmental Management,* 21**,** 203-217.

WREN, D. G., BARKDOLL, B. D., KUHNLE, R. A. & DERROW, R. W. 2000. Field Techniques for Suspended-Sediment Measurement. *Journal of hydraulic engineering (New York, N.Y.),* 126**,** 97-104.

XIA, R. 2010. Different Characteristics of Suspended Sediment Transport in Dry and Wet Years Revisited. *In:* ENGINEERS, U. A. C. O. (ed.) *2nd Joint Federal Interagency Conference.* Las Vegas: Advisory Committee on Water Information (ACWI).

XU, J. 2014. The influence of dilution on downstream channel sedimentation in large rivers: the Yellow River, China. *Earth Surface Processes and Landforms,* 39**,** 450-462.

ZIMMERMANN, A. E. 2013. 9.20 Step–Pool Channel Features. *In:* SHRODER, J. F. (ed.) *Treatise on Geomorphology.* San Diego: Academic Press.